PB-230 800

ORTHOKINETIC FLOCCULATION OF POLY-DISPERSED SYSTEMS

Howard S. Harris, et al

California University

Prepared for:

Public Health Service

July 1966

DISTRIBUTED BY:

NTIS

National Technical Information Service
U. S. DEPARTMENT OF COMMERCE
5285 Port Royal Road, Springfield Va. 22151

PB 230 800

ORTHOKINETIC FLOCCULATION OF POLYDISPERSED SYSTEMS

By

Howard S. Harris
and
Warren J. Kaufman

Prepared Under

U. S. Public Health Service
Research Grant No. WP-00658

July 1966

Sanitary Engineering Research Laboratory
College of Engineering
and
School of Public Health
University of California
Berkeley, California

SERL REPORT NO. 66-2

Reproduced by
NATIONAL TECHNICAL
INFORMATION SERVICE
U S Department of Commerce
Springfield VA 22151

ABSTRACT

The flocculation of colloidal material naturally present in water has long been employed in water purification practice prior to phase separation in other elements of a treatment plant. Flocculator performance is largely determined by its effectiveness in promoting orthokinetic flocculation resulting from stirring-induced velocity gradients. Because the kinetics of flocculation are imperfectly understood, the design and operation of flocculators have been based to a great extent upon empirical criteria. The purpose of this investigation was to identify the major parameters of significance in orthokinetic flocculation and to express their interrelationship in the form of a rate equation.

Theoretical equations expressing the rate of flocculation of a polydispersed system were developed from the Smoluchowski equation and other considerations. These equations accommodate the major parameters determining the performance of process units. The validity of the equations was demonstrated in two ways. First, the progress of flocculation in a series of continuous stirred-tank reactors was simulated by repeated computer application of the basic Smoluchowski equation and the computed floc size distributions compared with those predicted by the theoretically derived equations. Second, the flocculation of kaolin by alum was experimentally studied in a laboratory-scale reactor and the results compared with those predicted by the integrated rate equation after substitution of parameters susceptible to laboratory measurement.

The degree of completion of the flocculation reaction obtained in continuous flow or batch reactors is a function of the product of a rate constant, the mean velocity gradient, the amount of floc in the system, the retention period, and a parameter characterizing the floc size distribution. The compartmentalization of a continuous flow flocculator exerts a significant influence on the degree of flocculation attained and on overall system economy. In terms of performance at a constant overall residence time, a single completely mixed reactor is the least satisfactory, while an infinitely large number of infinitely small reactors is most efficient. The increase in the degree of flocculation with mean velocity gradient reaches a limit that depends upon floc strength, thus limiting the range of conditions over which the kinetic equations apply. The flocculation rate constant appears to be a function of the physical-chemical parameters generally associated with coagulation.

Preceding page blank

TABLE OF CONTENTS

	Page
ABSTRACT	iii
LIST OF TABLES	viii
LIST OF FIGURES	ix
Chapter	
I. INTRODUCTION	1
Coagulation and Flocculation in Water Purification	1
Research on Flocculation Kinetics	2
Objectives of the Study	2
Sponsorship and Acknowledgments	3
II. THEORY OF COLLOIDAL SYSTEMS	4
Stability Factors	4
Perikinetic Flocculation	7
Orthokinetic Flocculation	10
Flocculation in Water Purification	13
III. GENERALIZATION OF THE SMOLUCHOWSKI EQUATION	17
Introduction	17
Rate Equation for Total Floc Concentration — Unlimited Floc Size	17
Rate Equation for Total Floc Concentration — Limited Floc Size	23
Rate Equation for Primary Floc Concentration — Unlimited Floc Size	26

TABLE OF CONTENTS (continued)

Chapter		Page
	Rate Equation for Primary Floc Concentration — Limited Floc Size	27
	Additional Comments on Rate Equations as Applied to Water Purification	28
	Summary	31
IV.	SIMULATION OF FLOCCULATION	32
	Introduction	32
	Computer Programs	33
	Analysis of Computed Size Distrubutions	37
	Analysis of Kinetics of Simulated Flocculation	46
	Summary	54
V.	LABORATORY REACTOR CHARACTERISTICS	55
	Theory of Residence Time Distribution	55
	Laboratory Reactor	58
	Residence Time Distribution	61
	Energy Input	65
VI.	LABORATORY INVESTIGATION OF FLOCCULATION KINETICS	69
	Rate Equation for Experimental Results	69
	Additional Comments on the Experimental System	71
	Flocculation-Sedimentation Experiments	73
	Analysis of Experimental Results	78
	Flocculation Rate Parameters	78
	Rate Constant	87
	Batch Reactor Analysis	91

TABLE OF CONTENTS (continued)

Chapter		Page
	Summary	93
VII.	IMPLICATIONS OF RESULTS IN PROCESS DESIGN AND OPERATION	95
	Previous Design Equations	95
	Application of the Rate Equation to the Design of a Series of Reactors	95
	Solids Contact Units	98
VIII.	SUMMARY AND CONCLUSIONS	99
	APPENDIXES	
	A. List of Symbols	103
	B. Computer Program	109
	C. Chemical Analysis of Tap Water	117
	D. Results of Flocculation - Sedimentation Experiments	121
	First reactor in series	123
	Second reactor in series	125
	Fourth reactor in series	127
	REFERENCES	129

LIST OF TABLES

Table	Title	Page
I.	β Function for a System of Two Flocs of Various Relative Sizes	21
II.	Summary of Rate Equations and Size Distribution Functions	29
III.	Summary of Computer Program Parameters and Floc Size Distribution Functions	40

LIST OF FIGURES

Figure	Title	Page
1.	Schematic Representation of the Double Layer	6
2.	Net Potential Energy as a Function of Distance	6
3.	Sphere of Influence in Orthokinetic Flocculation . . .	11
4.	Computer Program Flow Diagram for Floc II	34
5.	Relation of Floc Numbers in Selected Sizes to Iteration Number	39
6.	Floc Size Distributions for $\theta = 0.02$	41
7.	Floc Size Distributions for $\theta = 0.225$	42
8.	Floc Size Distributions for $\theta = 1.00$	43
9.	Floc Size Distributions for $\theta = 3.00$	44
10.	Floc Size Distributions from Batch Computer Run	45
11.	Computed Change in Total Number of Flocs in a Series of Continuous Stirred-Tank Reactors	47
12.	Computed Change in Number of Size One Flocs in a Series of Continuous Stirred-Tank Reactors	48
13.	Computed Change in Number of Size One Flocs in a Batch Reactor	49
14.	Relation Between γ Function and Relative Number of Total Flocs	50
15.	Relation Between δ Function and Relative Number of Size One Flocs	51
16.	Relation Between δ'_m Function and Relative Number of Size One Flocs	52
17.	F- and C- Diagrams for Ideal Reactors	56
18.	Flocculatio Reactors	59
19.	Laboratory Reactors	60

LIST OF FIGURES (continued)

Figure	Title	Page
20.	Residence Time Function for a Single Reactor with 229 Second Retention Period	62
21.	Residence Time Function for a Single Reactor with 463 Second Retention Period	63
22.	Residence Time Function for a Single Reactor with 901 Second Retention Period	64
23.	Residence Time Function for Two Reactors in Series	66
24.	Energy Imparted by Stirring as a Function of Paddle PPM	67
25.	Kaolin Particle Size Distribution	72
26.	Light Transmission Characteristics of a Dilute Suspension of Kaolin in Distilled Water	74
27.	Light Transmission Characteristics of Kaolin in Distilled Water and Tap Water	75
28.	Relationship Between Kaolin Concentration and Turbidity as Measured with a Hellige Turbidimeter.	75
29.	Light Transmission Characteristics of a Coagulated Kaolin Suspension in Tap Water	76
30.	Supernatant Clarity after Flocculation and Sedimentation (Jar Test Procedure)	77
31.	Effect of Alum Dosage upon Degree of Flocculation (Continuous Flow Basis)	77
32.	Effect of Settling Time on Clarity of Coagulated Kaolin Suspensions	79
33.	Effect of Mean Velocity Gradient on Degree of Flocculation	80
34.	Effect of Retention Period on Degree of Flocculation.	82
35.	Effect of Floc Mass on Degree of Flocculation	83
36.	KD for Reactor 1	84
37.	KD for Reactor 2	85

LIST OF FIGURES (continued)

Figure	Title	Page
38.	KD for Reactor 4	86
39.	Experimentally Determined Values of D Function and δ_m' from Flocculation Simulation Studies	88
40.	Degree of Flocculation in a Series of Continuous Stirred-Tank Reactors	89
41.	D Function as Derived from Hudson's Jar Test Data . . .	92
42.	Role of Compartmentalization in Flocculator Performance	97

I. INTRODUCTION

COAGULATION AND FLOCCULATION IN WATER PURIFICATION

The rapid growth of municipal water purification and distribution systems during the past century has been the result of increasing municipal and industrial demand for supplies of water of high quality. The initial consideration in purification practice was the protection of public health against water-borne disease. As experience with chlorination and watershed sanitation has accumulated and as the more inadequate systems of waste disposal have yielded to the modern water pollution control plant, nearly all questions of disease transmission by potable water have been resolved and emphasis in treatment practice increasingly has been directed toward improving the aesthetic properties of the treated water.

Coagulation and filtration of impurities in surface waters has proven a most effective process for producing a sparking clear potable water. Colloidal and suspended clay particles, bacterial and algal cells, and organic debris which may impart turbudity and color to the water are efficiently removed. While this removal is of primarily health and aesthetic value, it has significant economic value to certain industries. Moreover, the consumer appears quite willing to pay the slightly higher price that treatment to improve appearance requires.

Coagulation and sedimentation were originally considered to be only preparatory steps to the process of filtration, but with greater understanding of the chemical nature of the phenomena involved, the importance of coagulation has slowly been recognized. Indeed, coagulation and flocculation may be the more important steps, as in the absence of adequate coagulation the effectiveness of subsequent processes may be seriously impaired.

The major consideration in the design of water treatment flocculators is to provide adequate opportunity within the unit for the growth of particle aggregates of such size and density (and perhaps surface properties) that maximum separation may occur elsewhere in the plant. The performance of the unit is in large measure determined by its effectiveness in promoting orthokinetic flocculation by stirring-induced velocity gradients as the mixing of chemicals and perikinetic flocculation by Brownian motion are rapidly accomplished. Proper design may avoid costly expenditures, either initially for overdesigned units or subsequently due to excessive coagulant requirements. Rational design criteria, however, have not been available. Design is based upon criteria which tend to be subjective and empirical, largely because the designer does not have a general theory describing the flocculation process in terms of the decisions he must make.

RESEARCH ON FLOCCULATION KINETICS

Research concerned with colloidal systems has tended to emphasize either of two aspects. The first of these, coagulation, concerns primarily the factors affecting sol stability and the means of reducing stability through the addition of electrolytes, chemical coagulants, and coagulant aids. This research is producing a vast body of knowledge of both theoretical interest and practical value. The second aspect is flocculation or the aggregation of the colloidal system once instability has been attained. Only minor effort has been directed toward greater understanding of flocculation phenomena.

Research into flocculation phenomena by colloid chemists and others has well established the validity of certain theoretical relationships. The systems investigated have tended to have certain common characteristics. The colloidal particles are less than one micron in diameter with the result that Brownian motion is the principal agent causing aggregation (perikinetic flocculation). The colloidal particles are discrete solids of approximately uniform size. The progress of flocculation has been followed only to the point where the average aggregate is composed of very few of the primary particles. Observations have ceased before any physical factor, such as shear strength of the aggregates, might limit the further increase in floc size. The experiments have been conducted on a batch basis. The flocculation kinetics of these relatively simple systems may be described quite accurately.

The more complex systems such as those of interest in water treatment have received little attention. In addition to the primary discrete particles, there are present loose aggregates of the primary particles which may be several orders of magnitude larger in size. Flocculation is promoted primarily by velocity gradients induced by stirring, but the maximum floc size is limited by these gradients and the strength of the floc. Furthermore, flocculation is achieved in practice with a series of continuous stirred-tank reactors (CSTR) in which a broad spectrum of velocity gradients exists, resulting in both flocculation and breakup within the same reactor.

OBJECTIVES OF THE STUDY

Fundamental information regarding the kinetics of orthokinetic flocculation should permit improved design and operation of flocculation units. The investigation was directed toward the following specific objectives:

1. Development of a theoretical generalized rate equation accommodating the major parameters determining flocculator performance.

2. Laboratory investigation of the degree of flocculation obtained in a series of continuous stirred-tank reactors.

3. Determination of the extent to which rate equations derived for an idealized system are useful in describing the rate of flocculation observed for a complex real system.

SPONSORSHIP AND ACKNOWLEDGMENTS

This research was supported in part by research grant WP-00658 from the National Institutes of Health, U. S. Public Health Service.

The many stimulating discussions with, and difficult questions posed by, Professor Ray B. Krone of the Davis Campus are greatly appreciated. The writer is indebted to Mr. John T. Heibel who developed the program which made the computer studies possible.

II. THEORY OF COLLOIDAL SYSTEMS

Studies of colloidal systems have tended to emphasize either of two aspects. The first of these, which will be termed coagulation in this report, is concerned with the origin and nature of the stabilizing forces within the sol and the effects of additions of electrolytes, coagulants, and coagulant aids in lessening stability. The second aspect will be designated flocculation and is the process of aggregation of the sol once instability has been attained. Research related to coagulation has produced a vast body of knowledge of both theoretical significance and practical importance. However, a detailed consideration of coagulation is beyond the scope of this report.

Flocculation may be described as perikinetic or orthokinetic, depending upon whether Brownian motion or velocity gradients within the fluid are the principal agents causing the close approach and collision of the colloidal particles. To a certain extent, all particles are subject to flocculation by both mechanisms, their relative effectiveness in promoting flocculation being related to the characteristic particle size of the suspension, and, to a lesser extent, to temperature and to the energy dissipated in creating velocity gradients. The rate of perikinetic flocculation appears to be a function of the net repulsive or attractive forces between particles and the bridging action of polymeric molecules attached to the particle surfaces. It is to be expected that a similar situation exists relative to orthokinetic flocculation, but that a lesser dependence exists on particle charge and other surface properties.

The nature of forces between colloidal particles will be briefly considered. Various theories of perikinetic and orthokinetic flocculation will then be reviewed, together with the extent to which the kinetics of flocculation have been applied to water purification systems.

STABILITY FACTORS

An important characteristic of a sol or suspension is its stability or resistance to flocculation. A relatively stable sol may exhibit little flocculation after a period of months, while the flocculation of an unstable system may be essentially complete in minutes. In a stable sol, Brownian motion is sufficient to keep the solid phase dispersed uniformly throughout the fluid, but because of the spectrum of kinetic energies of the individual particles, perikinetic flocculation occurs, though often extremely slowly.

The stability of hydrophobic colloidal particles is associated with the electrical charge carried on their surfaces. Several theories have been advanced to explain the origin of this charge, including ionization of groups present on the particle surface, isomorphic substitution, and ion adsorption. This charge may be altered by the

addition of electrolytes (especially highly charged ions of sign opposite to that on the particle), by the interaction with colloidal particles of opposite charge, by changes in pH, and by additions of polyelectrolytes that may interact in a particular manner with the particle surface or serve to link particles together.

The aluminum and ferric ions used as coagulants in water purification form hydrolysis products which have marked tendencies to polymerize and these have been shown to be more significant than the ions in causing coagulation. The hydrogen ion concentration is especially significant in coagulation with iron and aluminum salts as the hydrolysis product formed and its average charge is thereby determined.

The presence of an electrical charge upon the surface of a colloidal particle affects the distribution of ions within the dispersing medium, especially in the immediate vicinity of the particle. The excess ions on the solid phase and the excess ionic charge of opposite sign distributed in the dispersion medium near the particle constitute a double layer. Several theoretical distributions of ionic charge within the double layer have been proposed. The Gouy-Chapman [1,2] treatment yields an approximately exponential drop in potential with increasing distance from the solid (cf. Figure 1). The assumptions are made that the ions are point charges able to approach to within an infinitesimal distance from the solid surface. The derived relationships do not agree well with experimental data, particularly in the vicinity of the surface. Stern [3] has proposed a correction which is equivalent to considering the first layer of ions to be at a small distance (δ) from the surface rather than at the surface.* A second modification proposed by Stern is that a layer of ions is adsorbed to the wall at this same small distance. A further development has been proposed by Grahame [4] who has hypothesized that the Stern layer actually contains only anions, which have been adsorbed with a partial loss of their hydration shell. Cations tend to remain hydrated and are not able to approach as closely. In summary, all of these theories predict an approximately exponential decrease in potential with distance, beginning at least some small distance beyond the particle surface.

The presence of strong repulsive forces between particles is often sufficient to reduce the rate of flocculation and the reduction or elimination of these forces allows the functioning of a short-range attractive force, the London–Van der Waals force, which is responsible for the aggregation of unstable particles which have closely approached or collided. The net potential of the particle is the resultant of these repulsive and attractive forces (cf. Figure 2). The presence of a small net repulsion at an intermediate distance may not insure sol stability if occasional approaching particles possess sufficient kinetic energy to overcome the barrier and enter the region of net attraction (cf. Figure 2, curve B). Other net potentials may be attractive at all distances.

---

*Symbols used in this report are defined in Appendix A.

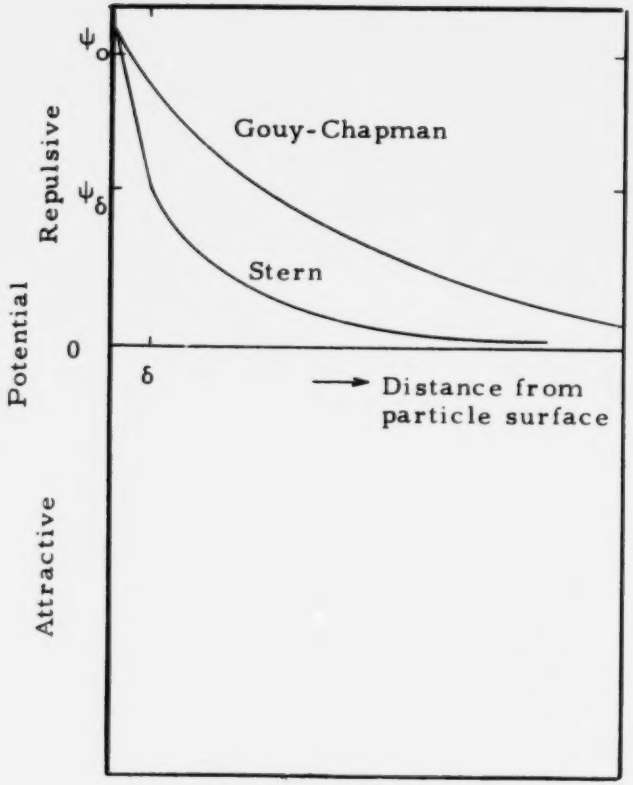

FIGURE 1 -- Schematic Representation of the Double Layer

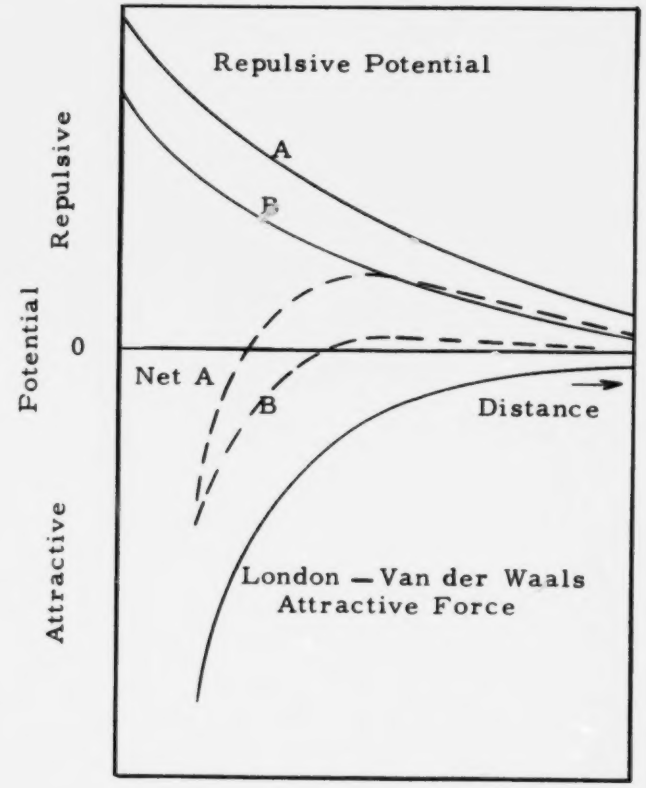

FIGURE 2 -- Net Potential Energy as a Function of Distance

PERIKINETIC FLOCCULATION

Because of a difference in the significant physical mechanicms causing flocculation, the study of flocculation kinetics may be conveniently divided into two parts. In the first, perikinetic flocculation, Brownian motion is the principal agent causing the close approach or collision of colloidal particles. In the second, orthokinetic flocculation, the approach results principally from fluid velocity differences. Brownian motion is more effective in flocculating very small particles while larger ones are affected more by velocity gradients. A brief summary of theories of perikinetic flocculation is presented below, following the treatment by Overbeck [5].

A theory of perikinetic flocculation was first presented by Smoluchowski [6,7,8]. Assuming spherical particles and the absence of repulsive forces between particles, the rate at which particles diffuse through a sphere around a central particle is given by Fick's first diffusion equation as

$$I = 4\pi r^2 D \frac{dn}{dr} \tag{1}$$

where I is the number of collisions per unit time with the central particle; r, the distance from the center of the central particle; D, the diffusion constant of the particles; and n, the number of particles per unit volume. For the boundary conditions:

$$n = n_o \quad \text{for} \quad r = \infty$$

$$n = 0 \quad \text{for} \quad r = R$$

$$I = 4\pi D R n_o \tag{2}$$

where n_o is the initial number of particles per unit volume and R is the distance between the centers of two particles at which a lasting contact is formed.

As the central particle is also subject to Brownian motion, the proper diffusion constant is

$$D_{ij} = D_i + D_j \tag{3}$$

and the total number of collisions per unit time is

$$I_{ij} = 4\pi D_{ij} R_{ij} n_i n_j \ . \tag{4}$$

For a size distribution of n_1 primary particles, n_2 secondary particles, and generally n_i i-fold particles, the rate of change in concentration of k-fold particles is

$$\frac{dn_k}{dt} = \frac{1}{2} \sum_{\substack{i=1 \\ j=k-i}}^{j=k-1} 4\pi D_{ij} R_{ij} n_i n_j - n_k \sum_{i=1}^{\infty} 4\pi D_{ik} R_{ik} n_i \ . \qquad (5)$$

The first term expresses the rate at which k-fold particles are created as a result of collisions between i-fold and j-fold ($k = i + j$) and the second term expresses the rate at which k-fold particles disappear as the result of collision with other particles.

The radius of interaction, R_{ij}, is about equal to $(r_i + r_j)$ where r is the radius of the particle. The diffusion constant D_i is inversely proportional to the particle radius r_i. Then

$$D_{ij}R_{ij} = (D_i + D_j)(r_i + r_j) = D_1 R_1 \left(\frac{1}{r_i} + \frac{1}{r_j}\right)(r_i + r_j) \ . \qquad (6)$$

Smoluchowski makes the approximation that $(1/r_i + 1/r_j)(r_i + r_j) = 4$, which is exact for $r_i = r_j$ and increasing in error as the size difference increases. Then

$$D_{ij}R_{ij} = 4D_1 r_1 \ , \qquad (7)$$

or for situations where it cannot be assumed that the collision distance is equal to the sum of the particle radii,

$$D_{ij}R_{ij} = 2D_1 R \ . \qquad (8)$$

Equation 5 may now be simplified to

$$\frac{dn_k}{dt} = 4\pi D_1 R \left[\sum_{\substack{i=1 \\ j=k-i}}^{j=k-1} n_i n_j - 2n_k \sum_{i=1}^{\infty} n_i \right] \ . \qquad (9)$$

The rate of change of total number of particles is then

$$\frac{d\sum_{k=1}^{\infty} n_k}{dt} = 4\pi D_1 R \left[\sum_{i=1}^{\infty}\sum_{j=1}^{\infty} n_i n_j - 2\sum_{k=1}^{\infty}\sum_{i=1}^{\infty}\right] n_i n_k$$

$$= -4\pi D_1 R \sum_{i=1}^{\infty}\sum_{j=1}^{\infty} n_i n_j = -4\pi D_1 R \left(\sum_{k=1}^{\infty} n_k\right)^2$$

$$\frac{dn_t}{dt} = -4\pi D_1 R n_t^2 \qquad (10)$$

where n_t is the total number of particles per unit volume. The usual form of this equation is obtained by integrating with respect to time (batch basis). Thus,

$$n_t = \frac{n_o}{1 + 4\pi D_1 R n_o t} = \frac{n_o}{1 + \frac{t}{T}} \qquad (11)$$

where $T = 1/4\pi D_1 R n_o$, the coagulation time or time in which the number of particles is reduced one half.

That the initial rate of rapid flocculation of a monodispersed sol is adequately expressed by Equation 11 has been demonstrated many times. The collision distance is often observed to be two to three times the particle radius, indicating that not only has the repulsive force between particles been eliminated, but that a net attractive force exists. For a sol which was not monodispersed, Muller [9,10] showed that the rate of flocculation could be expressed by replacing the coefficient 4 in Equation 7 by a larger coefficient computed from Equation 6 using the actual radii. This approach is adequate for a sol consisting of two sizes of particles, but has not been generalized for a size distribution.

The above derivation assumes that all collisions result in aggregation (i.e., rapid flocculation). For conditions of slow flocculation, where there remains slight repulsive forces between particles, Smoluchowski proposed a theory only slightly different from that above. He assumed that of the close approaches expressed by Equation 11, only a fraction α resulted in aggregation of the particles. Then the time of flocculation becomes

$$T = \frac{1}{4\pi D_1 R n_o \alpha} \cdot \qquad (12)$$

While this equation does indeed express the rate at which some slow flocculations proceed, in other cases it is not adequate. Fuchs [11] successfully developed an equation expressing the rate of slow flocculation as a function of the remaining potential between particles. The theory, however, has not been extended to collisions of multiple-sized particles.

ORTHOKINETIC FLOCCULATION

It has long been observed that gentle stirring promotes flocculation. Similar accelerations of the process have been observed as a consequence of sedimentation or centrifugation of a sol. Smoluchowski [12] developed a theory to explain these effects based upon the existence of velocity gradients. The theory has been extended by others [13,14].

Although the distribution of velocity gradients in stirred liquids is generally complex, assume that the gradient is constant, at least locally. As a result of the gradient, particles may approach to within such a distance that collision and aggregation results. Let R_{ij} again be the collision radius of a j-particle with a central i-particle. The probability of collision is the product of the concentration of j-particles (n_j) and the rate of flow of liquid to within a distance R_{ij} of the central particle (cf. Figure 3). For flow in the y direction and a velocity gradient du/dz, the velocity at a height z is z du/dz. The differential area with this velocity is $2\sqrt{R_{ij}^2 - z^2}\,dz$. Then

$$J_{ij} = 2\int_0^{R_{ij}} n_j\left(z\,\frac{du}{dz}\right) 2\sqrt{R_{ij}^2 - z^2}\,dz$$

$$= \frac{4}{3}\,n_j(R_{ij})^3\,\frac{du}{dz}\,. \qquad (13)$$

If the concentration of central particles is n_i, the frequency of collision between i and j particles is

$$J_{ij} = \frac{4}{3}\,n_i n_j(R_{ij})^3\,\frac{du}{dz}\,. \qquad (14)$$

For a system of particles of uniform size

$$J = \frac{4}{\pi}\,\frac{du}{dz}\,\Phi n_T \qquad (15)$$

where Φ is the volume fraction of particles.

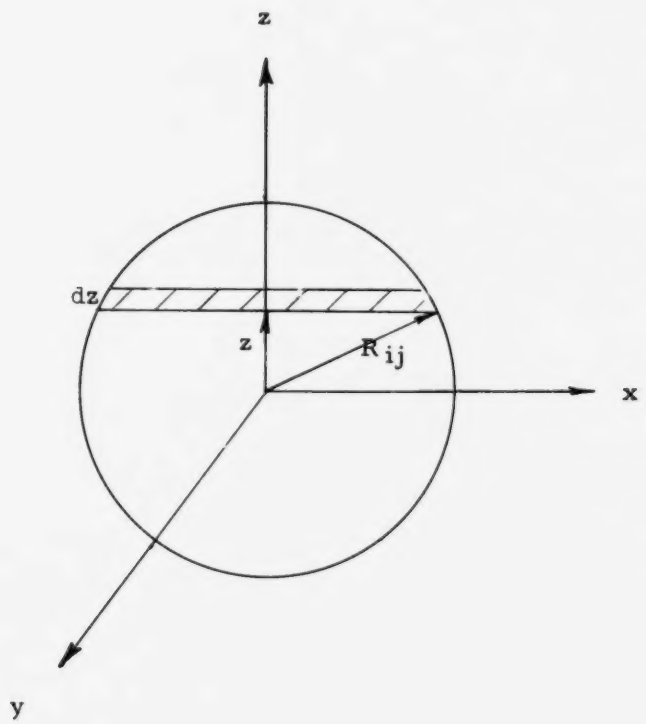

FIGURE 3 -- Sphere of Influence in Orthokinetic Flocculation

The relative effectiveness of stirring and Brownian motion in promoting flocculation may be determined by comparing Equations 14 and 4.

$$\frac{J_{ij}}{I_{ij}} = \frac{(R_{ij})^2 \frac{du}{dz}}{3\pi D_{ij}} . \tag{16}$$

Using the Einstein equation for an estimate of the particle diffusion coefficient,

$$\frac{J_{ij}}{I_{ij}} = \frac{\mu(R_{ij})^3 \frac{du}{dz}}{2kT} \tag{17}$$

where μ is the liquid viscosity; k, the Boltzmann constant; and T, the absolute temperature. Assuming a water temperature of 20°C and a velocity gradient of 20 sec^{-1}, the ratio is unity for a collision distance of

$$R_{ij} = \sqrt[3]{\frac{(2)(1.38 \times 10^{-16})(293)}{(0.0101)(20)(10^{-12})}} = 0.74 \mu .$$

Assuming two equal particles whose radii are one half the collision distance, the flocculation of particles with a radius smaller than 0.37 microns is more strongly influenced by Brownian motion, while the flocculation of particles with a radius greater than 0.37 microns is more greatly affected by velocity gradients.

Levich [15] has considered flocculation in turbulent flow where the flocculation radius R is very small in comparison with the microscale of turbulence. Comparing the collision rate as a result of turbulence to that of Brownian motion, he concluded that Brownian motion is more significant for particles smaller than 0.1 microns (in water at room temperature).

Experimental verification of Equation 15 has been attempted by Manley and Mason and by Swift and Friedlander. Manley and Mason [16] observed the frequency of collision of spherical glass beads (137-micron diameter) suspended in corn syrup between counterrotating coaxial cylinders. A total of 1437 observations were made at velocity gradients of 0.4 to 1.9 per second and volume fractions of the beads of 0.00398 to 0.0234. The average ratio of observed to theoretical collision frequency was 1.01.

Swift and Friedlander [17] investigated the initial rate of flocculation of Dow polystyrene latex spheres (0.871-microns diameter) in distilled water. Velocity gradients of 1 to 80 per second were produced between rotating coaxial cylinders. Under the experimental conditions both velocity gradient and Brownian motion promoted flocculation, the ratio of effectiveness ranging from 0.069 to 5.50. Based upon the assumption that the collision rates due to Brownian motion and velocity gradient are additive (and the results seem to indicate that this is so), it was shown that the kinetics were first order with respect to particle concentration and that the rate constant was proportional to shear rate as predicted. The observed rate constant was 37.5 per cent of the theoretical. As this same percentage of the theoretical rate was observed during perikinetic flocculation, it was concluded that $\alpha = 0.375$ for this system.

FLOCCULATION IN WATER PURIFICATION

In 1921 Langelier [18] first described the significance of agitation for securing adequate flocculation in water purification units. Based upon the results of jar tests and a model three-compartment continuous-flow flocculator, he demonstrated an increase in rate of flocculation and a decrease in time required to produce satisfactory floc as the paddle speed was increased. The use of compartmented flocculators with individual paddles was advocated as giving greater flexibility in operation. The value of multiple compartments in reducing the short circuiting of a portion on the flow was recognized and a reduction in velocity in each succeeding compartment was recommended.

Camp, Root, and Bhoota [19] investigated the effect of temperature upon the rate of floc formation and concluded that changes in temperature have no measurable effect upon the time of floc formation. The authors hypothesized that the formation of floc takes place in three steps. The first is the formation of precipitates as the result of chemical reaction, then the formation of colloidal floc particles by Brownian motion, and finally floc growth as a result of velocity gradients. It was concluded from their experimental results that the Brownian motion phase was probably near completion in 6 to 10 seconds.

Camp and Stein [20] in 1943 published an especially significant paper introducing several concepts into the fluid mechanics literature in a form convenient for engineering design. The Smoluchowski orthokinetic flocculation equation was developed for the rate of collision between two sizes of particles. Expressions were developed for the root-mean-square velocity gradients in both stirred and baffled channel flocculators. For the stirred flocculator

$$\left(\frac{du}{dz}\right)_{mean} = G = \sqrt{\frac{W}{\mu}} \qquad (18)$$

where W is the total power dissipated per unit volume of fluid and μ is the viscosity of the fluid.

In 1955 Camp [21] summarized the conclusions of his earlier articles. Based upon operation at design capacity, Camp estimated that the mean velocity gradient G at 20 U.S. water treatment plants was between 20 and 74 sec^{-1}. The product of G and T (flocculation period in seconds) ranged from 23,000 to 210,000. To obtain a satisfactory floc he recommended that the sum of the GT values for a series of basins should be the same as the value for a single basin. The results of laboratory jar tests by P. C. Stein were quoted as indicating an optimum velocity gradient of 20 sec^{-1}, whereas 40 sec^{-1} disrupted the floc.

Camp developed formulas for the dissipation function W for rotating paddles and for reciprocating blades. For paddles

$$W = \frac{239\, C_D (1 - k)^3 S^3}{V} \sum Ar^3 \qquad (19)$$

where C_D is the coefficient of drag; k, the ratio of fluid velocity to that of the blade; S, the shaft speed in revolutions per second; V, the fluid volume; A, the area of the blade; and r, the distance from the center of the shaft to the center of the blade. Based upon experiments at the Cambridge treatment plant, k was found to be 0.24 at high speed and 0.32 at low.

Fair and Gemmel [22] reviewed the various theories of flocculation kinetics and the application of these concepts to water treatment practice. Using a digital computer and Smoluchowski's equations, the progress of flocculation on a batch basis was simulated for various system parameters and modes of floc breakup. A number of particle size distributions as a function of time were determined; however, the analysis of flocculation kinetics was inconclusive.

The appearance of floc developed at values of G from 3.2 to 9.3 sec^{-1} on a batch basis was recorded photographically and analyzed as a function of floc size distribution, flocculation time, and GT. Flocs with areas as small as 0.023 sq mm were included in some floc size distributions. It was demonstrated that the mean size of the larger flocs tends to increase to a maximum and then decrease slightly with further flocculation time. The effectiveness of flocculation in removing color (produced by instant coffee) and turbidity (kaolin) as a function of G and T was investigated. Qualitative conclusions were drawn, but a kinetic analysis was not presented.

Tambo [23], in a comprehensive study of coagulation and flocculation in water purification practice, reviewed the literature of flocculation kinetics. He pointed out that the Smoluchowski-Camp equation for orthokinetic flocculation assumed laminar flow conditions and did not adequately describe the mechanism of turbulent flocculation.

Based upon the Levich equation describing the rate of flocculation of particles very much smaller than the scale of turbulence, Tambo developed the following equation for the rate of flocculation in turbulent flow.

$$\frac{d\sum_{k=1}^{\infty} n_k}{dt} = \frac{1}{2} A \left\{ \sum_{k=1}^{\infty} \sum_{i=1}^{\infty} [1^{1/3} + (k-i)^{1/3}]^3 n_i n_{k-i} - 2 \sum_{k=1}^{\infty} \sum_{i=1}^{\infty} (i^{1/3} + k^{1/3})^3 n_k n_i \right\} \qquad (20)$$

$$A = \frac{3}{2} \pi \beta \sqrt{\frac{W}{\mu}} d_1^3 n_o^2$$

where β is a proportionality constant. Using a digital computer and Equation 20, particle size distributions were developed for flocculation on a batch basis.

Tambo investigated flocculation in the laboratory in two ways. First, a micro-floc was formed during 2 minutes of stirring at 300 rpm, followed by a floc-forming period of 0 to 240 seconds at 50 rpm. The rate of settling was then observed using a sedimentation balance. The rate of accumulation was compared with curves derived from the computer studies to estimate a value of A for the system. However, it was not demonstrated that the Levich equation could be properly applied to this experimental system. Second, flocculation was observed in a four-compartment model flocculator. Per cent removal of turbidity was determined and presented as a function of the sum of the retention period–mean gradient product.

Hudson [24] recently has presented several equations describing the rate of change of concentration of colloidal particles in a flocculating system. The equations are obtained directly from the Smoluchowski-Camp equation by considering only aggregation of fine or primary particles with the large flocs present and by neglecting the floc volume fraction of the fines. The equations are:

$$\frac{N}{N_o} = \exp\left(-\frac{\alpha \Phi G T}{\pi}\right) \qquad (22)$$

$$= \exp\left(-\frac{\alpha A G T}{\pi S}\right) \qquad (23)$$

where N_o is the colloidal material naturally present (excluding floc from the coagulant); N, the unflocculated material remaining after time T; α, the fraction of collisions resulting in aggregation ("sticking ratio"); Φ, the floc volume fraction; G, the mean velocity gradient; A, the coagulant dose; and S, the concentration of coagulant in the floc. The effectiveness of flocculation in a series of jar tests was evaluated by measuring turbidity after flocculation and sedimentation. It was concluded by Hudson that at constant G the volume of floc was proportional to the alum dose and that the density of the floc can be increased more than 10 times by extended agitation. Analysis of Hudson's data by a different approach will be presented in Chapter VI.

Michaels and Bolger [25,26] have studied the settling and plastic flow characteristics of flocculated kaolin suspensions. They concluded that small flocs rather than the primary clay particles are the fundamental structural units. The flocs are considered to be rigid spheres which tend to cluster together in weak aggregates. A number of experimental relationships were observed. Specifically, a tendency was noted for aggregate size to decrease as velocity gradients increased, although the change was small in the range 21-42 sec^{-1}. The water-clay ratio in the aggregate was 30-60 to 1.

Krone [27], in an investigation of the rheologic properties of a number of estuarial sediments, was able to identify and measure changes in physical properties with changes in aggregate structure. The various structures were identified as primary particles, primary particle aggregates, aggregates of primary particle aggregates, etc. A decrease in density and shear strength was observed with increasing order of aggregation.

Numerous other articles could be cited which contain some reference to the kinetics of flocculation in water purification practice. Generally the data presented permit qualitative conclusions to be drawn about the effect of stirring and time of flocculation for the particular conditions investigated. A more general analysis is usually not possible for two reasons. First, no quantitative measure of the progress of flocculation was made. Qualitative measures are used such as a description of floc appearance or the relative settling rate (of the visible flocs). Second, the relative stirring is recorded in some manner such as paddle tip velocity. Identification of flocculator geometry and relative rotation velocity of the water is not made.

III. GENERALIZATION OF THE SMOLUCHOWSKI EQUATION

INTRODUCTION

The application of the Smoluchowski equation to orthokinetic flocculation has been hindered by the absence of a generalized form. The equation as written predicts the collision frequency of a system of particles of uniform size (Equation 15) or of a system of particles of two sizes (Equation 14). Use of the equation for a general system consisting of many sizes of particles has not been feasible (except to a very limited extent using a digital computer). Furthermore, the inability to consider the effects of limitation on particle growth negates direct application to most real systems.

In the further development of the Smoluchowski orthokinetic equation, a number of assumptions of the original derivation will be retained.

1. Flocs shall be considered as consisting of one or more primary particles, the number being written as a subscript. Primary particles are assumed to be of uniform size.

2. Flocs will be assumed to be spherical and of constant density, independent of size. The volume of a resulting floc is, therefore, equal to the sum of the volumes of the colliding flocs.

3. Only collisions of two flocs at a time will be considered.

4. The collision radius of a floc is a constant multiple of the particle radius.

5. If the aggregation of two flocs creates a floc larger than the limiting size, the oversized floc is broken into two fragments of unspecified size.

RATE EQUATION FOR TOTAL FLOC CONCENTRATION — UNLIMITED FLOC SIZE

The frequency of collisions between i-fold and j-fold particles was shown to be

$$J_{ij} = \frac{4}{3} n_i n_j (R_{ij})^3 \frac{du}{dz} . \qquad (14)$$

If it is assumed that each collision results in aggregation, the rate of change in concentration of k-fold particles is equal to the rate at which k-fold particles are created as the result of the collision of i-fold and j-fold particles (i + j = k), less the rate at which k-fold particles disappear as a result of collisions with other particles. For the case of no limitation upon maximum floc size

$$\frac{dn_k}{dt} = \frac{1}{2} \sum_{\substack{i=0 \\ j=k-i}}^{k} \frac{4}{3} n_i n_j (R_{ij})^3 \frac{du}{dz} - \sum_{i=0}^{\infty} \frac{4}{3} n_i n_k (R_{ik})^3 \frac{du}{dz} . \quad (24)$$

The factor 1/2 arises because of the summations indicated. For the general case of $i \neq j$, each combination is considered twice (e.g., $i = x$, $j = k - x$ and $j = x$, $i = k - x$). For the occasional case where $i = j$, the factor 1/2 arises from the number of combinations of n_i things taken two at a time: $n!/2!(n-2)! = 1/2\ n(n-1) \cong 1/2\ n^2$.

The volume of a floc is

$$V_i = \frac{4}{3} \pi r_i^3 = \frac{4}{3} \pi i r_1^3 \quad (25)$$

$$r_i^3 = i r_1^3 . \quad (26)$$

Also, the collision distance is taken as the sum of the two collision radii. Then

$$R_{ij} = R_i + R_j . \quad (27)$$

By definition

$$a = \frac{R}{r} . \quad (28)$$

Based upon the relationships above,

$$\begin{aligned} (R_{ij})^3 &= (R_i + R_j)^3 = (ar_i + ar_j)^3 \\ &= [ar_1(i)^{1/3} + ar_1(j)^{1/3}]^3 \\ &= (ar_1)^3[(i)^{1/3} + (j)^{1/3}]^3 . \end{aligned} \quad (29)$$

Equation 24 may now be written as

$$\frac{dn_k}{dt} = \frac{4}{3}(ar_1)^3 \frac{du}{dz}\left\{ \sum_{\substack{i=0 \\ j=k-i}}^{k} \frac{n_i n_j}{2} [(i)^{1/3} + (j)^{1/3}]^3 - \sum_{i=0}^{\infty} n_i n_k [(i)^{1/3} + (k)^{1/3}]^3 \right\} . \qquad (30)$$

The rate of change of total number of flocs may be found by summing over all possible k values.

$$\frac{d \sum_{k=0}^{\infty} n_k}{dt} = \frac{4}{3}(ar_1)^3 \frac{du}{dz}\left\{ \sum_{k=0}^{\infty} \sum_{\substack{i=0 \\ j=k-i}}^{\infty} \frac{n_i n_j}{2} [(i)^{1/3} + (j)^{1/3}]^3 - \sum_{k=0}^{\infty} \sum_{i=0}^{\infty} n_i n_k [(i)^{1/3} + (k)^{1/3}]^3 \right\} . \qquad (31)$$

The index k goes to infinity in the double summation related to creation of k-fold flocs, and both i and j may have any value up to infinity independently. Physically this means that no matter how great i and j are, a larger floc k can be formed, since all combinations of i and j are considered. Therefore the summation indices may be replaced

$$\sum_{k=0}^{\infty} \sum_{\substack{i=0 \\ j=k-i}}^{\infty} \frac{n_i n_j}{2} [(i)^{1/3} + (j)^{1/3}]^3$$

$$= \sum_{i=0}^{\infty} \sum_{j=0}^{\infty} \frac{n_i n_j}{2} [(i)^{1/3} + (j)^{1/3}]^3$$

$$= \sum_{i=0}^{\infty} \sum_{k=0}^{\infty} \frac{n_i n_k}{2} [(i)^{1/3} + (k)^{1/3}]^3 \quad . \qquad (32)$$

The following function of the floc size distribution is defined:

$$\beta = \frac{\sum_{j=0}^{\infty} \sum_{i=0}^{\infty} n_i n_j [(i)^{1/3} + (j)^{1/3}]^3}{\sum_{j=0}^{\infty} \sum_{i=0}^{\infty} n_i n_j (i + j)} \quad . \qquad (33)$$

This function is an index of the degree of dispersion of floc sizes. The magnitude of β is four for a monodispersed system and decreases to one for a strongly polydispersed system. For a size distribution where one size (or a narrow size range) predominates, β will approach four. Values of β for a system of two sizes of flocs are shown in Table I.

TABLE I

β FUNCTION FOR A SYSTEM OF TWO FLOCS OF VARIOUS RELATIVE SIZES

i/j	(i + j)	$[(i)^{1/3} + (j)^{1/3}]^3$	β=
1	2	8.00	4.00
10	11	31.26	2.84
100	101	179.4	1.78
1,000	1,001	1331	1.33
10,000	10,001	11,451	1.14
100,000	100,001	106,630	1.07
1,000,000	1,000,001	1,030,301	1.03
∞	-	-	1.00

Substituting Equations 32 and 33 into Equation 31

$$\frac{d \sum_{k=0}^{\infty} n_k}{dt} = -\frac{\beta}{2} \left(\frac{4}{3}\right) (ar_1)^3 \frac{du}{dz} \left[\sum_{k=0}^{\infty} \sum_{i=0}^{\infty} n_i n_k (i + k) \right]$$

$$= \frac{-2\beta}{3} (ar_1)^3 \frac{du}{dz} \left[\sum_{k=0}^{\infty} \sum_{i=0}^{\infty} i n_i n_k + \sum_{k=0}^{\infty} \sum_{i=0}^{\infty} k n_i n_k \right]$$

$$= \frac{-2\beta}{3} (ar_1)^3 \frac{du}{dz} \left[\left(\sum_{k=0}^{\infty} n_k \right) \left(\sum_{i=0}^{\infty} i n_i \right) + \left(\sum_{k=0}^{\infty} \right) \left(\sum_{i=0}^{\infty} n_i \right) \right] . \tag{34}$$

The volume of floc per unit volume of sol, Φ, is

$$\Phi = \frac{4}{3} \pi r_1^3 \sum_{k=0}^{\infty} k n_k = \frac{4}{3} \pi r_1^3 \sum_{i=0}^{\infty} i n_i . \tag{35}$$

The total concentration of floc is

$$n_t = \sum_{i=0}^{\infty} n_i = \sum_{k=0}^{\infty} n_k .$$

Therefore,

$$\frac{d \sum_{k=0}^{\infty} n_k}{dt} = -\frac{2\beta}{3} (ar_1)^3 \frac{du}{dz} \left[\frac{\Phi n_t}{4/3\pi r_1^3} + \frac{\Phi n_t}{4/3\pi r_1^3} \right] \tag{36}$$

and

$$\frac{dn_t}{dt} = \frac{-\beta a^3}{\pi} \frac{du}{dz} \phi n_t \quad . \qquad (37)$$

Equation 37 may be compared with Equation 15 for the trivial case of a monodispersed system ($\beta = 4$). The size distribution function β may be computed for a known size distribution with Equation 33. In addition to the effect of β, the rate of decrease of total floc concentration is first order with respect to the total floc concentration, velocity gradient, and floc volume fraction.

RATE EQUATION FOR TOTAL FLOC CONCENTRATION — LIMITED FLOC SIZE

In the previous section it was assumed that there was no limit to the size to which a floc might grow. This condition is approached during the initial stages of flocculation occurring on a batch basis or for the first of a series of continuous stirred-tank reactors (where the retention period is short compared to the reaction constant). Generally, however, consideration must be given to a limitation on the maximum size. For the systems of interest in water purification, the limitation arises from the inability of the floc to resist shearing or surface erosion within the velocity gradient. A similar situation arises in aerosol and emulsion systems where shearing of liquid droplets may be significant.

Several mechanisms for breaking up flocs exceeding the size limit may be postulated. Oversized flocs might be broken into two (or more) equal fragments. Or the size of one fragment might be specified to be equal to the limiting size. It might be hypothesized that collision does not result in aggregation if the resulting aggregate would exceed the size limit. If it is assumed that the breakup is into two fragments, then there is no change in total floc concentration, irrespective of the size of the fragments. Although the exact mechanism must be known to predict the resulting floc size distributions, it need not be known if the size distribution is know.

If p is the maximum size of floc permitted, the rate of change of k-fold flocs is

$$\frac{dn_k}{dt} = \frac{1}{2} \sum_{\substack{i=0 \\ j=k-i}}^{k} \frac{4}{3} n_i n_j (R_{ij})^3 \frac{du}{dz} - \sum_{i=0}^{p-k} \frac{4}{3} n_i n_k (R_{ik})^3 \frac{du}{dz}$$

$$= \frac{4}{3} (ar_1)^3 \frac{du}{dz} \left\{ \sum_{\substack{i=0 \\ j=k-i}}^{k} \frac{n_i n_j}{2} [(i)^{1/3} + (j)^{1/3}]^3 \right.$$

$$\left. - \sum_{i=0}^{p-k} n_i n_k [(i)^{1/3} + (k)^{1/3}]^3 \right\} . \qquad (38)$$

The rate of change of total number of flocs is

$$\frac{d \sum_{k=0}^{p} n_k}{dt} = \frac{4}{3} (ar_1)^3 \frac{du}{dz} \left\{ \sum_{\substack{k=0 \\ j=k-i}}^{p} \sum_{i=0}^{k} \frac{n_i n_j}{2} [(i)^{1/3} + (j)^{1/3}]^3 \right.$$

$$\left. - \sum_{k=0}^{p} \sum_{i=0}^{p-k} n_i n_k [(i)^{1/3} + (k)^{1/3}]^3 \right\} . \qquad (39)$$

This equation is similar to Equation 31, except for the change in limits over which the summation is to be performed. The first summation above may be written as

$$\sum_{k=0}^{p} \sum_{\substack{i=0 \\ j=k-i}}^{k} = \sum_{j=0}^{p} \sum_{i=0}^{p} - \sum_{j=(p-i)+1}^{p} \sum_{i=0}^{p} = \sum_{j=0}^{p} \sum_{i=0}^{p} - \sum_{j=(p-i)+1}^{p} \sum_{i=0}^{p} ,$$

(40)

and the second summation as

$$\sum_{k=0}^{p}\sum_{i=0}^{p-k} = \sum_{k=0}^{p}\sum_{i=0}^{p} - \sum_{k=0}^{p}\sum_{i=(p-k)+1}^{p} . \qquad (41)$$

Both of these transformations are based upon the fact that the desired summation is the difference between the summation of all possible combinations of sizes and the summation of all undesired possibilities. Making these substitutions into Equation 39,

$$\frac{d\sum_{k=0}^{p} n_k}{dt} = \frac{4}{3}(ar_1)^3 \frac{du}{dz}\left\{ -\frac{1}{2}\sum_{j=0}^{p}\sum_{i=0}^{p} n_i n_j \left[(i)^{1/3} + (j)^{1/3}\right]^3 \right\}$$

$$+\frac{1}{2}\sum_{j=(p-i)+1}^{p}\sum_{i=0}^{p} n_i n_j \left[(i)^{1/3} + (j)^{1/3}\right]^3 \Bigg\}$$

$$\frac{dn_t}{dt} = -\frac{4}{6}(ar_1)^3 \frac{du}{dz}\left\{ \sum_{j=0}^{p-i}\sum_{i=0}^{p} n_i n_j \left[(i)^{1/3} + (j)^{1/3}\right]^3 \right\} . \qquad (42)$$

A function γ of the floc size distribution is defined

$$\gamma = \frac{\sum_{j=0}^{p}\sum_{i=0}^{p-j} n_i n_j \left[(i)^{1/3} + (j)^{1/3}\right]^3}{\sum_{j=0}^{p}\sum_{i=0}^{p} n_i n_j (i + j)} . \qquad (43)$$

Substitution into Equation 42 yields

$$\frac{dn_t}{dt} = -\frac{\gamma a^3}{\pi}\frac{du}{dz}\Phi n_t . \qquad (44)$$

The form of this equation is identical to that expressing the rate when the maximum floc size is not limited (Equation 37), except that a different size distribution function is defined. The γ function is a measure of the dispersion of the floc size distribution. The maximum

value of γ is 4 for a monodispersed system of size p/2-fold or smaller. The minimum value is 0, which is obtained when all flocs are larger than p/2-fold.

RATE EQUATION FOR PRIMARY FLOC CONCENTRATION – UNLIMITED FLOC SIZE

The rate of decrease of primary floc (k = 1) may be deduced from Equation 30

$$\frac{dn_1}{dt} = \frac{4}{3}(ar_1)^3 \frac{du}{dz} \left\{ 0 - \sum_{i=0}^{\infty} n_i n_1 [(i)^{1/3} + (1)^{1/3}]^3 \right\}$$

$$= -\frac{4}{3}(ar_1)^3 \frac{du}{dz} n_1 \sum_{i=0}^{\infty} n_i [(i)^{1/3} + 1]^3 . \qquad (45)$$

Let δ be a function of the size distribution such that

$$\delta = \frac{\sum_{i=0}^{\infty} n_i [(i)^{1/3} + 1]^3}{\sum_{i=0}^{\infty} i n_i} = \frac{1}{n_o} \sum_{i=0}^{\infty} n_i [(i)^{1/3} + 1]^3 . \qquad (46)$$

The maximum value of δ is 8 for a distribution consisting of only primary (i = 1) particles. The minimum value of δ approaches 1 as the number of particles approaches 1.

Substituting Equation 46 into Equation 45,

$$\frac{dn_1}{dt} = -\frac{4}{3}(ar_1)^3 \frac{du}{dz} n_1 \delta n_o = -\delta \frac{a^3}{\pi} \frac{du}{dz} \phi n_1 . \qquad (47)$$

The maximum value of the δ function is 8 for a monodispersed system. This value is consistent with the value of 4 for both β and γ functions, since the aggregation of two particles results in a decrease of two n_1 particles but only one particle in total.

RATE EQUATION FOR PRIMARY FLOC CONCENTRATION – LIMITED FLOC SIZE

Consideration must be given to the size distribution of floc fragments resulting from the breakup of oversized flocs. If the primary floc can form an aggregate with any floc present and if the breakup of oversized flocs does not yield a primary floc as a fragment, then the resulting rate equation is identical to Equation 47 utilizing the δ function. Appropriate equations can be developed if other assumptions are made. One additional example will be given.

Assume that the rate of collision of primary and p-size particles is equal to the rate at which n_1 particles are produced as the result of breakup of oversized particles. This is the equivalent of assuming that the collision of n_1- and n_p-size particles does not result in aggregation. Then,

$$\frac{dn_1}{dt} = \frac{4}{3} (ar_1)^3 \frac{du}{dz} \left\{ 0 - \sum_{i=0}^{p-1} n_i n_1 [(i)^{1/3} + 1]^3 \right\} . \quad (48)$$

Defining a function ϵ of the floc size distribution such that

$$\epsilon = \frac{1}{n_o} \sum_{i=0}^{p-1} n_i [(i)^{1/3} + 1]^3 \quad (49)$$

$$= \delta - \frac{n_p}{n_o} [(i)^{1/3} + 1]^3 , \quad (50)$$

and substituting into Equation 48 gives

$$\frac{dn_1}{dt} = - \frac{4}{3} (ar_1)^3 \frac{du}{dz} n_1 n_o \epsilon = - \frac{\epsilon a^3}{\pi} \frac{du}{dz} \phi n_1 . \quad (51)$$

The equation in the continued derivation will employ the δ function. However, as the experimental information is insufficient to indicate the correct mechanism for the breakup of flocs, the use of δ does not imply the supporting of any particular theory of breakup.

ADDITIONAL COMMENTS ON RATE EQUATIONS AS APPLIED TO WATER PURIFICATION

The rate equations derived previously, together with the definitions of the various size distribution functions, are summarized in Table II. It should be noted that the form of all of the equations is similar, differing only in size distribution function.

The objective of flocculation as conventionally practiced in water treatment is the aggregation of colloids initially present in the water to the extent that separation will occur as the result of sedimentation and filtration. It is the rate of disappearance of these primary particles which is the major consideration in process design, especially where separation by sedimentation is the principal objective. The rate of change of total numbers of floc is of slight interest. The series of equations derived without limitation on floc size may be considered as special situations of the size limited case. For these reasons, attention hereafter will be directed to the equation expressing the rate of decrease of primary particles, considering both a limitation on maximum floc size and the possibility that all collisions and very close approaches of flocs do not result in aggregation ($\alpha \neq 1.0$).

$$\frac{dn_1}{dt} = \frac{-\alpha\delta a^3}{\pi} \frac{du}{dz} \phi n_1 \ . \qquad (52)$$

The values of the functions β, γ, δ, and ϵ can be computed exactly for a given size distribution. If all other terms in the rate equation are specified, a value of the function may be computed. Because each value of the function does not correspond to a unique size distribution, no specific conclusions concerning the size distribution are anticipated as a result of an experimental determination of the function.

The rate equation may be integrated for both batch and continuous flow conditions. For the batch condition (no addition of reactants during the reaction),

$$\int_{n_o}^{n_1} \frac{dn}{n} = \int_0^T -\frac{\alpha\delta a^3}{\pi} \frac{du}{dz} \phi dt \ . \qquad (53)$$

If δ is constant,

$$\ln \frac{n_o}{n_1} = \frac{\alpha\delta a^3}{\pi} \frac{du}{dz} \phi T \ . \qquad (54)$$

TABLE II

SUMMARY OF RATE EQUATIONS AND SIZE DISTRIBUTION FUNCTIONS

Floc Size Limit	Total Number of Flocs	Primary Particles
Maximum Floc Size Unlimited	$\frac{dn_t}{dt} = -\frac{\beta\alpha a^3}{\pi}\frac{du}{dz}\phi n_t$	$\frac{dn_1}{dt} = -\frac{\delta\alpha a^3}{\pi}\frac{du}{dz}\phi n_1$
Maximum Floc Size Limited to p-fold	$\frac{dn_t}{dt} = -\frac{\gamma\alpha a^3}{\pi}\frac{du}{dz}\phi n_t$	$\frac{dn_1}{dt} = -\frac{\epsilon\alpha a^3}{\pi}\frac{du}{dz}\phi n_1$

$$\beta = \frac{\sum_{j=0}^{\infty}\sum_{i=0}^{\infty} n_i n_j \left[i^{1/3} + j^{1/3}\right]^3}{\sum_{j=0}^{\infty}\sum_{i=0}^{\infty} n_i n_j \left[i + j\right]}$$

$$\delta = \frac{\sum_{i=0}^{\infty} n_i \left[i^{1/3} + 1\right]^3}{\sum_{i=0}^{\infty} i n_i}$$

$$\gamma = \frac{\sum_{j=0}^{p}\sum_{i=0}^{p-j} n_i n_j \left[i^{1/3} + j^{1/3}{}^3\right]}{\sum_{j=0}^{p}\sum_{i=0}^{p} n_i n_j \left[i + j\right]}$$

$$\epsilon = \frac{\sum_{i=0}^{p-1} n_i \left[i^{1/3} + 1\right]^3}{\sum_{i=0}^{p} i n_i}$$

However, δ is not a constant since it is a function of the changing size distribution. As δ cannot now be related to some other parameter, integration of Equation 53 cannot properly be performed. Experimental data can be plotted in a form similar to that indicated by Equation 54 and the value of δ determined as a slope.

For a series of identical continuous-flow reactors with n_o as the feed concentration, the effluent from the first reactor is

$$n_o + \left(- \frac{\alpha \delta a^3}{\pi} \frac{du}{dz} \phi n_1 \right) \frac{T}{m} = n_1$$

$$\frac{n_o}{n_1} = 1 + \frac{\alpha \delta a^3}{\pi} \frac{du}{dz} \phi \frac{T}{m} . \qquad (55)$$

Assuming that δ is a constant, the effluent from the second identical reactor is

$$\left(\frac{n_o}{n_1} \right)_2 = \left[1 + \frac{\alpha \delta a^3}{\pi} \frac{du}{dz} \phi \frac{T}{m} \right]^2 \qquad (56)$$

$$\left(\frac{n_o}{n_1} \right)^{\frac{1}{2}} - 1 = \frac{\alpha \delta a^3}{\pi} \frac{du}{dz} \phi \frac{T}{m} , \qquad (57)$$

and in general for the m identical reactors

$$\left(\frac{n_o}{n_1} \right)_m = \left(1 + \frac{\alpha \delta a^3}{\pi} \frac{du}{dz} \phi \frac{T}{m} \right)^m . \qquad (58)$$

Since δ is not a constant, Equation 56 must be written as

$$\left(\frac{n_o}{n_1} \right)_2 = \left[1 + \frac{a \delta_1 a^3}{\pi} \frac{du}{dz} \phi \frac{T}{m} \right] \left[1 + \frac{a \delta_2 a^3}{\pi} \frac{du}{dz} \phi \frac{T}{m} \right] . \qquad (59)$$

This equation may be solved using the two appropriate values of the δ function. Under those conditions where it is desirable to determine the character of the effluent from a series of identical reactors, an overall function (δ'_m) can be defined.

$$\left(\frac{n_o}{n_1}\right)_m = \prod_{i=1}^{m} \left(1 + \frac{\alpha\delta_i a^3}{\pi} \frac{du}{dz} \phi \frac{T}{m}\right)$$

$$= \left(1 + \frac{\alpha\delta'_m a^3}{\pi} \frac{du}{dz} \phi \frac{T}{m}\right)^m . \qquad (60)$$

δ'_m is an average value for the reactor series. Equation 60 therefore is the general equation which may be useful in water purification practice.

SUMMARY

Equations describing the rate of orthokinetic flocculation of a polydispersed system were developed. These equations are generalizations of the Smoluchowski orthokinetic flocculation equation. Assumptions made are consistent with those implied in the derivations of the Smoluchowski orthokinetic and perikinetic equations. Equations are derived for the rate of change of concentration of total number of floc particles or of number of primary floc particles only for the conditions of unlimited or of limited maximum floc size.

The rate of change is shown to be first order with respect to the velocity gradient, floc volume fraction, and the number concentration of the flocs of interest (total number or primary). The rate is also shown to be first order with respect to a floc size distribution function. Appropriate definitions of the function are made for the several cases considered. The maximum and minimum values of the functions are deduced and the corresponding size distributions identified.

The equation describing the rate of change of concentration of primary flocs when the maximum size of floc is limited is identified as being most appropriate for use in water purification. Equations are developed for the change in concentration for reaction on a batch basis or for reaction in a series of continuous reactors.

IV. SIMULATION OF FLOCCULATION

INTRODUCTION

In the preceding chapter, several equations were derived to express the rate of decrease of total number of flocs or of primary flocs only for the conditions of unlimited or limited maximum floc size. In all instances, reduction to a final usable equation was accomplished with the definition of an appropriate function of the particle size distribution. The equations are of a form which may be readily used to predict the rate of flocculation of a system with a known particle size distribution. The equations are not of a form which facilitates prediction of floc size distributions arising from a given initial size distribution. The very great number of mathematical operations necessary to compute a final size distrubution from an initial distribution and reaction parameters suggests that distributions could best be obtained using a digital computer.

A program was undertaken to study flocculation kinetics based upon numerical calculation by an IBM 7094 computer. The aims of the program were to:

1. Compute steady state floc size distributions within a simulated continuous stirred-tank reactor for various initial size distributions and operating parameters.

2. Compute floc size distributions for a simulated batch process as a function of time and operating parameters.

3. Test the validity of the proposed flocculation equations.

4. Compute the size distribution functions γ and δ.

5. Determine the effective order of the orthokinetic flocculation reaction.

A general computer program was written which would simulate the progress of flocculation either for a batch system or for one of a series of continuous stirred-tank reactors. For an initial floc size distribution within the simulated reactor, the resulting change in numbers of flocs was computed. The initial distribution was then changed by the computed differences, together with the influent and effluent increments in the case of a CSTR. The process was then repeated until the steady state size distribution was approached. Periodically the complete size distribution was printed out, together with operating variables and special functions of the size distribution. Although the computations were made on the basis of numbers of flocs, the results are equally valid as relative concentrations of flocs.

COMPUTER PROGRAMS

Two complete computer programs were developed. The first was written in FORTRAN IV, IBSYS, which is a precompiled language for IBM digital computers. Each program iteration required in excess of 15 seconds. Due to the high cost of using the computing machinery and the great number of iterations desired, a faster program was required. Several modifications were considered. First, the time represented by each iteration was increased by scaling the reaction coefficient. Only a moderate reduction was made to prevent the introduction of significant errors due to the noncontinuous addition of feed and removal of outflow. Second, the number of calculations per iteration could be reduced. Reduction of the number of floc sizes was rejected as unduly increasing the deviation of the computer model from a real system. However, the number of calculations was reduced by using a subroutine to calculate the value of $[(i)^{1/3} + (j)^{1/3}]^3$ and storing the results. Third, the entire program could be written in a faster language. Accordingly, the program was rewritten in FAP with FORTRAN II routines for input-output, initial calculations, and final size distribution function calculations. Fourth, the number of size distributions printed out was reduced to after every tenth iteration (after the first ten iterations) and the output routine buffered to facilitate simultaneous calculation and print out. After these changes, the iteration time was about 1.1 seconds. A flow diagram of the final program is shown in Figure 4. A copy of the entire program is given in Appendix A.

The initial floc size distribution (PART), input floc size distribution (FINP), reaction coefficient (ALPHA), and fraction of contents wasted (BETA) were read into the computer and immediately printed out as reference for the run. The change in numbers of particles of each size ($\Delta_{i,j,k}$) was calculated for all values of i, j, and the appropriate n_i and n_j. Any resulting k-flod flocs greater in size than 100 were divided into two equal flocs. After the change in number of flocs of each size was computed, the numbers in the inflow were added and the outflow subtracted and this increment added to the previous distribution. The new reactor floc size distribution was then printed out, together with the iteration number. The calculations were repeated until the specified number of iterations was reached. Finally, additional cards were punched with the reactor outflow distribution. Using these cards as input, the flocculation in the next reactor of the series was simulated.

One hundred quantized floc sizes were allowed. This limitation was necessary because of the finite capacity of the computer. Thus the computer program investigated only the case where maximum floc size was limited, and no results were obtained for the case where maximum floc size was unlimited. Several mechanisms may be hypothesized for breaking up flocs larger than the limiting size. For this study it was assumed that flocs larger than the limit split into two flocs of equal volume. The distribution of floc sizes between 50 and 100 was significantly influenced by this breakup mechanism. The distribution of floc sizes 1 to 49 was only indirectly affected.

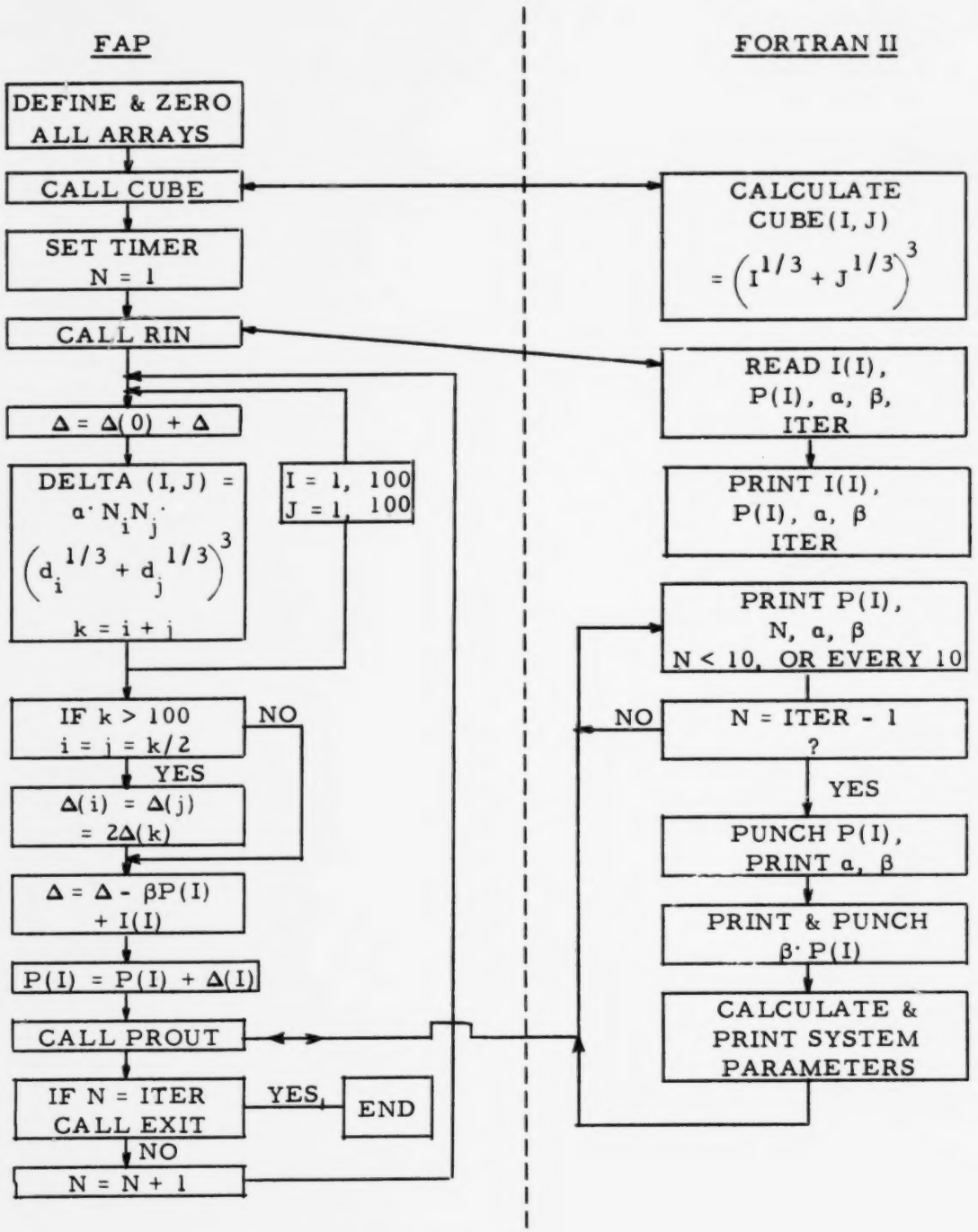
FAP
FORTRAN II
DEFINE & ZERO ALL ARRAYS
CALL CUBE
SET TIMER N = 1
CALL RIN
Δ = Δ(0) + Δ
DELTA (I, J) = α · N_i N_j · (d_i^1/3 + d_j^1/3)^3
k = i + j
I = 1, 100
J = 1, 100
IF k > 100 i = j = k/2
NO
YES
Δ(i) = Δ(j) = 2Δ(k)
Δ = Δ - βP(I) + I(I)
P(I) = P(I) + Δ(I)
CALL PROUT
IF N = ITER CALL EXIT
YES,
END
NO
N = N + 1
CALCULATE CUBE(I, J) = (I^1/3 + J^1/3)^3
READ I(I), P(I), α, β, ITER
PRINT I(I), P(I), α, β ITER
PRINT P(I), N, α, β N < 10, OR EVERY 10
NO
N = ITER - 1 ?
YES
PUNCH P(I), PRINT α, β
PRINT & PUNCH β · P(I)
CALCULATE & PRINT SYSTEM PARAMETERS

FIGURE 4 -- Computer Program Flow Diagram for Floc II

The main computer program permitted the computation of floc distributions for a single CSTR based upon a specified initial floc distribution (PART) and a specified feed floc size distrubution (FINP). A fraction BETA of all floc sizes within the CSTR was removed each iteration corresponding to reactor outflow. The number of iterations specified (ITER) was such that the final size distribution was that to be expected after the reaction had progressed for three retention periods. By specifying BETA and FINP as zero, the program simulated batch reactions.

The rate equation used for these computations was the Smoluchowski equation (Equation 14).

$$J_{ij} = \frac{4}{3} n_i n_j (R_{ij})^3 \frac{du}{dz} . \qquad (14)$$

It may be recalled that this equation describes the rate of collision of i-fold and j-fold flocs. If all collisions result in aggregation ($\alpha = 1$), the equation also describes the rate of flocculation.

Substituting Equation 29

$$\Delta_{i,j,k} = \frac{4}{3} n_i n_j (ar_1)^3 [(i)^{1/3} + (j)^{1/3}]^3 \frac{du}{dz} . \qquad (61)$$

The equation above defines the reaction coefficient ALPHA

$$\text{ALPHA} = \frac{1}{2} \left(\frac{4}{3} (ar_1)^3 \frac{du}{dz} \right) . \qquad (62)$$

As a part of the final printout routine, several functions of the floc size distribution were computed. These functions are related to the size distrubution function defined in Equations 33, 43, 46, and 49. The functions are as follows:

$$\text{DELTA*NUMB} = \sum_{i=1}^{100} n_i \left((i)^{1/3} + 1 \right)^3 \qquad (63)$$

$$\text{GAMMA DENOMINATOR} = \sum_{i=1}^{100} \sum_{i=1}^{100} n_i n_j (i+j) \qquad (64)$$

$$\text{GAMMA NUMERATOR} = \sum_{j=1}^{100} \sum_{i=1}^{100} n_i n_j \left((i)^{1/3} + (j)^{1/3} \right)^3 \quad (65)$$

$$\text{BETTA FUNCTION} = \sum_{j=1}^{100} \sum_{i=1}^{100} n_i n_j \left((i)^{1/3} + (j)^{1/3} \right)^3 . \quad (66)$$

Using these relationships, the desired functions may be computed

$$\beta = \frac{\text{BETA FUNCTION}}{\text{GAMMA DENOMINATOR}} \quad (67)$$

$$\gamma = \frac{\text{GAMMA NUMERATOR}}{\text{GAMMA DENOMINATOR}} \quad (68)$$

$$\delta = \frac{\text{DELTA*NUMB}}{n_o} \quad (69)$$

$$\epsilon = \delta - \frac{n_p}{n_o} \left[(p)^{1/3} + 1 \right]^3 . \quad (70)$$

It may be recalled that the derivation of β assumes that the maximum size of floc is unlimited. Since a maximum size of 100 is used in these computer studies, values computed have significance only in the unusual situation where few, if any, flocs reach a size of 100. Values of ϵ have no meaning here since the appropriate breakup mechanism was not used.

The computer program variables ALPHA, BETA, and PART have a special relationship. From Equation 62

$$2\ \text{ALPHA} = \frac{4}{3} (a r_1)^3 \frac{du}{dz} .$$

The reciprocal of BETA is the ratio between the reactor volume and rate of removal or the retention period.

$$\frac{1}{\text{BETA}} = \frac{\text{PART}}{\text{FINP}} = \frac{T}{M} . \quad (71)$$

The total volume of floc per unit volume is related to the integrated floc size distribution, and from Equation 35

$$\sum \text{PART} = \sum in_i = \frac{\phi}{\frac{4}{3}\pi r_1^3} . \tag{72}$$

Combining these equations gives

$$2 \frac{\text{ALPHA}}{\text{BETA}} \sum \text{PART} = \frac{a^3}{\pi} \phi \frac{du}{dz} \frac{T}{m} \tag{73}$$

$$= \theta . \tag{74}$$

Equation 74 is the definition of the flocculation factor (θ) as employed in the computer studies. The rate of flocculation is directly proportional to θ. Any combination of parameters which yields equal products θ will produce the same reaction rate.

ANALYSIS OF COMPUTED SIZE DISTRIBUTIONS

The results of two computer runs may be compared to illustrate the effect of equal θ upon the floc size distribution. The operating parameters were:

Program Variable	1	10
ALPHA	0.5×10^{-8}	1.125×10^{-8}
BETA	0.004444	0.01
PART	10^5	10^5
θ	0.225	0.225
T	2.98	3.00

The simulated reactors initially contained 100,000 floc of size 1. After 670 interations for Run No. 1 and 300 iterations for Run No. 10 (the reactors being operated as CSTR's), the following numbers of selected floc sizes were computed:

Floc Size	1	10
1	43,992.38	44,101.80
33	8.68	8.64
67	1.69	1.68
100	0.37	0.37

The distributions are essentially identical in all respects.

In the computer studies simulating flocculation within a CSTR, the reactor contents were initially assumed to have the same size distribution as the reactor feed stream. As the computer performed the iterative calculations simulating flocculation, the size distribution within the reactor gradually coarsened. Although theoretically an infinitely large number of iterations are required to reach the corresponding steady state size distribution, the expense of computer time necessitated minimizing the number of iterations. The results of the first few computer runs indicated that the percentage change in floc numbers was small after two retention periods, typically 200 iterations. Consequently, three retention periods were selected as the standard duration of the computer runs. Figure 5 gives the relationship between numbers of selected floc sizes and iteration number for a typical computer run. For this run, 300 iterations represented three retention periods.

A summary of the operating parameters for each computer run simulating a CSTR and several functions of the final size distribution are shown in Table III.

Effluent floc size distributions from computer Runs No. 10 to 23 are shown in Figures 6 to 9. These runs simulated flocculation in a CSTR at various values of θ, the flocculation rate factor (cf. Equation 74). Figure 6 presents the floc size distribution in each of a series of four CSTR at θ of 0.02. The distributions become progressively coarser from the first reactor to the fourth and the total number of flocs in the effluent decreases as the number of compartments (m) is increased. The value of θ is so small that the numbers of flocs of size 20 or larger is very small, even in the fourth reactor. The floc size distributions computed for θ = 0.225 are shown on Figure 7. The distributions again become progressively coarser through the series of reactors, at least for flocs of size 50 and larger. Between sizes 49 and 50 the discontinuity in the distribution results from the mode of breakup arbitrarily assumed. The number of size 1 flocs decreases through the series of reactors while somewhat larger sizes, e.g., size 40, show an erratic pattern. At higher values of θ (Figures 8 and 9), the size distributions begin to show a constant pattern. The numbers of flocs of size 49 or less decrease in all instances through the series of reactors, and the total numbers of flocs of size 50 or larger increase. The numbers of size 50 to 100 flocs is somewhat constant in the first reactor, but the distributions in successive reactors show an increasing number of size 80 to 90 flocs and a corresponding decrease in other sizes.

Selected floc size distributions resulting from flocculation on a batch basis are shown in Figure 10. For θ = 0.04, the size distribution is characterized by a large fraction of the initial size 1 flocs still unreacted and only a trivial number of flocs larger than size 10. At the higher value of θ = 0.6, the numbers of size 1 flocs remaining is small while significant numbers of flocs occur up to the limiting size of 100. A discontinuity in the size distribution again appears at size 50 and results from the breakup routine biasing the numbers of flocs above size 49. It should be noted that the size distribution obtained from a batch reactor are significantly different from those obtained in a series of continuous stirred-tank reactors.

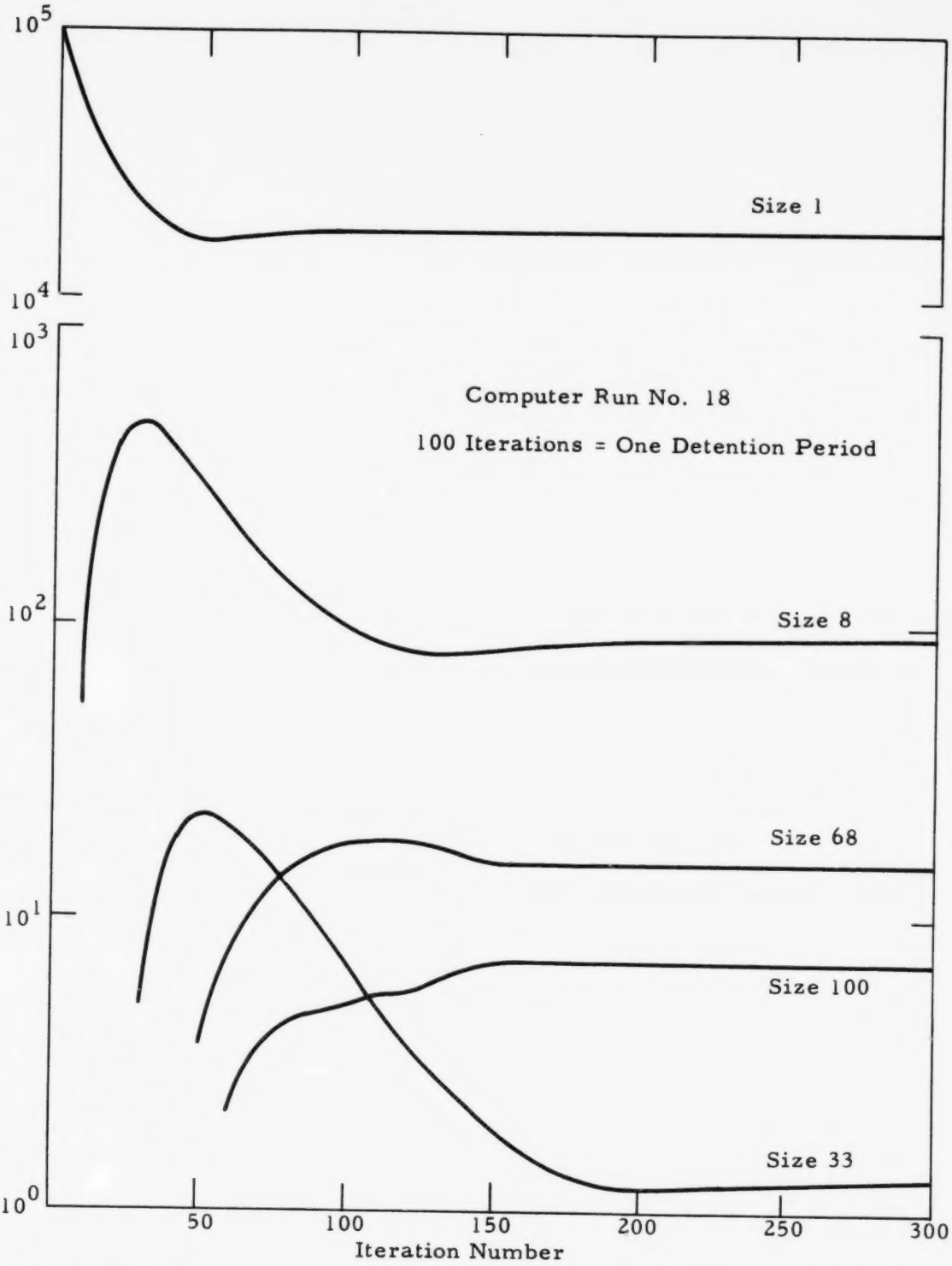

FIGURE 5 -- Relation of Floc Numbers in Selected Sizes to Iteration Number

TABLE III

SUMMARY OF COMPUTER PROGRAM PARAMETERS AND FLOC SIZE DISTRIBUTION FUNCTIONS

Computer Run Number	ALPHA x 10^9	BETA	Initial Reactor Contents and Feed Stream Size Distribution	θ	Position in Reactor Series m	γ	δ	Total Number of Flocs	Number of Size 1 Flocs	n_o/n_t	n_o/n_1	$\frac{1}{m}\sqrt{n_o/n_t}$	$\frac{1}{m}\sqrt{n_o/n_1}$	δ'_m [a]
10	11.25	0.01	10^5 Size 1	0.225	1	3.48	5.68	56,295	44,102	1.78	2.27	1.78	2.27	5.64
11	11.25	0.01	Run 10 output	0.225	2	3.04	4.27	33,620	22,610	2.97	4.42	1.73	2.10	4.89
12	11.25	0.01	Run 11 output	0.225	3	2.69	3.40	21,137	12,888	4.73	7.76	1.68	1.98	4.36
13	11.25	0.01	Run 12 output	0.225	4	2.39	2.85	13,889	7,902	7.20	12.66	1.64	1.89	3.96
14	1.00	0.01	10^5 Size 1	0.02	1	3.96	7.68	93,001	87,164	1.08	1.15	1.08	1.15	7.36
15	1.00	0.01	Run 14 output	0.02	2	3.92	7.38	86,550	76,368	1.16	1.31	1.08	1.14	7.20
16	1.00	0.01	Run 15 output	0.02	3	3.89	7.10	80,599	67,236	1.24	1.49	1.07	1.14	7.10
17	1.00	0.01	Run 16 output	0.02	4	3.85	6.83	75,108	59,468	1.33	1.68	1.07	1.14	6.95
18	50.00	0.01	10^5 Size 1	1.00	1	2.63	3.70	28,049	21,473	3.57	4.66	3.57	4.66	3.66
19	50.00	0.01	Run 18 output	1.00	2	1.99	2.41	9,669	6,353	10.34	15.74	3.22	3 97	2 97
20	50.00	0.01	Run 19 output	1.00	3	1.50	1.97	4,023	2,158	24.86	46.34	2.92	3.59	2.59
21	50.00	0.01	Run 20 output	1.00	4	0.96	1.80	2,137	777	46.79	128.70	2.62	3.37	2.37
22	150.00	0.01	10^5 Size 1	3.00	1	2.11	2.65	14,417	11,284	6.94	8.86	6.93	8.86	2.62
23	150.00	0.01	Run 22 output	3.00	2	1.34	1.80	3,156	1,783	31.69	56.09	5.61	7.49	2.16

[a] $\delta'_m = \frac{1}{\theta}\left[(n_o/n_1)^{1/m} - 1\right]$

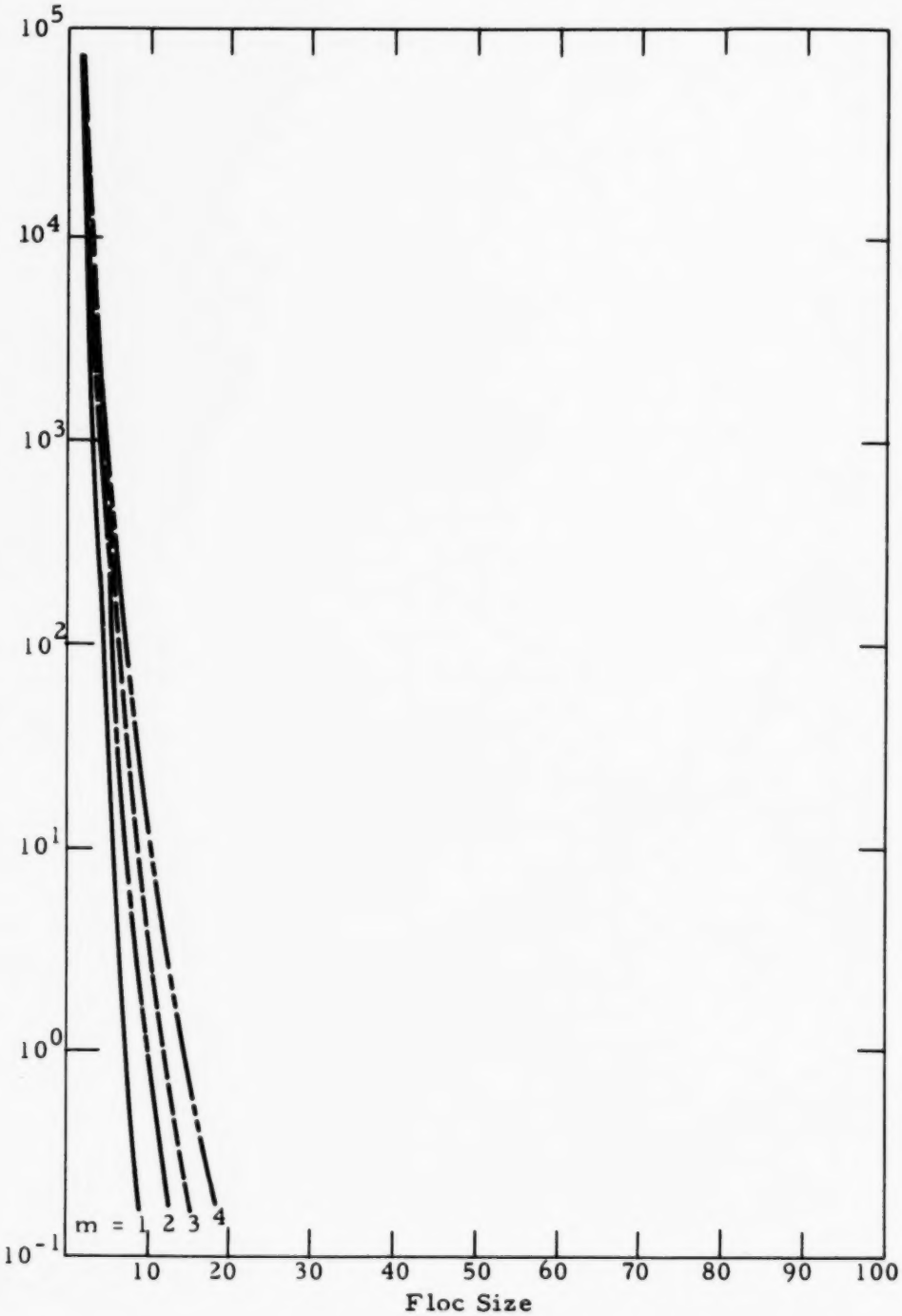

FIGURE 6 -- Floc Size Distributions for $\theta = 0.02$

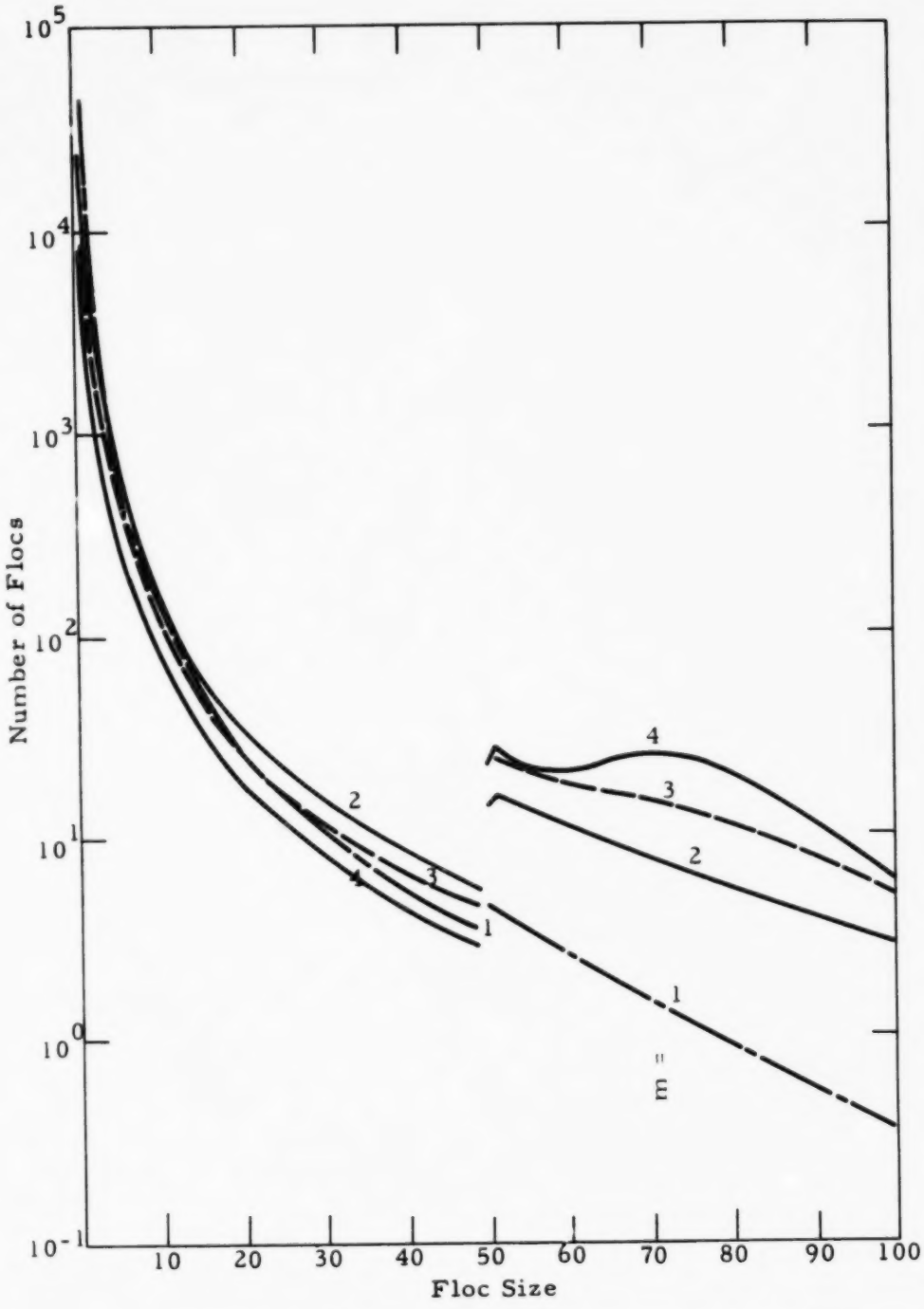

FIGURE 7 -- Floc Size Distributions for $\theta = 0.225$

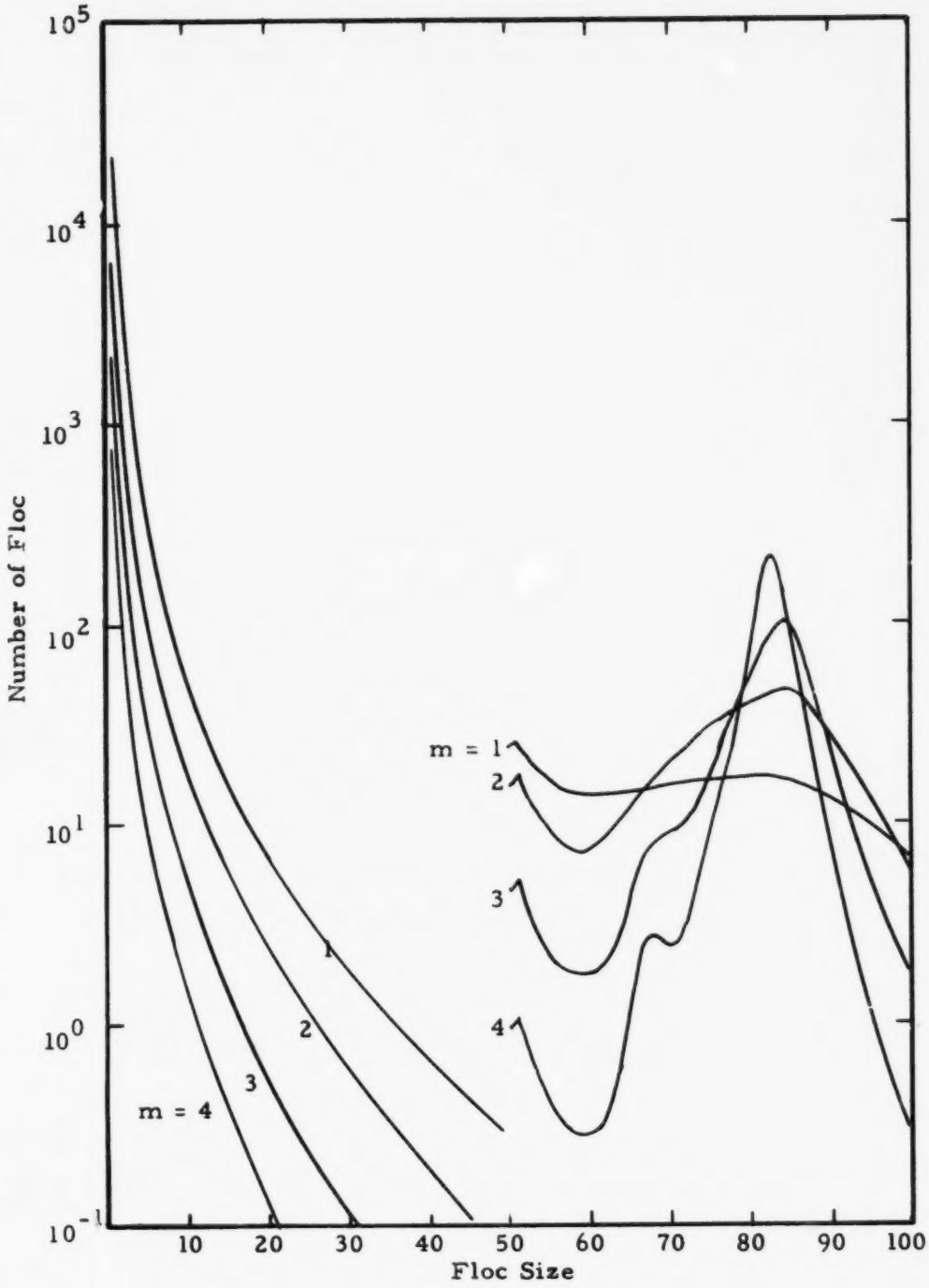

FIGURE 8 --Floc Size Distributions for $\theta = 1.00$

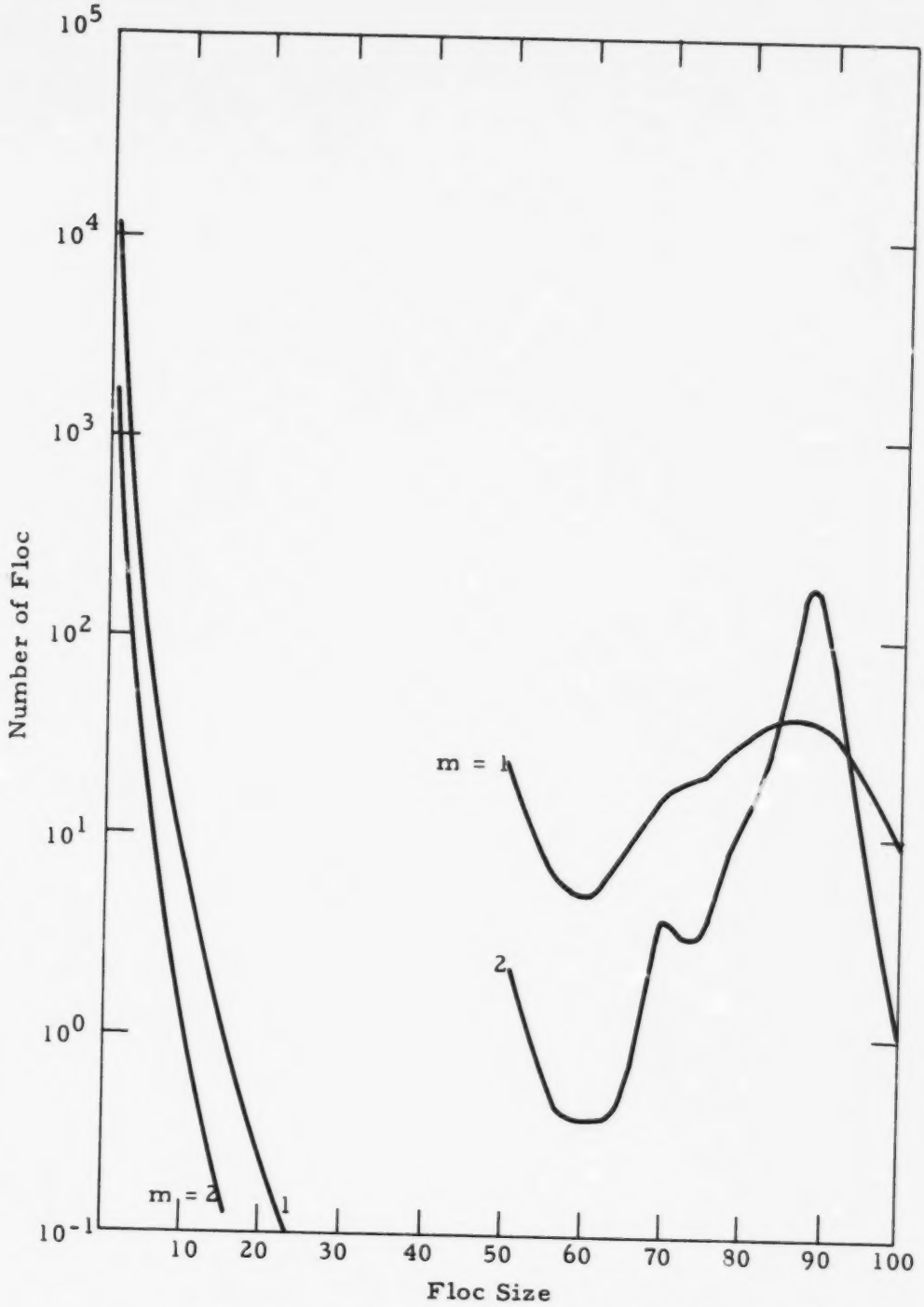

FIGURE 9 -- Floc Size Distributions for $\theta = 3.00$

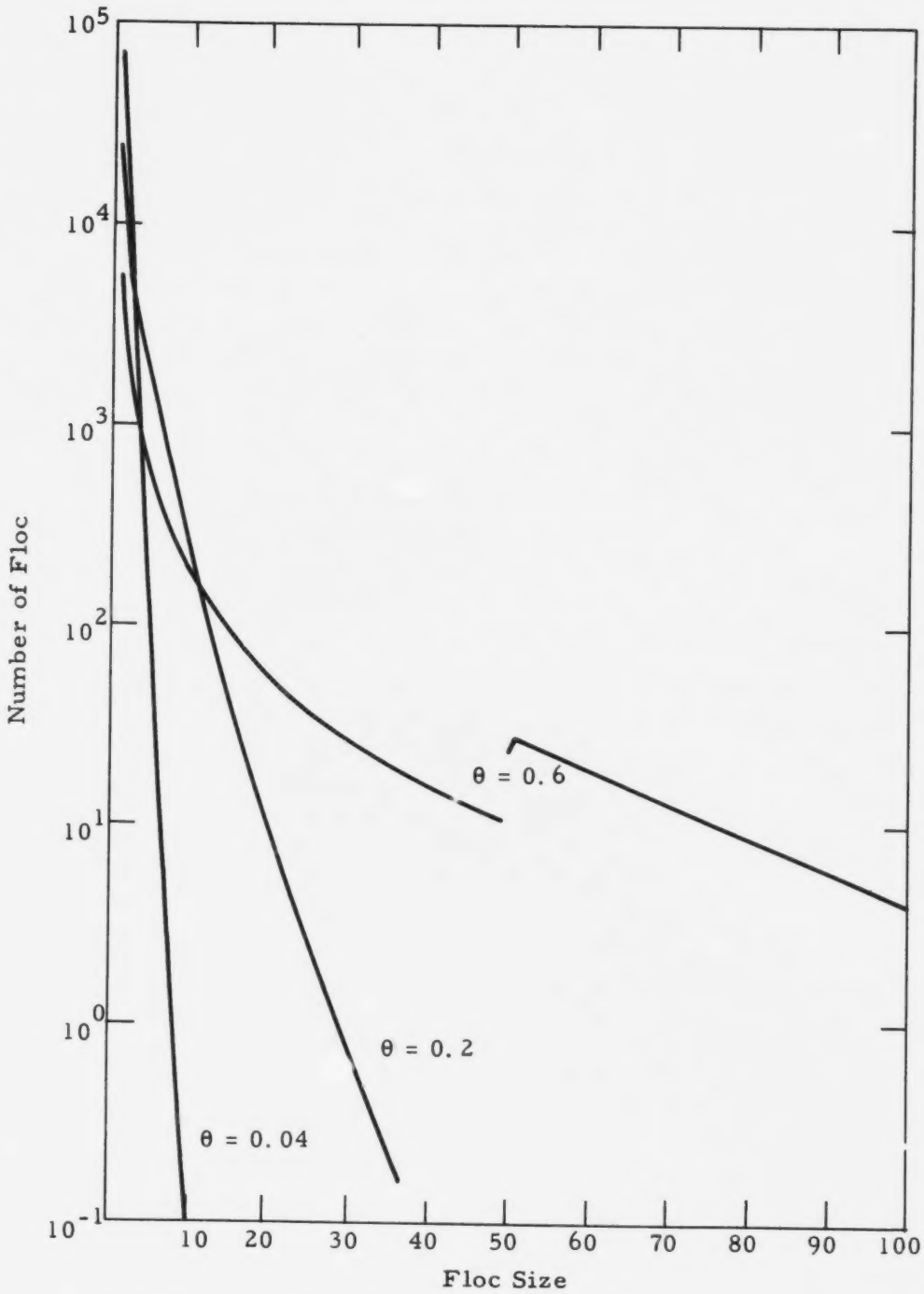

FIGURE 10 -- Floc Size Distributions from a Batch Computer Run

ANALYSIS OF KINETICS OF SIMULATED FLOCCULATION

The changes in total number of flocs and number of primary flocs are shown in Figures 11, 12, and 13 (cf. Equations 37 and 74). Also shown in each figure is the theoretical initial slope (γ or δ for a monodispersed system). It may be noted that the computed curves have the theoretical initial slope. The slope at any point is equal to the γ or δ function of the size distribution then existing. Except for low values of θ in reactor 1, the computed change in number deviates markedly from the change which would be predicted using a constant value of γ or δ equal to the theoretical maximum. That the decrease in rate increases progressively through a series of reactors is indicated by the decreasing magnitude of $(n_o/n_1)^{1/m}$ with increasing m (for a given value of θ, cf. Figure 12). However, despite this reduction in rate, the total reduction as indicated by the value of n_o/n_1 increases with m for a constant <u>total</u> θ. As an example, for a <u>total</u> θ of 3.00 divided equally among m reactors, Figure 12 indicates:

m	θ	$(n_o/n_1)^{1/m}$	n_o/n_1
1	3.0	8.86	8.86
2	1.5	5.02	25.2
3	1.0	3.60	46.3
4	0.75	2.96	76.8

Increasing from one reaction chamber or to two nearly triples the reduction in concentration of n_1 particles.

The form of a rate equation indicated by these figures is ($\alpha = 1$)

$$(n_o/n_1)_m = \left(1 + \frac{\alpha \delta'_m a^3}{\pi} \frac{du}{dz} \phi \frac{T}{m}\right)^m \qquad (60)$$

$$= (1 + \delta'_m \theta)^m .$$

Values of δ'_m can be calculated since all other terms can be evaluated from the computer results. In a similar manner individual values of δ and γ can be calculated.

Figures 14, 15, and 16 present the relationship between the effluent γ, δ, and δ'_m functions and the relative number of total or size 1 flocs. The relationship may be characterized as a family of somewhat similar curves having a common origin at $n_o/n_1 = 1$. The magnitude of the functions at $n_o/n_1 = 1$ are the theoretically deduced values. For a given value of n_o/n_1, δ or δ'_m increases in magnitude progressively with the position of a reactor in a series up to the value for the batch process (which might also be the limiting case

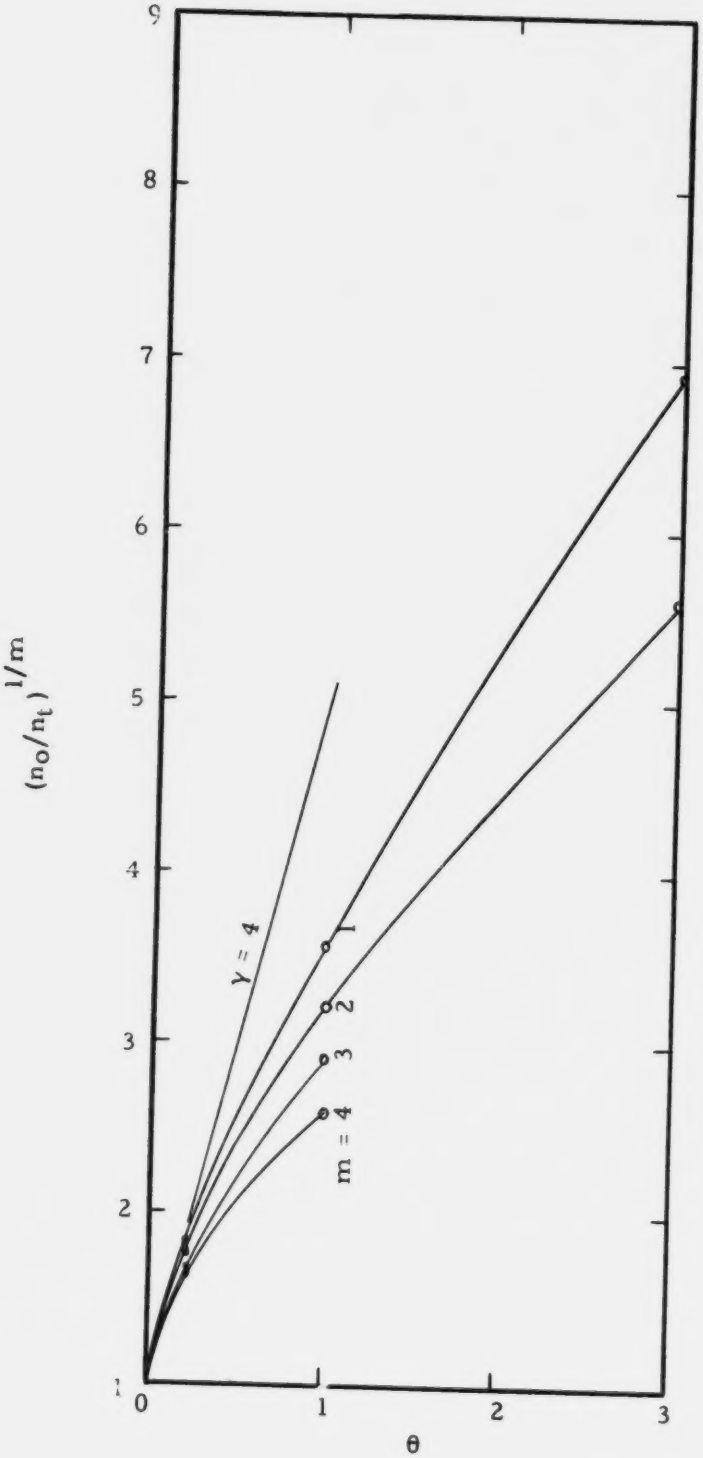

FIGURE 11 -- Computed Change in Total Number of Flocs in a Series of Continuous Stirred-Tank Reactors

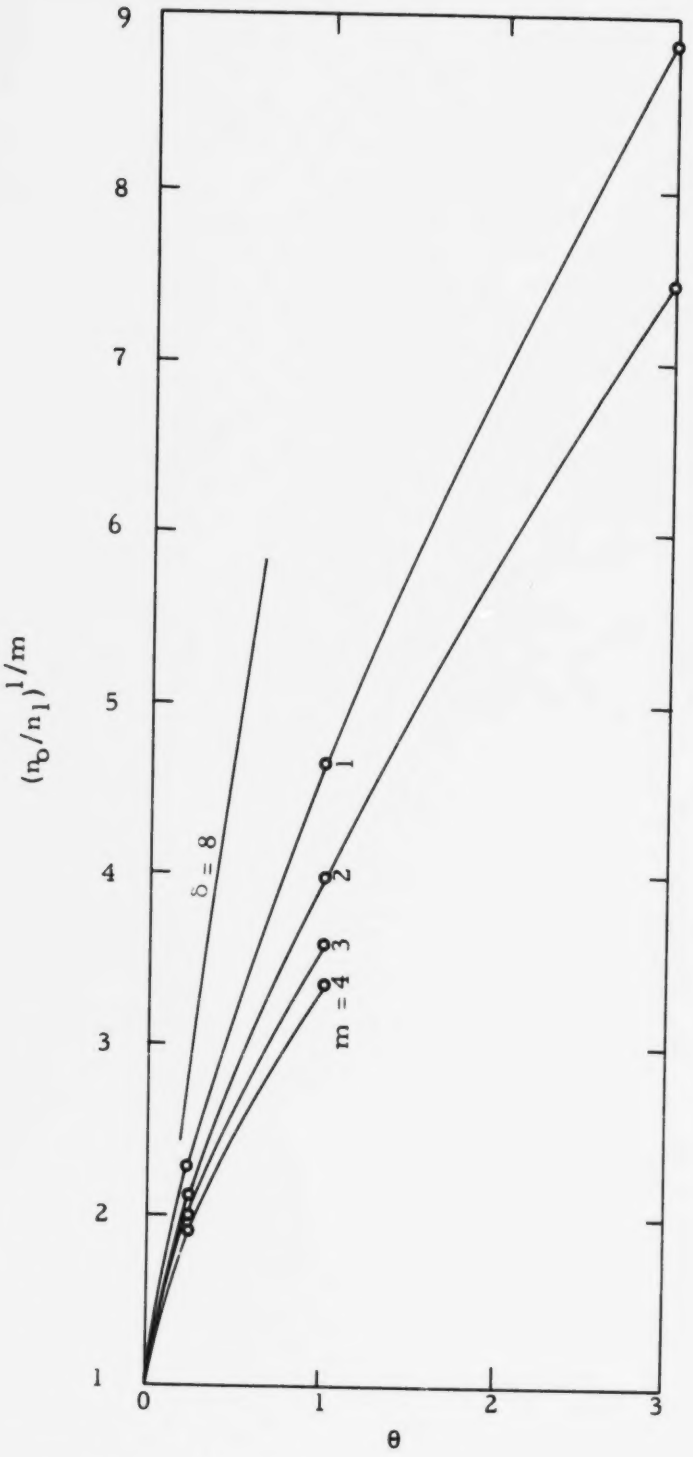

FIGURE 12 -- Computed Change in Number of Size 1 Flocs in a Series of Continuous Stirred-Tank Reactors

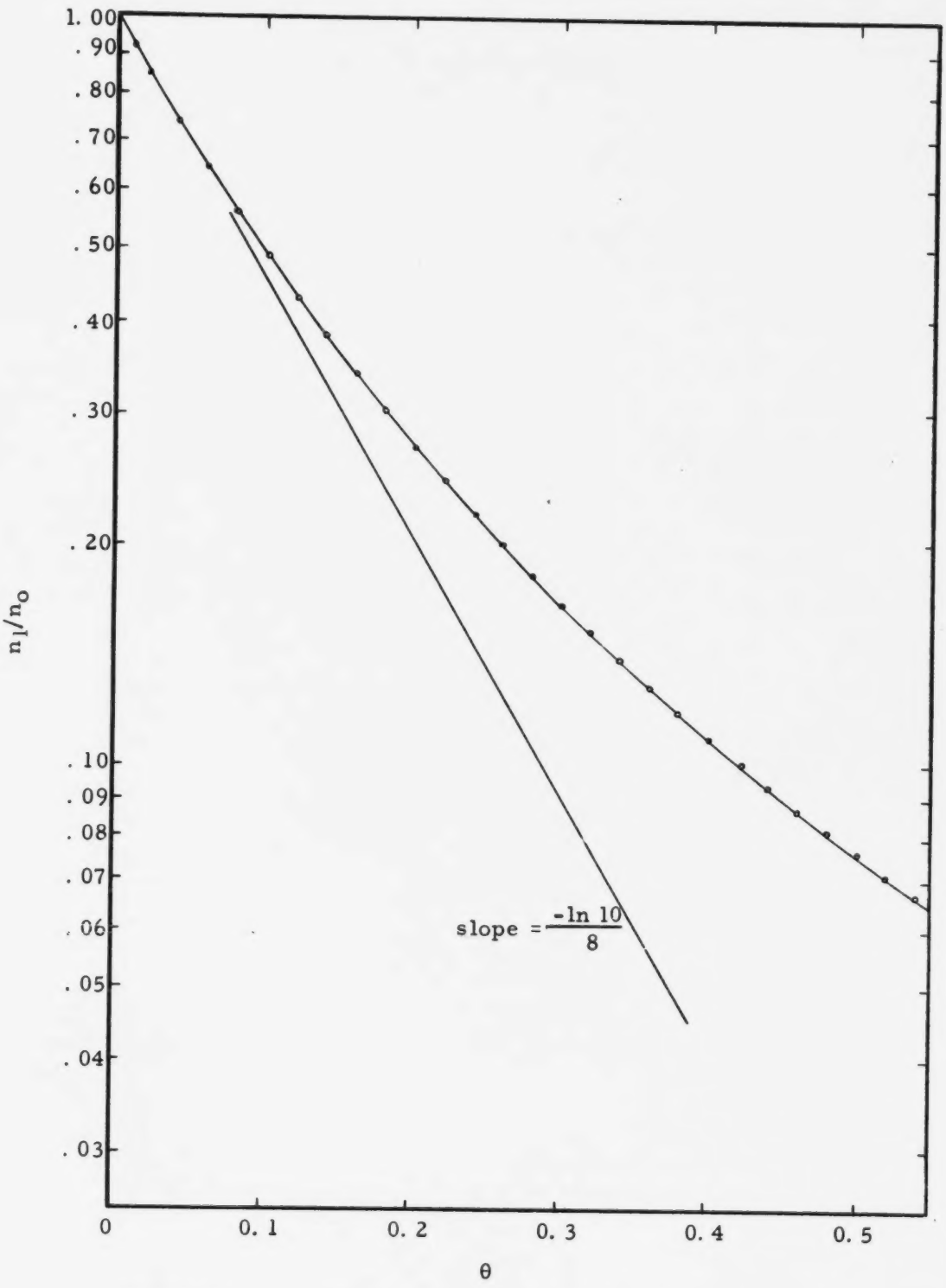

FIGURE 13 -- Computed Change in Number of Size 1 Flocs in a Batch Reactor

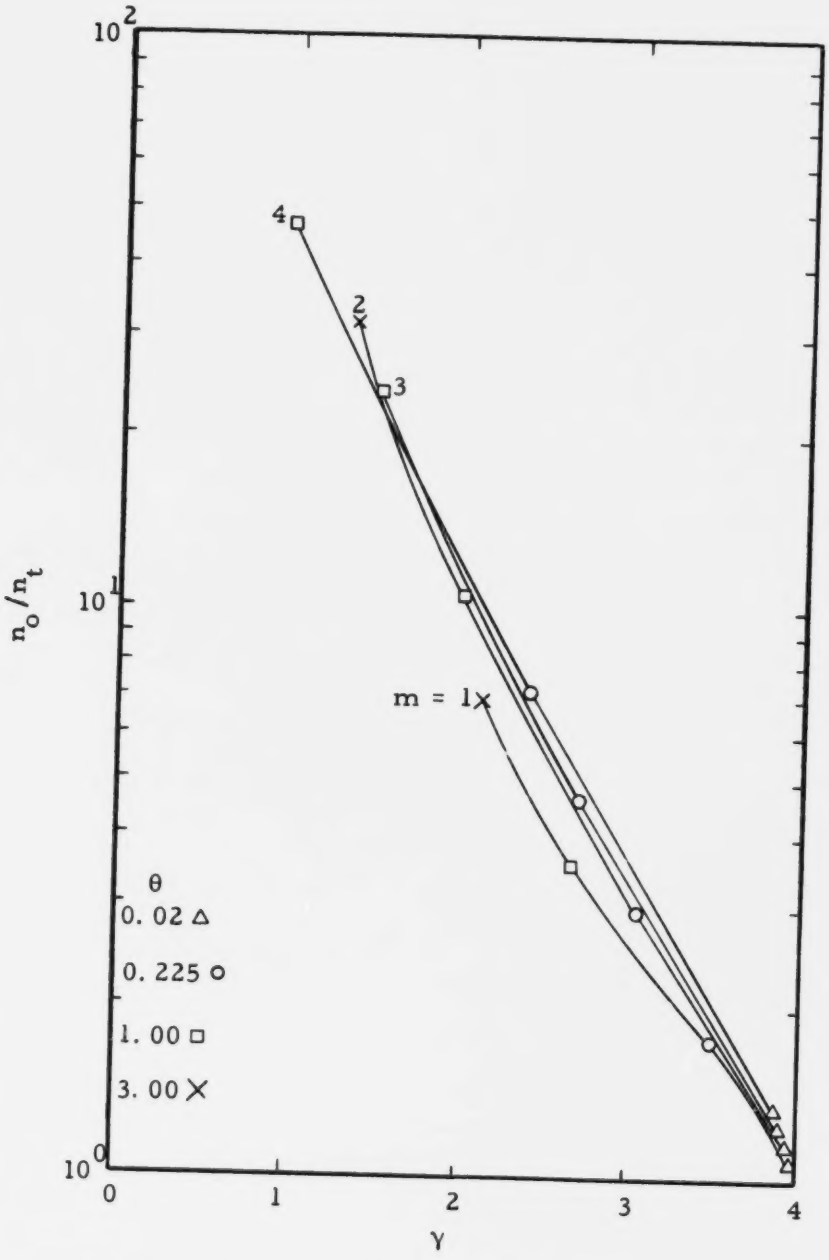

FIGURE 14 -- Relation Between γ Function and the Relative Number of Total Flocs

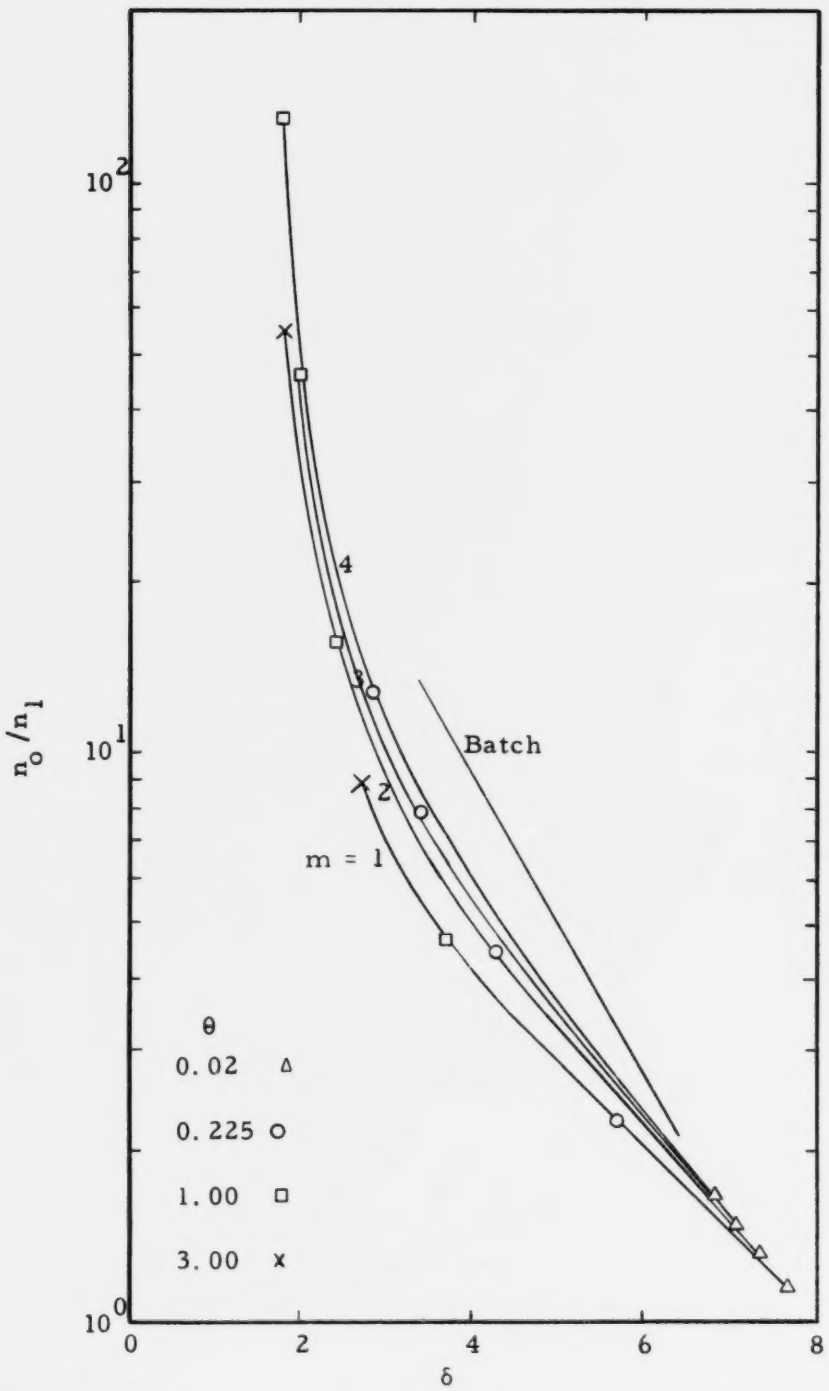

FIGURE 15 -- Relation Between δ Function and the Relative Number of Size 1 Flocs

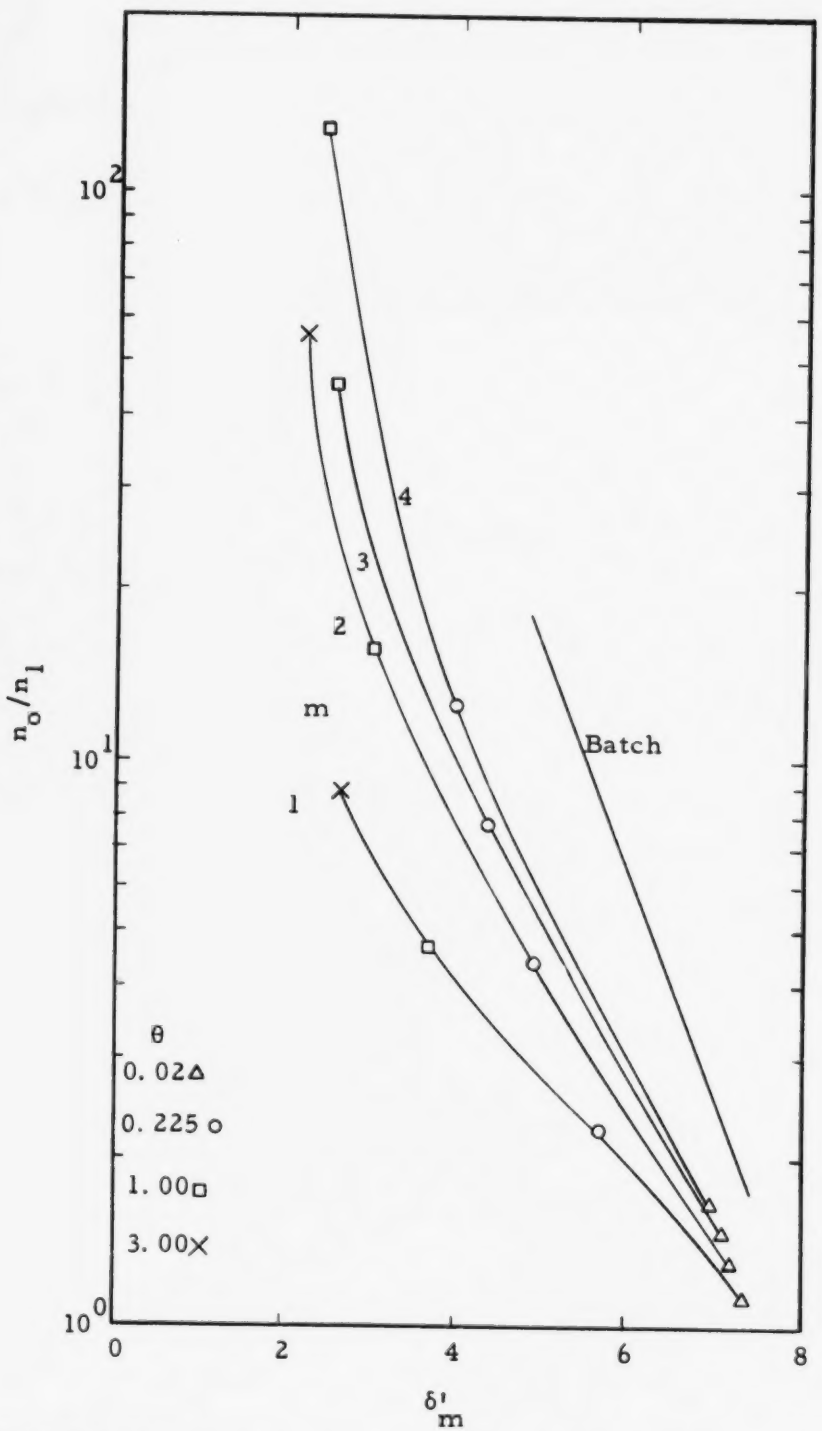

FIGURE 16 -- Relation Between δ'_m Function and the Relative Number of Size 1 Flocs

for an infinite number of reactors in series). Small values are associated with increasing deviation from a monodispersed system. The size distributions from Run No. 11 ($n_o/n_1 = 4.42$, $\delta = 4.27$) and No. 18 ($n_o/n_1 = 4.66$, $\delta = 2.41$) are an example of the difference for approximately equal values of n_o/n_1. The shape of the curves shown in Figures 14 to 16 cannot be assumed to be universal in nature. The value of the function at a given value of n_o/n_t or n_o/n_1 (except $n_o/n_t = 1$, $n_o/n_1 = 1$) would be greatly influenced by the permitted range of particle size and breakup mode. Because the range in size in a real system would be greater than the 100:1 used for computation, smaller values of these functions would be expected.

The validity of the size distribution functions may be readily demonstrated. For example, the value of δ_1 for Run No. 10 may be computed both from the size distribution and from kinetic considerations. As computed from the size distribution (Table III)

$$\delta_1 = 5.68 \ .$$

From the computed change in concentration

$$\delta_1 = \frac{n_o/n_1 - 1}{\theta} \qquad (60a)$$

$$= \frac{10^5/44{,}102 - 1}{0.225}$$

$$= 5.64 \ .$$

The slight difference is attributed to the fact the steady state distribution is only being closely approached.

A second example will be given. For Run No. 11, the value of δ_2' as indicated by kinetic considerations is

$$\delta_2' = \frac{1}{\theta}\left[(n_o/n_1)^{1/m} - 1\right] \qquad (60b)$$

$$= \frac{1}{0.225}\left[(4.42)^{1/2} - 1\right] = 4.89$$

The value of δ_2' as computed from the two appropriate size distributions is

$$\delta_2' = \frac{[(1+\delta_1\,\theta)(1+\delta_2\,\theta)]^{1/2} - 1}{\theta}$$

$$= \frac{[1+(0.225)(5.68)]\,[1+0.225)(4.27)] - 1}{0.225}$$

$$= 4.95 \ .$$

Although agreement between the values of the δ function computed by the two approaches substantiated the analysis leading to the general rate equation and the dependence of kinetics upon size distribution, the absolute validity of the computer results is much in doubt as was borne out in subsequent laboratory experiments. Because of the limit in computer capacity, the maximum size ratio was 100:1, whereas in the real system it is probably more nearly 10^9:1. The restricted spread in the computer analysis results in a greater proportion of small size particles and it is not possible for i to be very much greater than unity (cf. Equation 46). Thus δ, which should range from 8 (as $i \rightarrow 1$) to 1 (as $i \gg 1$) is biased toward the high value region. Moreover, as noted earlier, the breakup function was entirely arbitrary and bears no relationship to reality. However, the computer investigation did demonstrate certain expected characteristics of the rate equation applied to a CSTR and thus did provide a limited validation of that equation.

SUMMARY

The progress of flocculation was simulated using an IBM 7094 computer. Particle size distributions for both batch and continuous reactors were computed by repeated application of the Smoluchowski orthokinetic flocculation equation. A number of initial size distributions and operating parameters were used. It was demonstrated that similar size distributions were obtained for equal products of the operating parameters (θ).

The computed size distributions were characterized by the number of size 1 particles or by the total number of particles. The change in numbers of size 1 particles in a series of continuous reactors was equal to

$$(n_o/n_1) = (1 + \delta_m'\,\theta)^m \ . \qquad (60)$$

Similar values of δ_m' were computed from the particle size distributions and from the values of n_o/n_1 and θ. This agreement demonstrates the dependence of the rate upon the size distribution, as theoretically predicted. A maximum value of δ_m' of 8 was approached for the monodispersed system (n_o/n_1 approaching 1).

V. LABORATORY REACTOR CHARACTERISTICS

The analysis of data obtained from a laboratory or field flocculation unit requires that certain characteristics of the reactor be described. Two of the more important parameters are the distribution of residence time and the energy imparted to the water by the stirring mechanisms. As a preliminary to the conduct of laboratory experiments, the residence time distribution and energy input characteristics of the laboratory reactors were investigated.

THEORY OF RESIDENCE TIME DISTRIBUTION

Analysis of experimental data obtained from a model or the design of a reactor based upon a given rate equation requires knowledge of the residence time distribution within the reactor. Either of two assumptions is usually made:

1. The contents of the reactor are perfectly mixed; the composition of the effluent being identical to the composition at all points within the reactor, or

2. elements of the influent pass through the reactor as a plug unmixed with the contents of other elements.

Although in many cases the type of flow does correspond to one of these flow patterns, in the practical case it frequently does not. It appears unlikely that the types of flocculators used in water purification ever possess these ideal flow patterns.

Some knowledge of residence time characteristics of a reactor can be determined using a tracer added to the influent stream. Although the tracer can be added in a number of ways, the two most common are an instantaneous or slug addition of all of the tracer or a step addition where the concentration in the influent is suddenly changed to a different concentration. Analysis of the effluent time-concentration relationship obtained after either mode of addition can yield the same information about the residence time distribution.

The results of a tracer test made on a continuous flow reactor may be expressed in several ways. In Danckwerts' nomenclature [28] the fraction of tracer which spends less than a given time within the reactor is F. F-diagrams for plug and perfectly mixed flow systems are shown in Figure 17. Also shown is a C-diagram which is the first derivative of the F-diagram. The F-diagram is obtained directly by a step addition of tracer, while the C-diagram, or frequency distribution of residence times, is obtained from a slug or impulse addition. For the perfectly mixed reactor, the equation for the F-function is

$$F = 1 - e^{-t/T} \qquad (75)$$

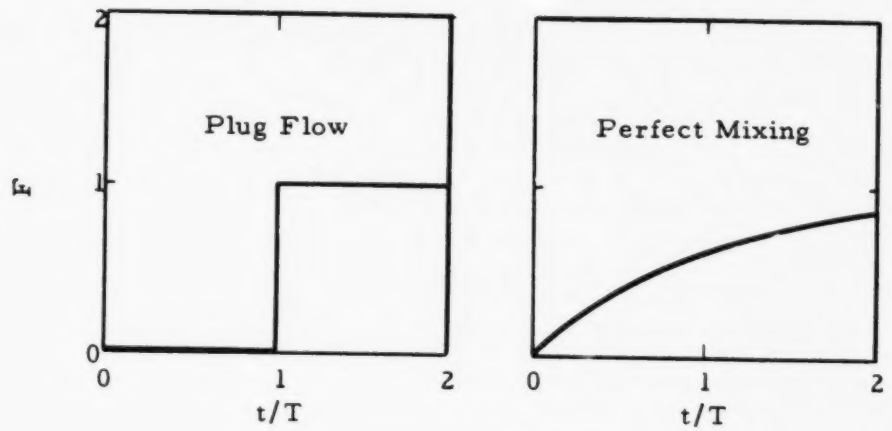

F-DIAGRAMS

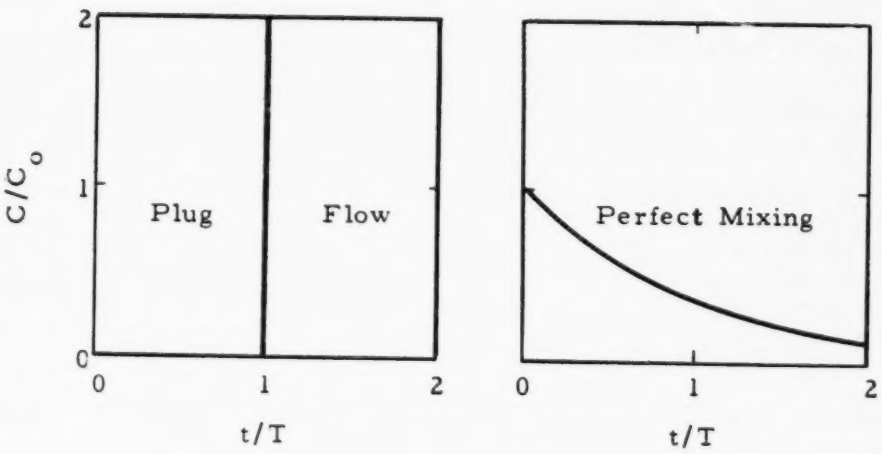

C-DIAGRAMS

FIGURE 17 -- F- and C-Diagrams for Ideal Reactors

for a single reaction chamber, and for m chambers in series

$$F = 1 - e^{-t/T} \left[\sum_{i=0}^{m-1} \frac{(t/T)^i}{i!} \right] . \qquad (76)$$

A number of models can be used to characterize nonideal flow patterns. Some models are more useful when the flow approaches ideal plug flow, while others are more useful in characterizing diviations from perfect mixing. Examples of the former type include dispersion models, where an analogy is drawn between mixing and a diffusional process, and tanks-in-series models which assume that the actual reactor can be represented by a series of equal sized perfectly mixed reactors. A summary of these methods is given by Levenspiel [29]. When the flow pattern differs greatly from plug flow and approaches perfect mixing, a mixed model is used. A mixed model is characterized by flow through a number of regions in series and parallel. The flow pattern in each region is assumed to be ideal, e.g., perfect mixing.

Wolf and Resnick [30] have developed a mixed model which considers deviations from perfect mixing caused by plug flow, dead space, partial short circuiting, error in residence time, and lag in system response. Based upon analysis of the residence time distribution data collected by a number of investigators, they observed that the F-functions could be represented as straight lines by plotting $\ln(1 - F)$ vs. t/T. These straight lines, however, normally possessed slopes different from -1 and did not pass through the origin, as would be obtained if there had been perfect mixing. The data may be expressed in the form

$$F(t) = 1 - e^{-\frac{\eta(t - \epsilon)}{T}}$$
$$F(t) \geq 0 \qquad (77)$$

where T is the average residence time. The term η is a measure of the efficiency of mixing, having a value of unity for perfect mixing and approaching infinity for plug flow. Dead space, short circuiting, and error in average residence time also influence the value of η. The term ϵ is a measure of phase shift in the system. ϵ/T is greater than zero for plug flow or system lag and negative in cases of short circuiting. Wolf and Resnick present the following table:

Values of η and ϵ/T for Several Models

Model	η	ϵ/T
Perfect mixing	1	0
Perfect mixing with plug flow	>1	>0
Perfect mixing with dead space	>1	0
Perfect mixing with short circuiting	<1	<0
Perfect mixing with error in T	$\gtrless 1$	0
Perfect mixing with systems lag	1	>0

Two facts must be recognized. First, although a theoretical model may depict or conform to experimental data reasonably well, it may not represent the physical situation within the reactor. Expecially with mixed models, several combinations of parameters may yield similar F-functions. Second, from a given tracer output curve, the conversion within the reactor can be predicted only for a first order (linear) reaction. For nonlinear rate equations the tracer information alone is insufficient. The accuracy of analysis is related to the precision with which the actual flow through the reactor can be described.

LABORATORY REACTOR

The investigation of orthokinetic flocculation kinetics was conducted using the reactors shown in Figures 18 and 19. The system was designed to operate as a series of four continuous stirred-tank reactors. The water supply system and variable-speed paddles were designed to permit operation over the range of paremeters used in water purification practice.

The reactors were constructed from acrylic plastic cylinders of inside diameter of 13-7/16 inches. Intermediate baffle plates 23 inches above the bottom of each cylinder divided them into an upper and lower reactor. A center hole and an annular space permitted flow between reactors. All experimental data reported herein were obtained with the baffle plates in place; however, the plates could be removed if it was desired to use only two large reactors in series. During operation the depth of water was such that the volume in the upper reactor was equal to that in the lower (13.90 gallons each). Sampling taps permitted withdrawal at several depths. Stainless steel stirring paddles were mounted on a vertical steel shaft coaxial with the reactor cylinder. A variable-speed motor connected directly to the top of the shaft drove the paddle system at any desired rate. Raising the motor permitted a torquemeter to be installed between the motor and shaft. Four stainless steel stators were mounted on the reactor top plate and on the reactor bottom plate, while eight stators were mounted on each baffle plate.

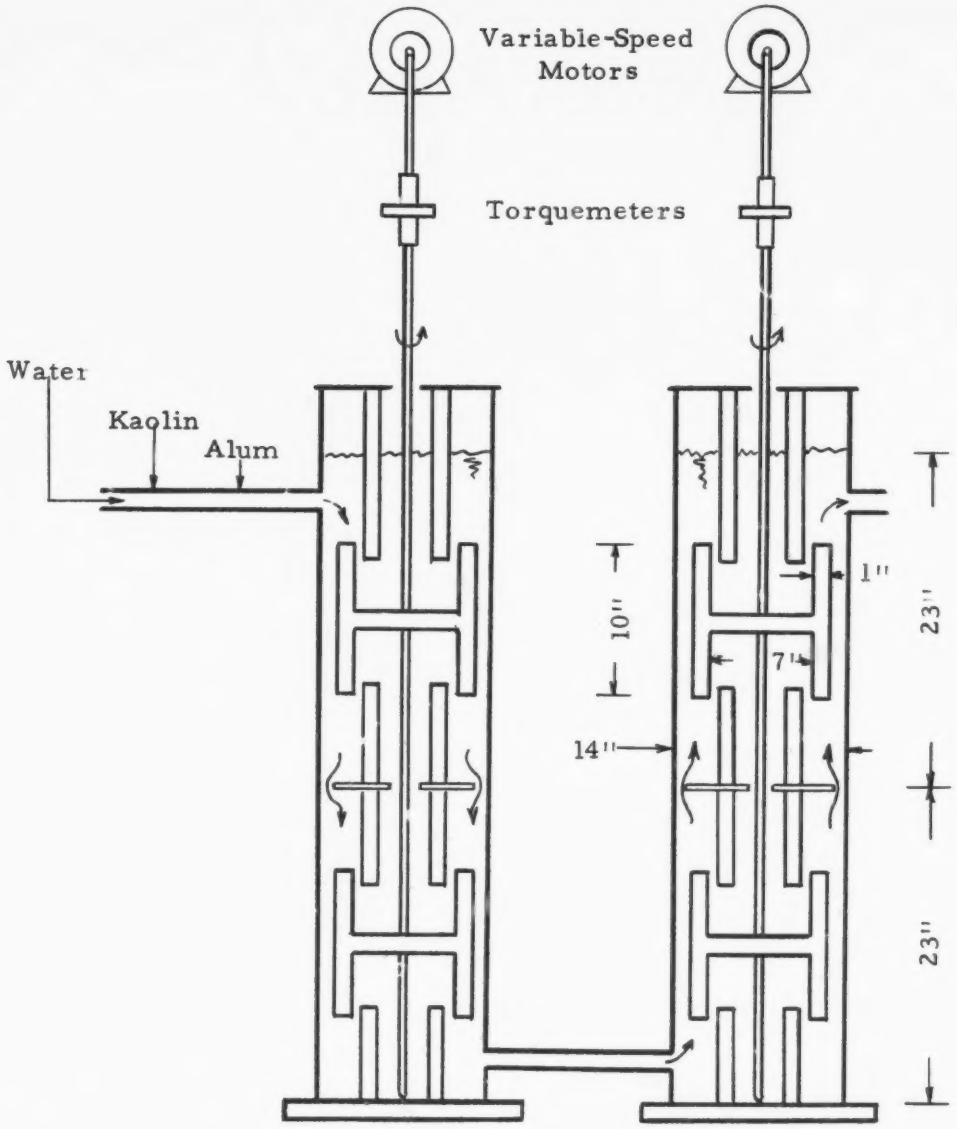

FIGURE 18 -- Flocculation Reactors

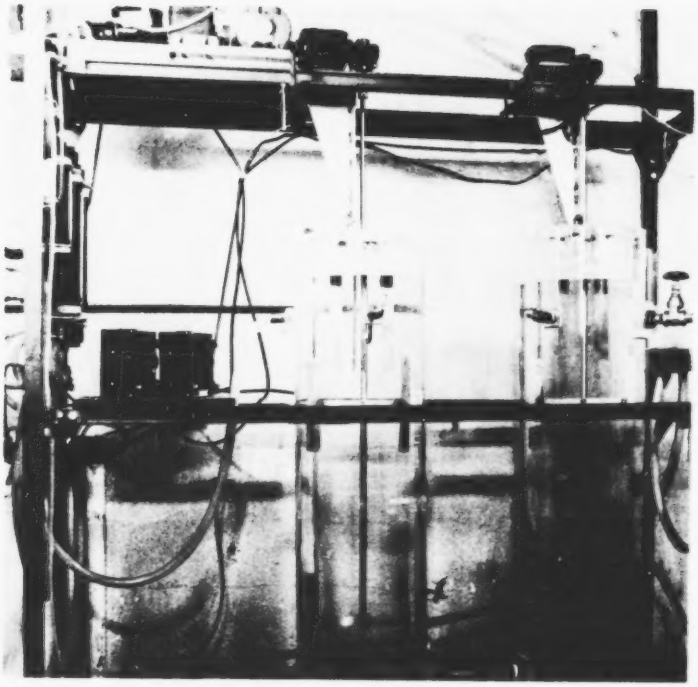

FIGURE 19 -- Laboratory Reactors

The flow of water, kaolin suspension and alum solution to the reactors was measured with Fischer and Porter Flowrators. The pressure of the water supply was maintained constant by an overflow weir, as was the water level in the reactors. The kaolin suspension and alum solution were fed by gravity from elevated storage tanks, the kaolin stock suspension being continuously agitated to maintain its uniformity. The incoming water was first mixed with the kaolin suspension and then with the alum coagulant. About 2 to 5 seconds were required for the mixture to pass through the connecting piping to the first reactor, depending upon the flow rate.

The water used in these experiments was the Mokelumne River supply of the East Bay Municipal Utility District. Treatment of the raw water included the addition of lime and chlorine and rapid sand filtration without coagulation and flocculation. The results of chemical analyses by EBMUD are shown in Appendix C.

RESIDENCE TIME DISTRIBUTION

A series of tracer tests was made to determine the residence time distribution characteristics of the reactors (the center baffle plates being in place). The tracer used was Pontacyl Brilliant Pink B. Tracer concentrations were determined with a G. K. Turner Associates Model III Fluorometer, using the procedures of Feuerstein and Selleck [31].

The first tests investigated the residence time distribution of a single upper reactor. With the stirrer turning, tap water with a constant concentration of tracer was supplied to the first reactor and wasted from the second. When steady state conditions were reached, the supply of tracer was stopped and, as the tracer was gradually eluted, water samples were collected from the bottom or effluent end of the reactor.

The results of several tracer tests performed on the first reactor are shown on Figures 20 and 22. For retention periods of 229 and 463 seconds, duplicate tracer tests were made at 15 and 35 rpm. Single runs were made at 15, 25, and 35 rpm for the 901-second retention period.

The results of these experiments (Figure 20) can be interpreted as indicating perfect mixing following a lag in response of about 23 seconds. At the longer retention period of 463 seconds (Figure 21), perfect mixing was approached at 15 rpm while a slight deviation is noted at 35 rpm. Again a brief delay in response is noted. At the longest retention period (Figure 22), only the data obtained at 15 rpm indicate an approach to perfect mixing. At higher paddle speeds there was a marked divergence from perfect mixing. It appears that under conditions of high energy input by stirring and low head loss between the first and second reactors (resulting from low hydraulic throughput), there is significant transfer of tracer from the second reactor back into the first. As stirring speed increases this transfer becomes more

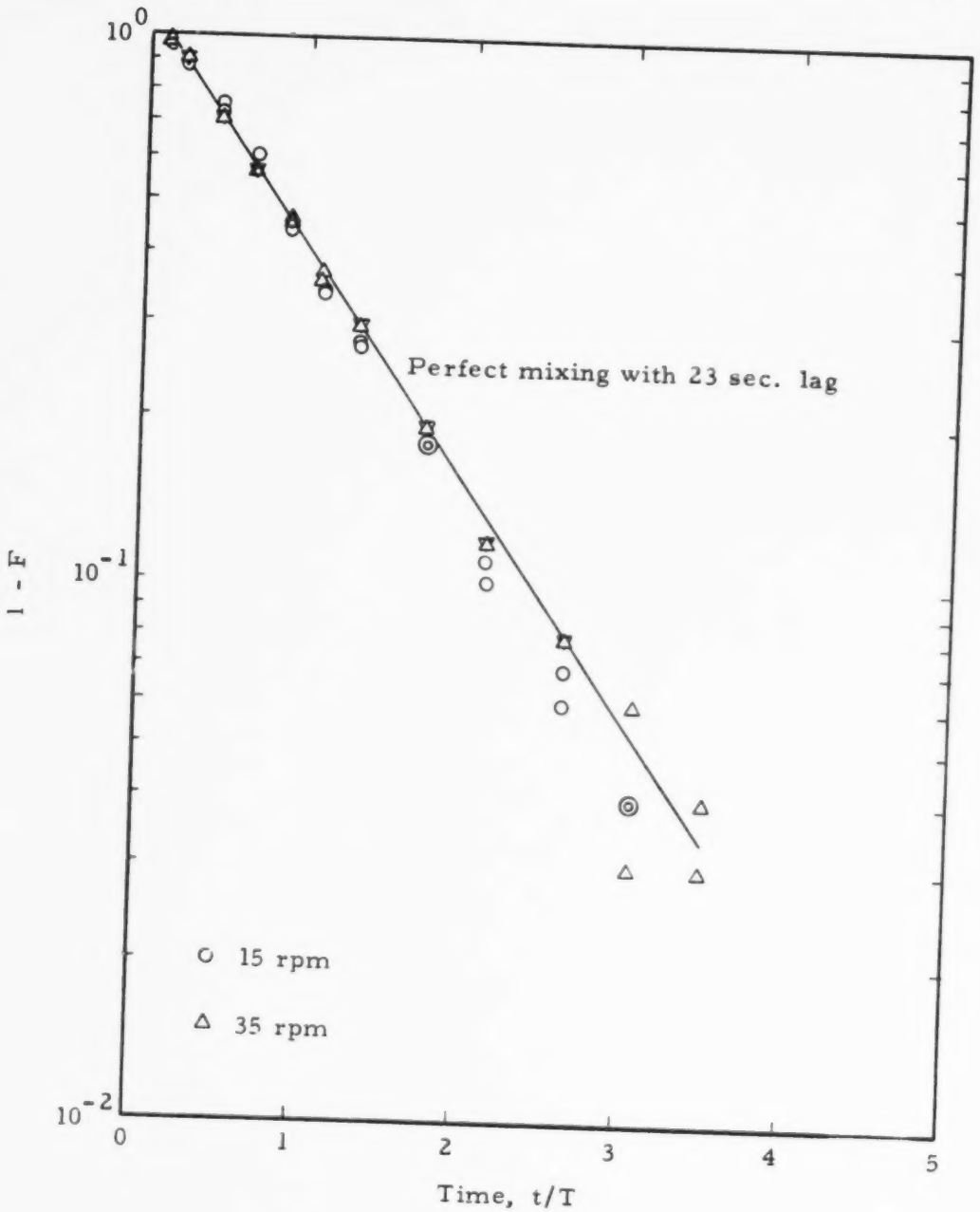

FIGURE 20 -- Residence Time Function for a Single Reactor With 229-Second Retention Period

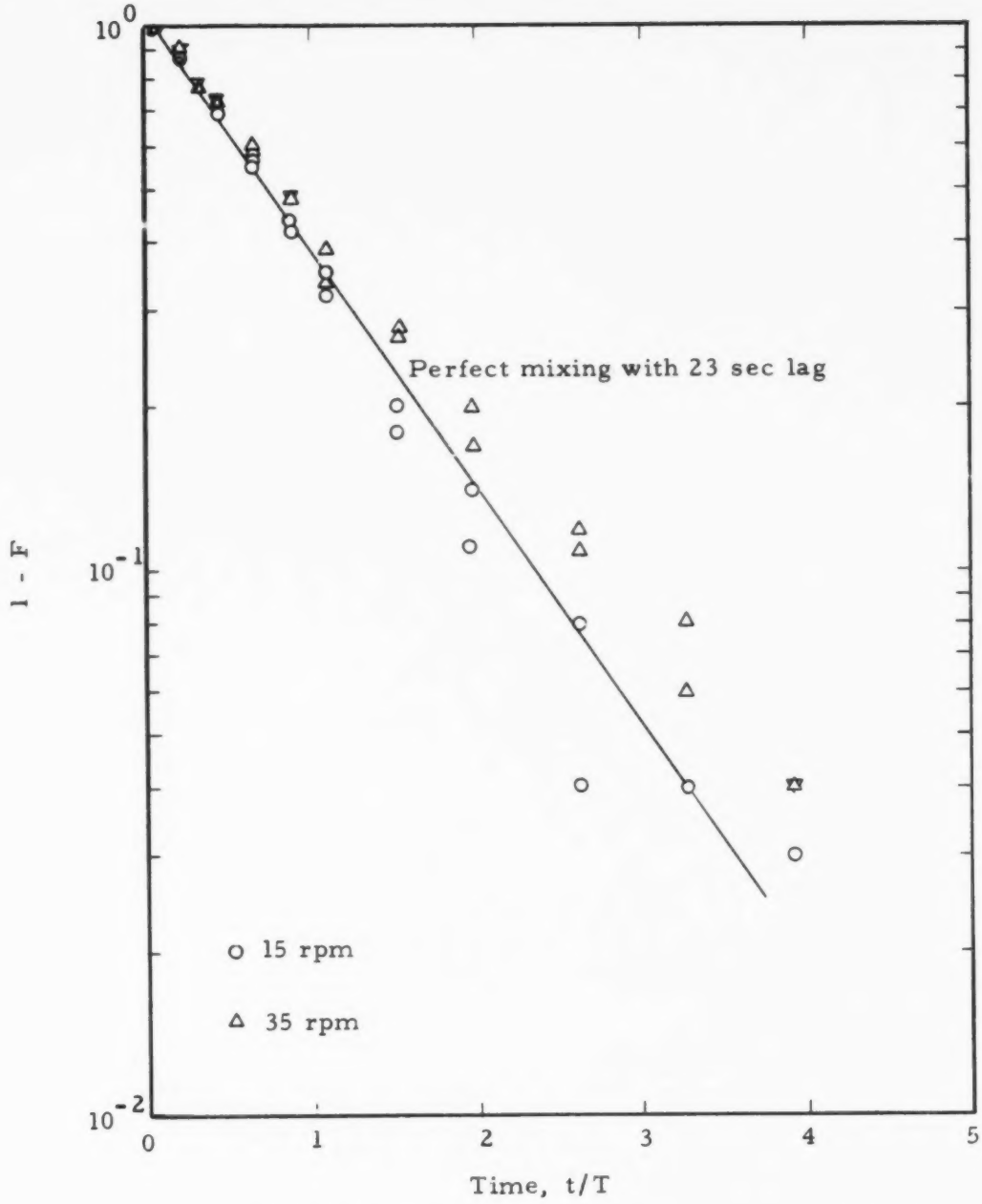

FIGURE 21 -- Residence Time Function for a Single Reactor With 463-Second Retention Period

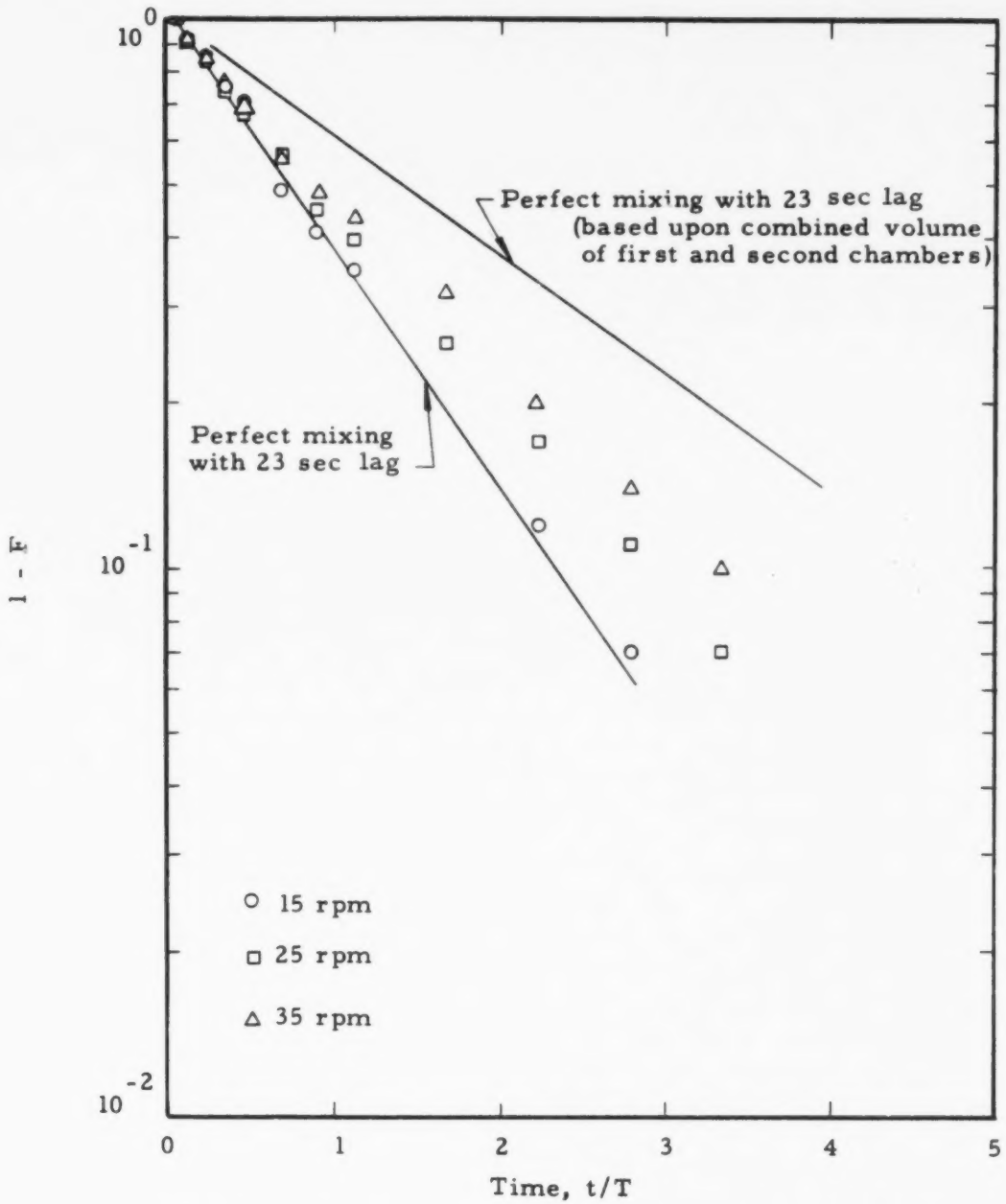

FIGURE 22 -- Residence Time Function for a Single Reactor With 901-Second Retention Period

pronounced until presumably at very high speeds the experimental results would indicate perfect mixing through the volume of both the upper and lower reactors.

The results of these experiments indicate a lag in response of about 23 seconds, assuming ideal mixing thereafter. The sources of this apparent lag are at least two-fold. First, the construction of the tracer feed system was such that a small amount of tracer could diffuse from the supply tube into the water system after the control valve was closed. Thus there was a slight amount of tracer added for a short period after time zero. Second, visual observation of tracer movement in the reaction chamber indicated that several seconds were required for the first traces of dye to be transported from the inlet through the reactor to the outlet.

Different sampling points in the first reactor were used for the tracer tests and for the flocculation-sedimentation experiments. In both cases, flow entered at the top and left at the bottom. Samples for tracer analysis were collected at the bottom of the chamber and samples for floc analysis were pipetted from 4 inches below the water surface. To the extent that perfect mixing is not attained, a difference in residence time distributions for these two points would be anticipated. For perfect mixing the distributions would be similar.

Figure 23 presents the results of tracer tests performed on two reactors in series for retention periods of 229, 463, and 901 seconds per reactor. The time scale has been adjusted to reflect a lag in response of 23 seconds. Also shown is the theoretical relationship between relative time and concentration for two equal, perfectly mixed reactors in series.

It may be concluded that under most operating conditions the reactors closely approached the condition of perfect mixing. Significant deviation is evident only at a retention period of 901 seconds with the stirrer operating at higher speeds.

ENERGY INPUT

The relationship between paddle rpm and energy dissipated was determined using two Power Instruments, Inc. Model 783C Torquemeters with 0.05 to 1.0 and 1.2 to 25 oz-in. ranges. By raising the stirring motor above its normal operating position and remounting it on a temporary spacer, the torquemeter could be installed between the motor and the shaft. Bearing friction was greatly reduced by inserting a Teflon bearing surface under the point of the shaft. To allow a correction for the effect of bearing friction, torque measurements were made with water at the normal operating level and with the reactor empty (but with sufficient water in the bottom to keep the bearing wet). The results of these experiments are shown in Figure 24. The experimental results can be compared with the theoretical relationship developed by Camp (Equation 19). First, the energy input per unit volume is a function of the stirrer rpm cubed, as predicted. Second, a value of k

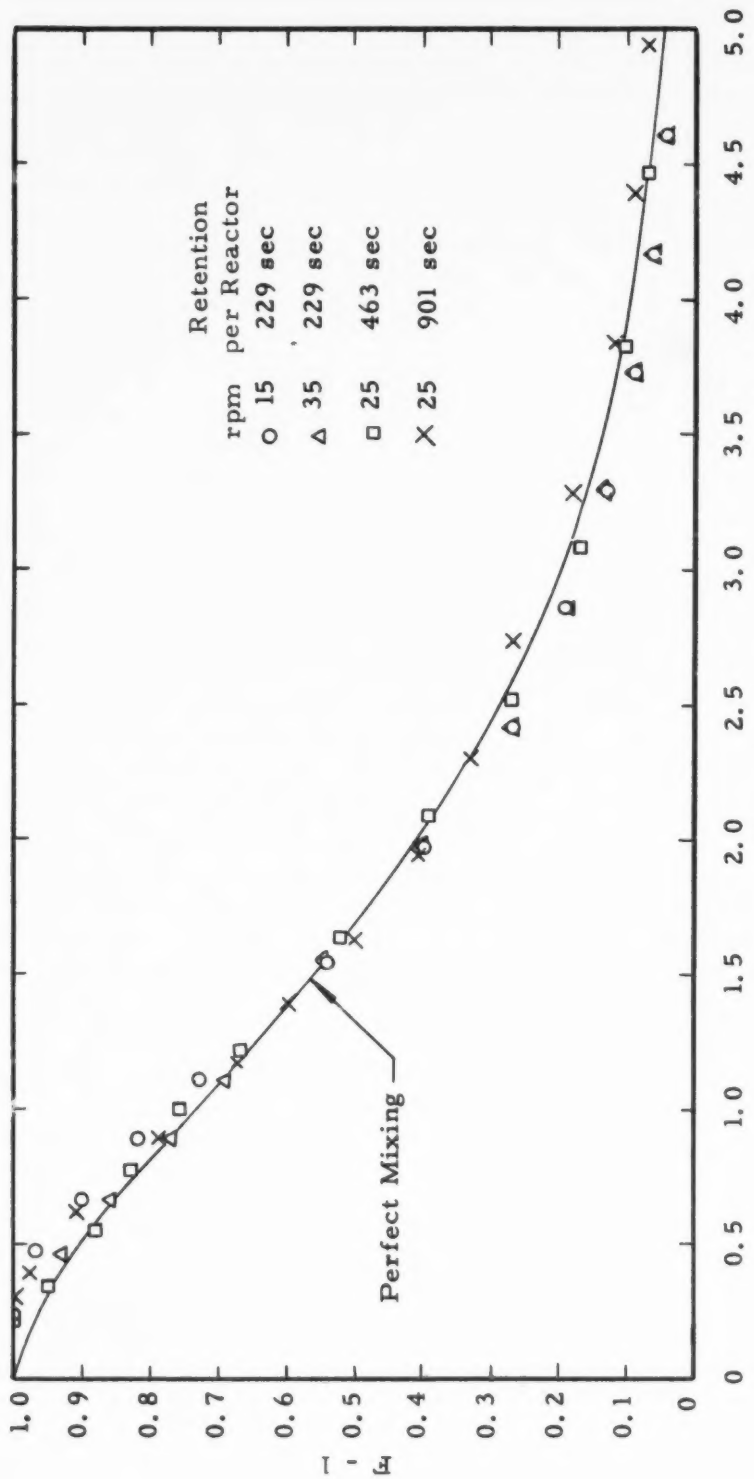

FIGURE 23 -- Residence Time Function for Two Reactors in Series

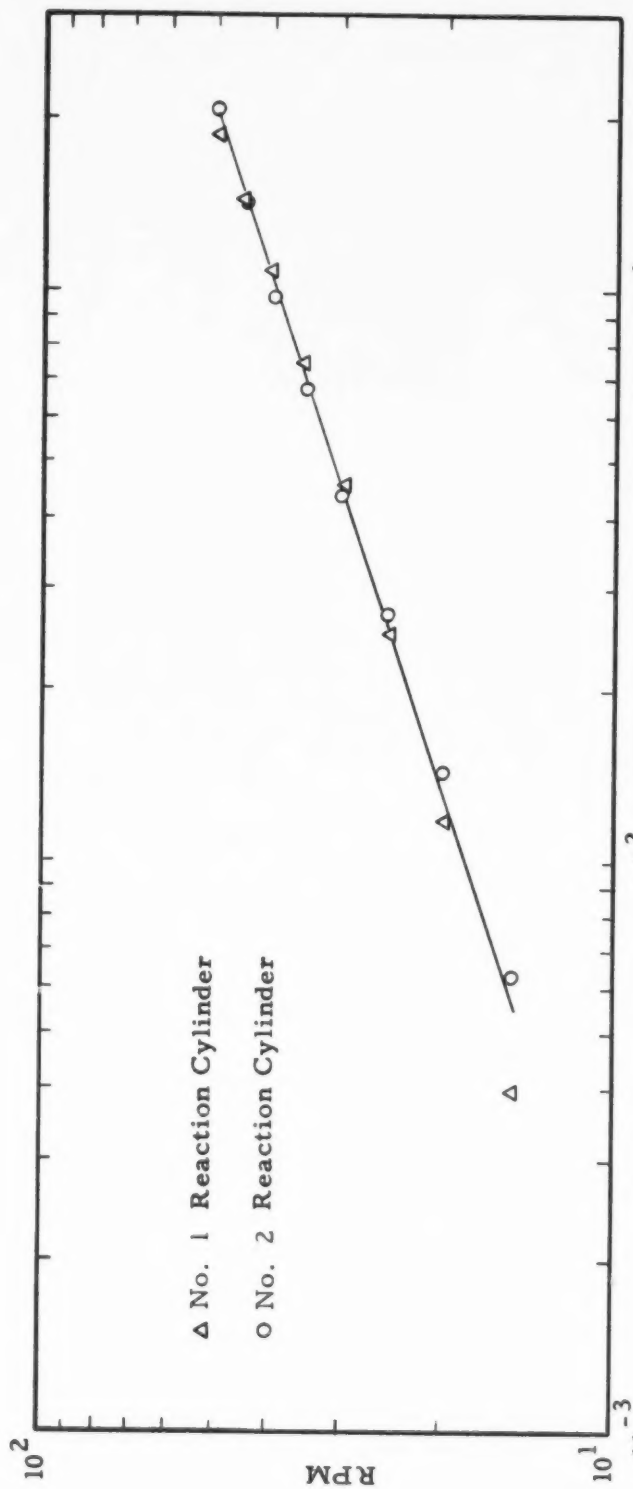

FIGURE 24 -- Energy Imparted by Stirring as a Function of Paddle RPM

can be calculated. For a drag coefficient of 1.9 [32], k was found to be equal to 0.355. Camp [21] observed values of 0.24 to 0.32 at the treatment plant in Cambridge, Mass.

Energy was transmitted to the mass of water in the first reactor both by stirring and by the kinetic energy of the incoming stream. The kinetic energy of the water passing into the third reactor was significant at high flow rates and short retention periods. The kinetic energy of water passing around the baffle plates into the second and fourth reactors could be neglected under all conditions. The computed values are:

Retention Period, sec	W, ft-lb/sec-cu ft	
	1st reactor	3rd reactor
229	0.0159	0.0018
463	0.0019	0.0002
901	0.0003	---

The viscosity of pure water [33] was used for all calculations. This procedure underestimates the viscosity of a suspension and the error may be estimated using the Einstein viscosity equation:

$$\frac{\mu_s}{\mu_o} = 1 + 2.5\phi \qquad (78)$$

where μ_s is the viscosity of the suspension; μ_o, that of the dispersion medium; and ϕ, the volume fraction occupied by hard, spherical particles. As will be shown later, an average value of ϕ for these experiments is about 0.00078.

Then

$$\frac{\mu_s}{\mu_o} = 1 + 2.5(0.00078)$$

$$= 1.00195 .$$

This is an error of about 0.2 per cent, which may be neglected.

VI. LABORATORY INVESTIGATION OF FLOCCULATION KINETICS

A series of equations has been developed to describe the rate of orthokinetic flocculation for an idealized system. The results of computer studies based upon the direct application of the basic Smoluchowski orthokinetic flocculation equation substantiated the form of the derived equations. To determine the usefulness of the equations when applied to a real system, a series of laboratory experiments was undertaken.

Two major considerations dictated the use of a continuous flow system rather than a batch or jar test procedure. First, floc size distributions in a continuous system would approximate the distributions encountered in water purification practice whereas size distributions from batch experiments would be expected to be significantly different. Second, the contents of the continuous flow reactor reach a steady state condition and can be investigated without respect to time of sampling. Since the characteristics of the contents of a batch reactor change continuously, proper sampling must be instantaneous and at a known time relative to the beginning of the experiment.

The experimental system investigated was a compromise between one which might best test the validity of the theoretical equations and one identical to that employed in water purification practice. The former consideration might indicate the use of uniform velocity gradients, perhaps at the expense of a better approach to perfect mixing, or the use of an emulsion rather than a sol so that the idealization of constant, additive volume of the dispersed media would be better approached. On the other hand, greater similarity to the problems encountered in water treatment would be obtained if a mixture of several organic materials were used to create turbidity and color. The experiments performed appear adequate to verify the theoretical equations while determining the characteristics of a system of engineering significance.

RATE EQUATION FOR EXPERIMENTAL RESULTS

Several substitutions may be made in the basic rate equation (Equation 60). The degree of flocculation attained will be based on the mass concentration of primary kaolin particles and small flocs with negligible settling velocity (N_o/N) rather than on the number concentration of size 1 particles (n_c/n_1). The ratio N_o/N will be referred to as the degree of flocculation.

The relationship between floc concentration based upon volume and upon mass may be determined from the densities of floc (ρ_f) and kaolin (ρ_k). Assuming that kaolin and water combine to form a floc on the basis of additive volumes, the volume of floc formed per unit mass of clay is

$$\phi/N = (x - 1/\rho_k)$$

where x is the amount of water associated with a unit mass of clay. Also

$$1 + x = \rho_f(x + 1/\rho_k) \ .$$

Then,

$$\phi/N = \frac{(\rho_k - 1)}{\rho_k(\rho_f - 1)} \ . \tag{79}$$

If N is expressed in mg/l

$$\phi/N = \frac{(\rho_k - 1)}{\rho_k(\rho_f - 1)} \times 10^{-6} \ . \tag{80}$$

The decrease in primary particles in a series of m reactors was shown to be

$$\left(\frac{n_o}{n_1}\right)_m = \left(1 + \frac{\alpha\delta'_m a^3}{\pi} \frac{du}{dz} \phi \frac{T}{m}\right)^m \ . \tag{60}$$

The form of the rate equation to be investigated experimentally is found by substitution

$$\left(\frac{N_o}{N}\right) = (1 + KDGN_o T/m)^m \tag{81}$$

where

$$K = \frac{\alpha a^3}{\pi} \frac{\phi}{N_o} \tag{82}$$

and D is the experimentally determined size distribution function. For a batch reaction

$$\ln N_o/N = KDGN_o T \ . \tag{83}$$

ADDITIONAL COMMENTS ON THE EXPERIMENTAL SYSTEM

Laboratory experiments were conducted in two large cylinders subdivided internally to give a total of four reactors in series. (Cf. Figures 18 and 19.) A general description of the system was given in Chapter V, together with the energy input and residence time distribution characteristics. Comments in this section will deal with the characteristics of the clay-alum system whose flocculation characteristics were studied.

The primary purpose of the research was to measure the rate of flocculation as a function of several physical parameters of the environment in which the reaction occurred. It was desirable therefore to standardize procedures so that the electro-chemical stability of the system would be constant from one run to the next. It was not the intent to describe all aspects of the colloidal system used. The goal of developing a readily reproducible system yielding a dense floc, which appeared to approach a spherical shape, was attained.

After a preliminary investigation, the following standard procedures were adopted. Twenty-four hours before the experiment was conducted, the desired amount of kaolin was weighed and suspended in several liters of distilled water. The suspension was shaken again several times prior to the test. Finally, the suspension was placed in the kaolin stock suspension tank and diluted with tap water to a volume of 25 liters. The concentration of kaolin in the stock suspension was typically 100 times the desired kaolin concentration in the reactor.

The water supply system was flushed for one hour or more immediately before each test period. Prolonged flushing was required for two reasons. First, it was necessary to have water of constant temperature (viscosity) during each test. Second, since the tap water was saturated or supersaturated with gases, any temperature rise which had occurred in the piping within the building resulted in dissolution of gas and excessive floating floc.

Each experiment began with the reactors empty. With the stirrer operating at the desired rpm, tap water with the selected concentrations of kaolin and alum was supplied to the first reaction chamber. To allow adequate time for flocculation to reach steady state, the reactors were operated after filling for a period of time equal to five retention periods, based upon the displacement volume up to the reactor being investigated. After completion of the settling and sampling schedule, the reactor contents were wasted. The reactors were brushed and rinsed prior to the next experiment.

All laboratory experiments were conducted using a suspension of kaolin in tap water, with alum as a coagulant. A single bottle of Baker and Adamson Kaolin Powder was used throughout. The size distribution, as determined by hydrometer analysis, is shown in Figure 25. The exchange capacity was 15.5 me/100 g. Matheson Coleman and Bell aluminum sulfate (technical, iron free) was used as the coagulant. The aluminum content was 7.73 per cent.

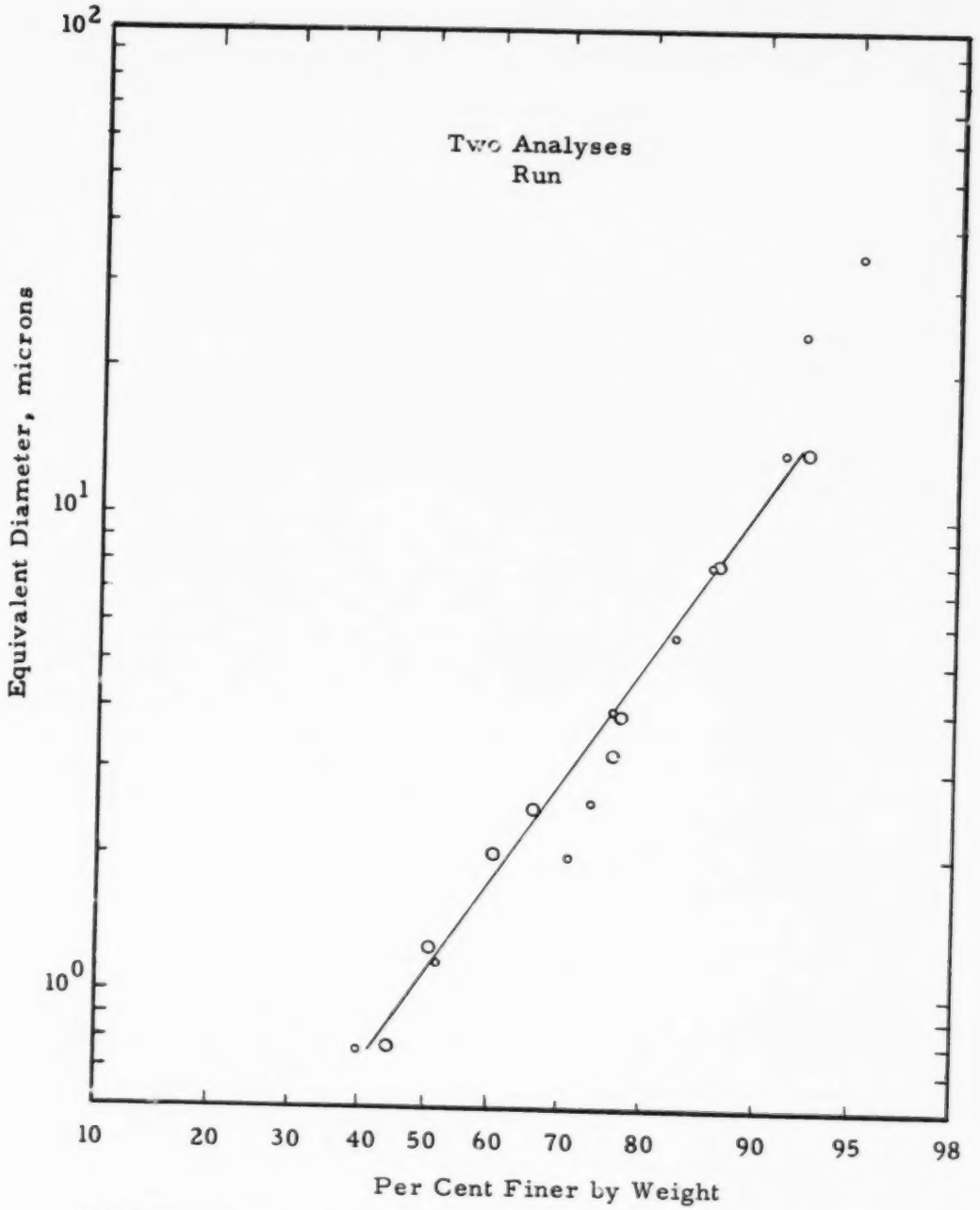

FIGURE 25 -- Kaolin Particle Size Distribution

The transmission characteristics of a suspension of kaolin in distilled water were measured with a Bausch and Lomb Spectronic 20 Colorimeter, using one-inch tubes. Minimum per cent transmission at maximum instrument sensitivity was obtained at a wavelength of 370 millimicrons, as shown in Figure 26. Distilled water was used as the standard. A wavelength of 375 mμ was selected for use, as it would then be possible to compensate for any lessening of instrument sensitivity. Figure 27 presents the results of measurements made with suspensions of kaolin in both distilled and tap water. Beer's Law is followed over the range of concentrations investigated. The 97.5 per cent transmission of tap water relative to distilled water was typical of the tap water during the period in which all tests were made. The relationship between kaolin concentration and turbidity as measured with a Hellige Turbidimeter is shown in Figure 28.

Figure 29 indicates the results of a series of jar tests performed with various concentrations of kaolin in tap water with an alum concentration of 25 mg/l. After 15 minutes of stirring, a representative sample was withdrawn and analyzed with the Spectronic 20 immediately after shaking violently for 5 seconds. Experience indicated that reproducible results were obtained only if the floc was dispersed by violent shaking and this procedure was employed immediately before all analyses. Turbidity in the coagulated sample was caused by the turbidity naturally present in the water and by the alum floc, in addition to the turbidity caused by the kaolin. Turbidity from these additional sources was accounted for by extrapolating the curve in Figure 29 to 100 per cent transmission and considering the intercept as the origin of an "equivalent kaolin concentration" scale. Thus the equivalent kaolin concentration exceeds the actual kaolin concentration by an increment related to the optical properties of the natural turbidity and alum floc. Experimental results are reported on the basis of equivalent kaolin concentrations.

A preliminary series of jar tests was conducted using tap water to which kaolin had been added in various amounts from 10 to 40 mg/l. After a 15-minute stirring period, followed by a 15-minute settling period, supernatant samples were withdrawn for analysis. For the range of kaolin concentrations investigated, an alum dosage of 25 mg/l gave maximum supernatant clarity in all cases (Figure 30). A similar series of experiments was performed on a continuous flow basis using the first reaction chamber (Figure 31). Again the maximum removal of turbidity occurred with 25 mg/l alum. All further experiments were conducted using 25 mg/l of alum.

FLOCCULATION-SEDIMENTATION EXPERIMENTS

Of the several theoretical flocculation equations developed, the equation expressing the rate of decrease in concentration of primary particles when the maximum floc size is limited appears to have the most direct application to water purification practice. This form was selected for experimental investigation. However, as no satisfactory means of determining the concentration of primary particles

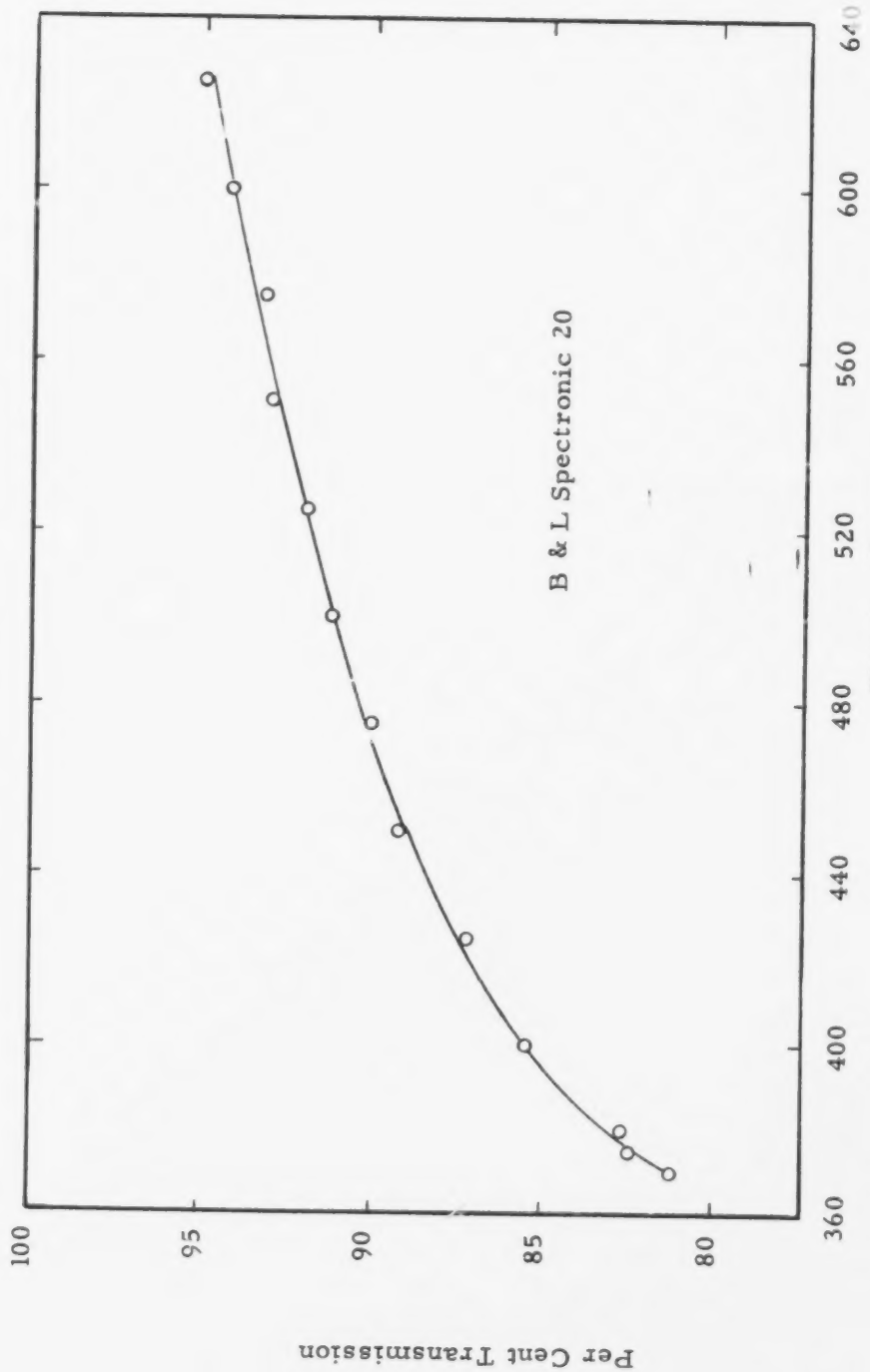

FIGURE 26 -- Transmission Characteristics of a Dilute Suspension of Kaolin in Distilled Water

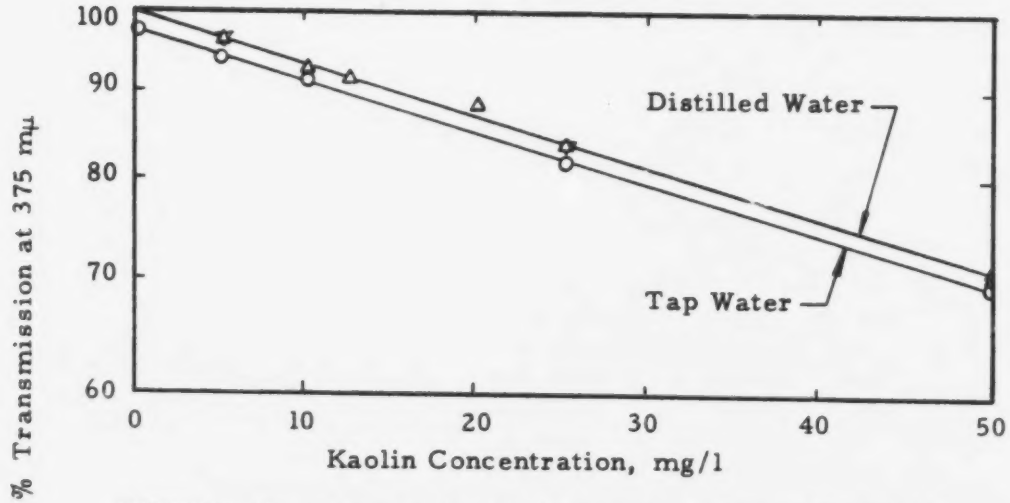

FIGURE 27 -- Transmission Characteristics of Kaolin in Distilled Water and Tap Water as Measured with a Spectronic 20

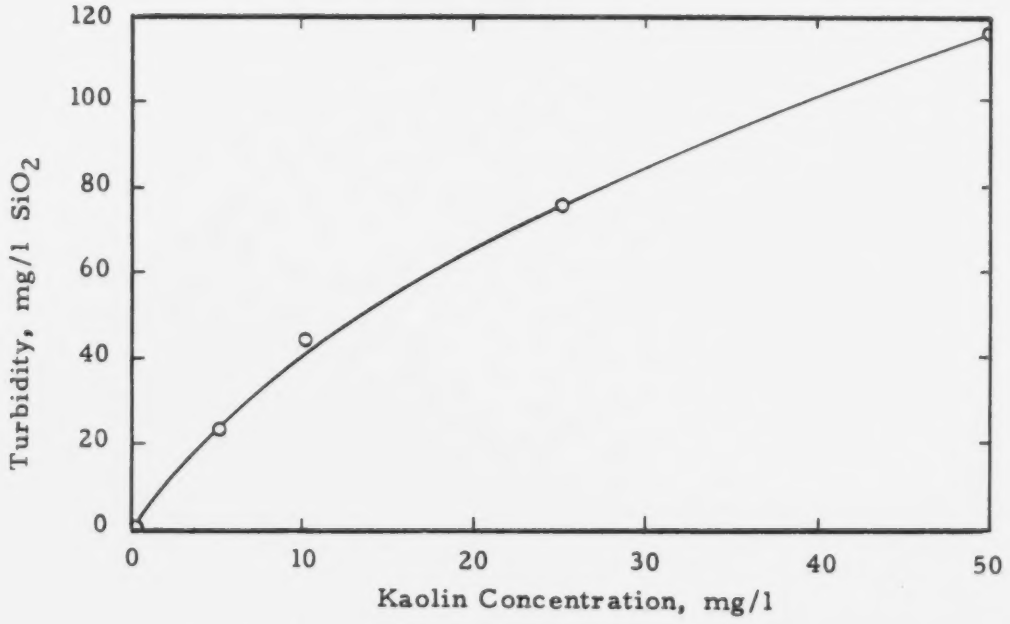

FIGURE 28 -- Relation Between Kaolin Concentration and Turbidity as Measured with a Hellige Turbidimeter

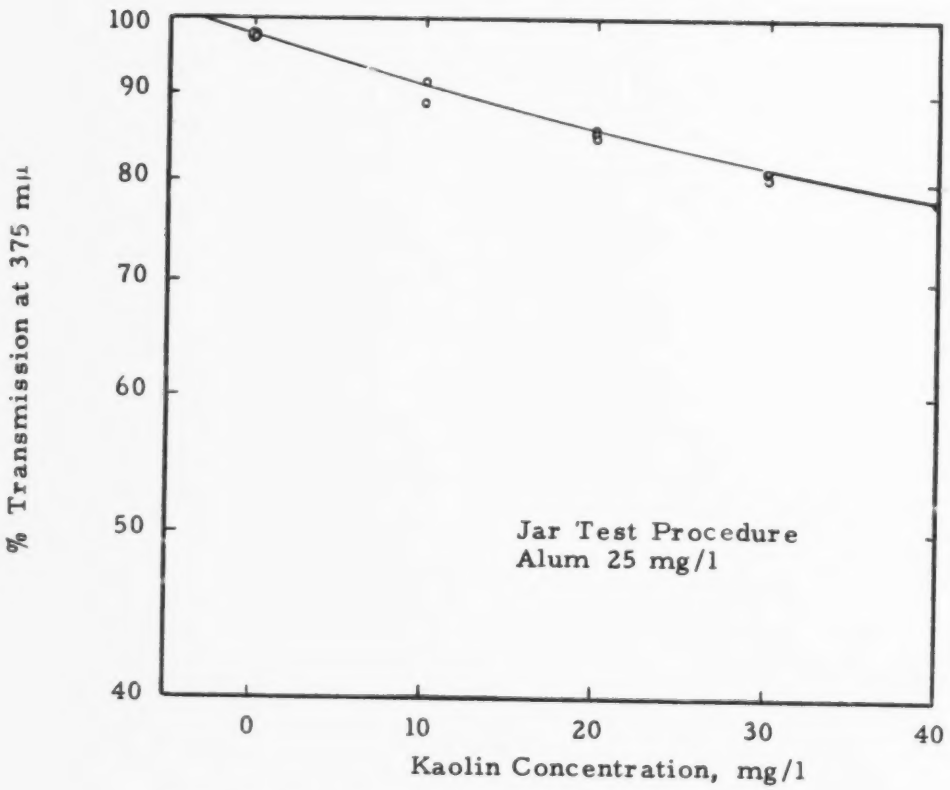

FIGURE 29 -- Transmission Characteristics of a Coagulated Kaolin Suspension in Tap Water

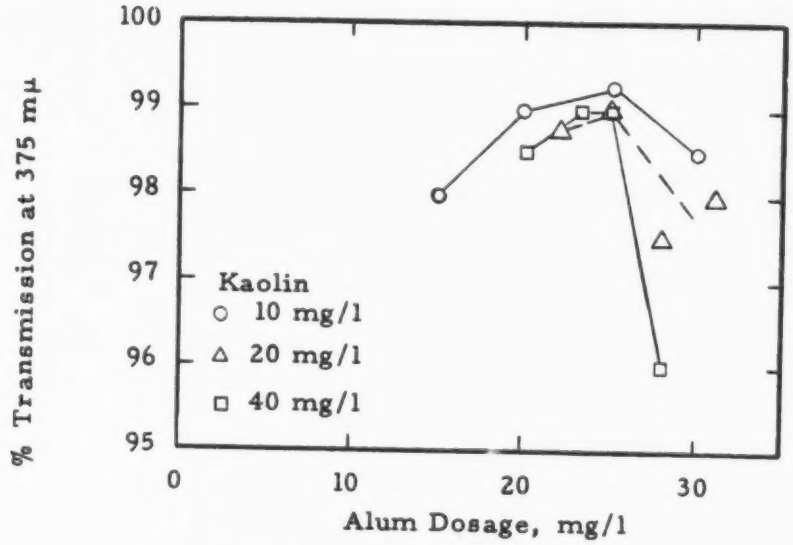

FIGURE 30 -- Supernatant Clarity After Flocculation and Sedimentation (Jar Test Procedure)

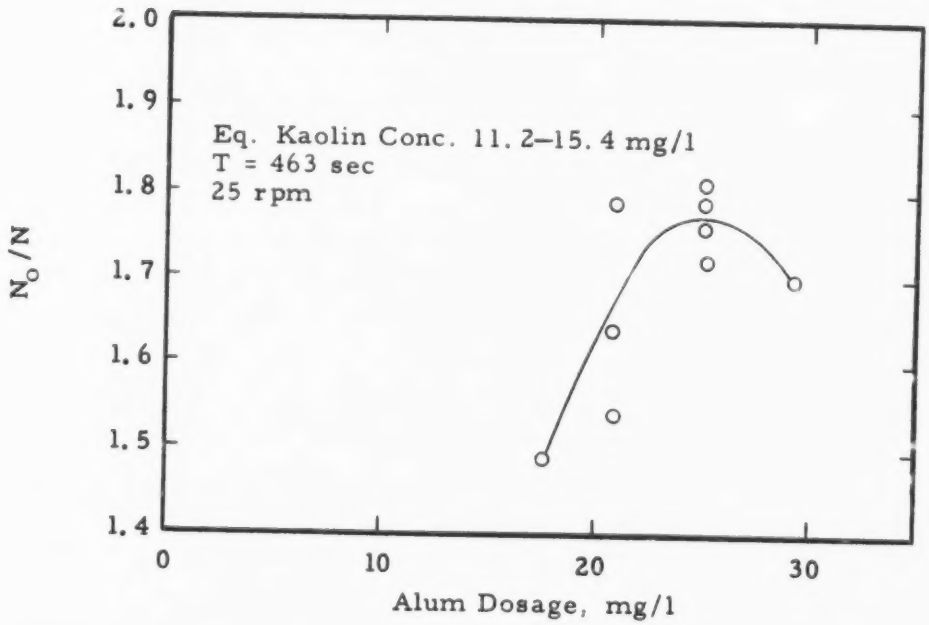

FIGURE 31 -- Effect of Alum Dosage Upon Degree of Flocculation (Continuous Flow Basis)

in a partially flocculated suspension could be devised, the parameter of performance selected was the concentration of primary particles and small flocs remaining in suspension after settling under standardized conditions.

Flocculation was observed at several operating conditions and the change in suspension transmission was determined as a function of settling time. As is shown by Figure 32, there was a rapid decrease in turbidity during the first 20 minutes and only little, if any, decrease thereafter. A settling period of 30 minutes was selected for use. Extremely long settling periods are undesirable since the additional flocculation caused by Brownian motion would become significant.

The first series of three suspension samples was collected with the reactor operating at steady state conditions. These samples were collected through a sampling tap in the reactor wall 3 inches below the water surface. The stirrer and all flows to and from the reactors were then stopped. After a 30-minute settling period the second series of samples was taken with a 50-ml pipette from a location 4 inches below the water surface. The samples were individually analyzed and the B & L Spectronic 20 readings averaged. The results of the first series of samples indicated the initial or total mass of floc (N_o), and the second series indicated the residual primary kaolin particles and small flocs (N).

Experimental parameters varied over a wide range as follows:

Retention period per reactor: T/m	229 to 1667 sec
Stirrer rpm:	15 to 50
Mean velocity gradient: G = du/dz	16.4 to 100 sec^{-1}
Stirrer tip velocity:	0.59 to 1.96 fps
Equivalent kaolin concentration: N_o	11.2 to 60 mg/l
Degree of flocculation: N_o/N	1.10 to 12.80
Reactor in series: m	1,2,4

All values of T, G, etc. are reported on the basis of each reactor. However, the experiments were conducted so that the values are essentially identical for each reactor of a series.

ANALYSIS OF EXPERIMENTAL RESULTS

Flocculation Rate Parameters

The results of the laboratory experiments are presented in Appendix D. The relationship between the degree of flocculation (N_o/N) and mean velocity gradient (G) for selected values of N_o and T is shown in Figure 33. For constant T and essentially constant N_o (21.1 to 28.0 mg/l), the relationship approaches first order (as would be indicated by a straight line relationship). The data points are expected to approach a straight line only to the extent that the size distribution function and the floc density are essentially constant. Figure 12

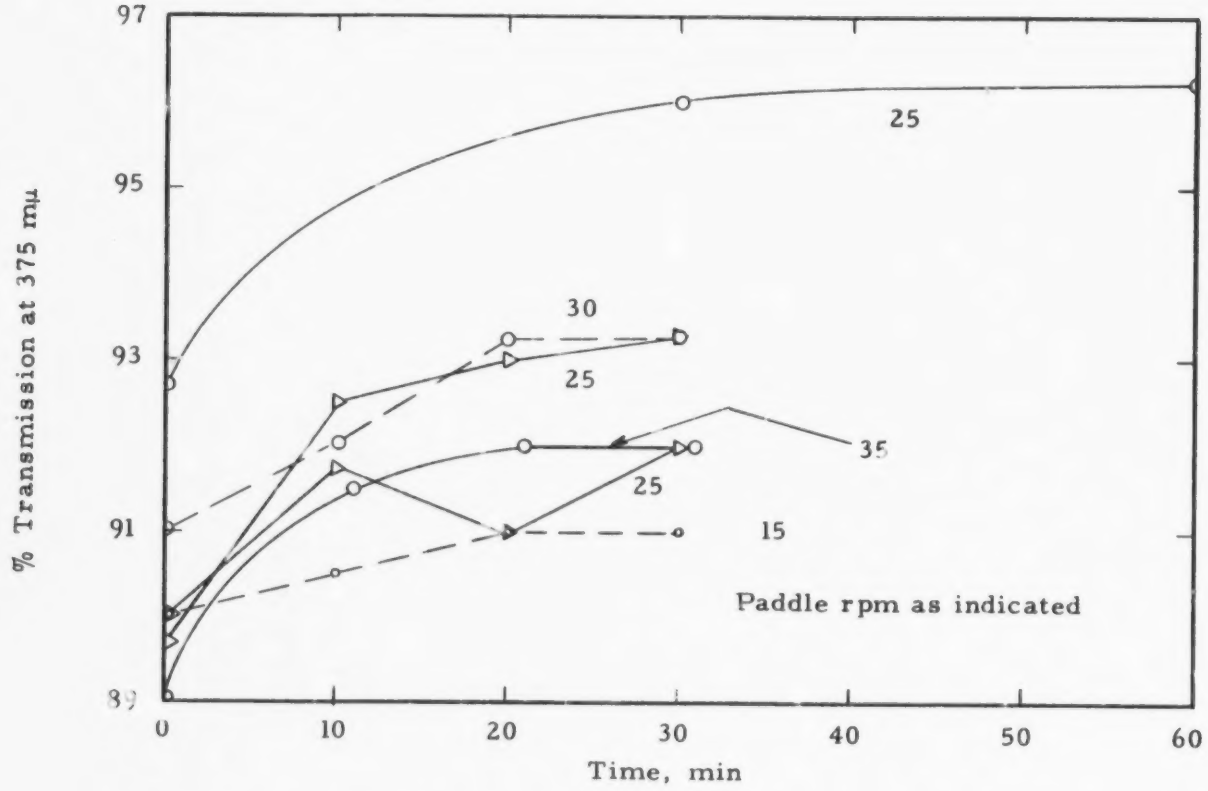

FIGURE 32 -- Effect of Settling Time on Clarity of Coagulated Kaolin Suspensions (Various Initial Concentrations)

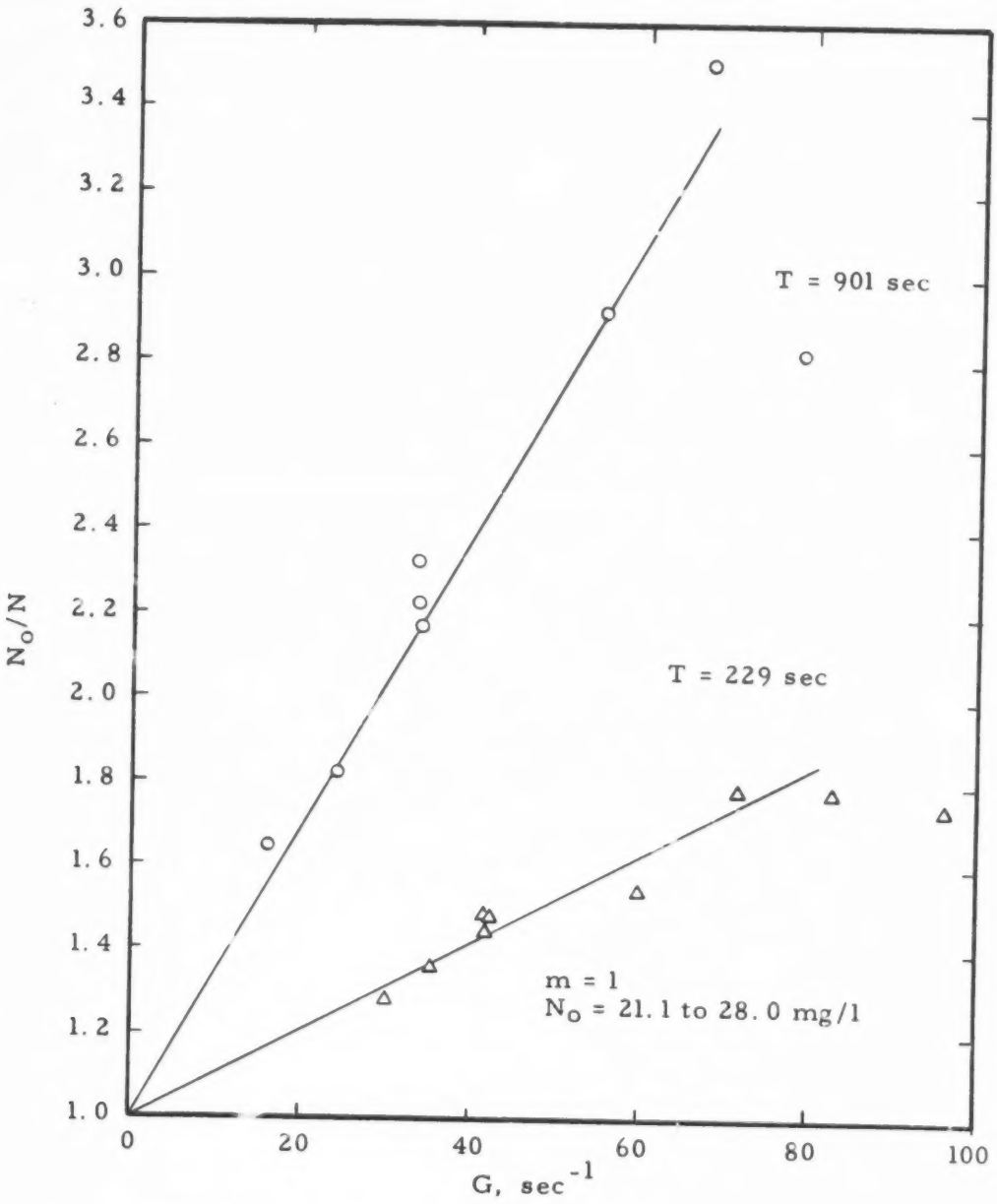

FIGURE 33 -- Effect of Mean Velocity Gradient on Degree of Flocculation

indicates that, based upon the computer studies, the relationship between n_o/n_1 and θ may be approximated by a straight line over the range $n_o/n_1 = 1.0$ to about $n_o/n_1 = 2.5$. Beyond this range the increase in n_o/n_1 is significantly less than directly proportional to the increase in θ. Considering this change in size distribution function, the data presented in Figure 33 indicate a first order dependence of the degree of flocculation upon mean velocity gradient. These results also indicate that the mean velocity gradient is a significant and useful parameter of flocculation rate, despite the distribution of gradients which existed within the reactor.

Figure 34 indicates the experimentally determined relationship between retention period and degree of flocculation for two groups of experiments conducted at approximately constant G and N_o. A direct dependence of N_o/N upon T is indicated, again subject to the assumption of essentially constant D. Finally the dependence of the degree of flocculation upon the floc mass present is presented in Figure 35. A first order dependence upon floc mass is indicated, but with considerable data scatter.

The product of the experimentally determined size distribution function (D) and the reaction constant (K) may be calculated from Equation 81 (see also Appendix D)

$$KD = \frac{\left(\frac{N_o}{N}\right)^{1/m} - 1}{GN_o T/m} . \qquad (81)$$

Figures 36 to 38 present the relation between the computed values of KD and N_o/N. Shown on Figure 36 are data collected under reactor conditions where perfect mixing was approached. As shown in Chapter V, these conditions were approached at T = 463 sec, 15-20 rpm, and at T = 229 sec, all rpm investigated. All data collected from the second and fourth reactors are shown in Figures 37 and 38.

Inspection of Figures 36 to 38 indicates that the value of KD is significantly different for the three reactors at a given N_o/N. As was shown previously, the magnitude of δ'_m at a given n_o/n is a function of m (cf. Figure 16). It was also shown that $\delta'_m = 8$ for a monodispersed system ($n_o/n = 1$). The magnitude of K may be calculated by noting that $KD = 6 \times 10^{-6}$ at $N_o/N = 1$ on all three figures. Then

$$K = \frac{1}{8} (6 \times 10^{-6}) = 0.75 \times 10^{-6} (mg/l)^{-1} .$$

Using this value of K and assuming that is constant, D may be calculated for other values of N_o/N. For example, at $N_o/N = 1.5$, m = 1

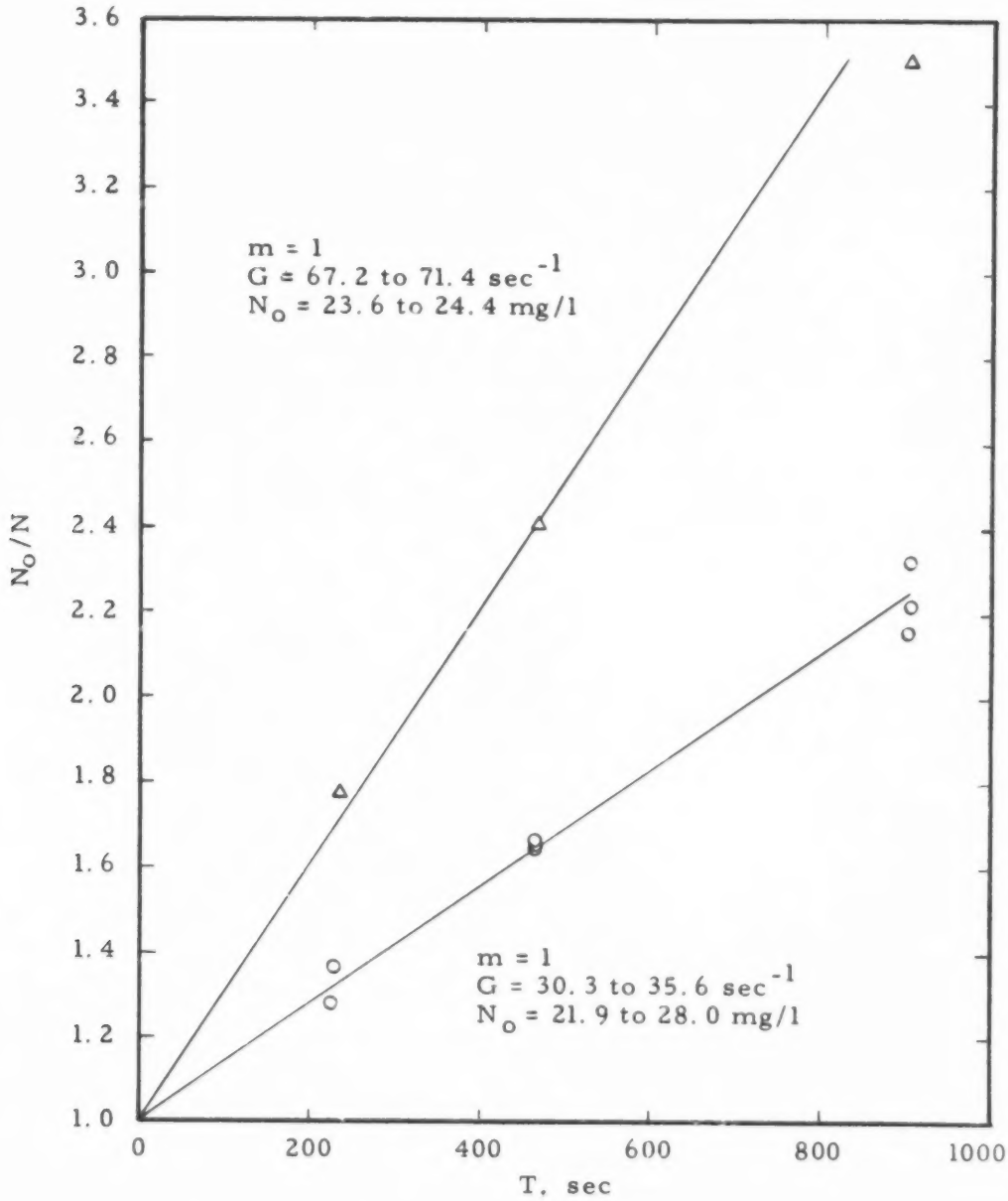

FIGURE 34 -- Effect of Retention Period on Degree of Flocculation

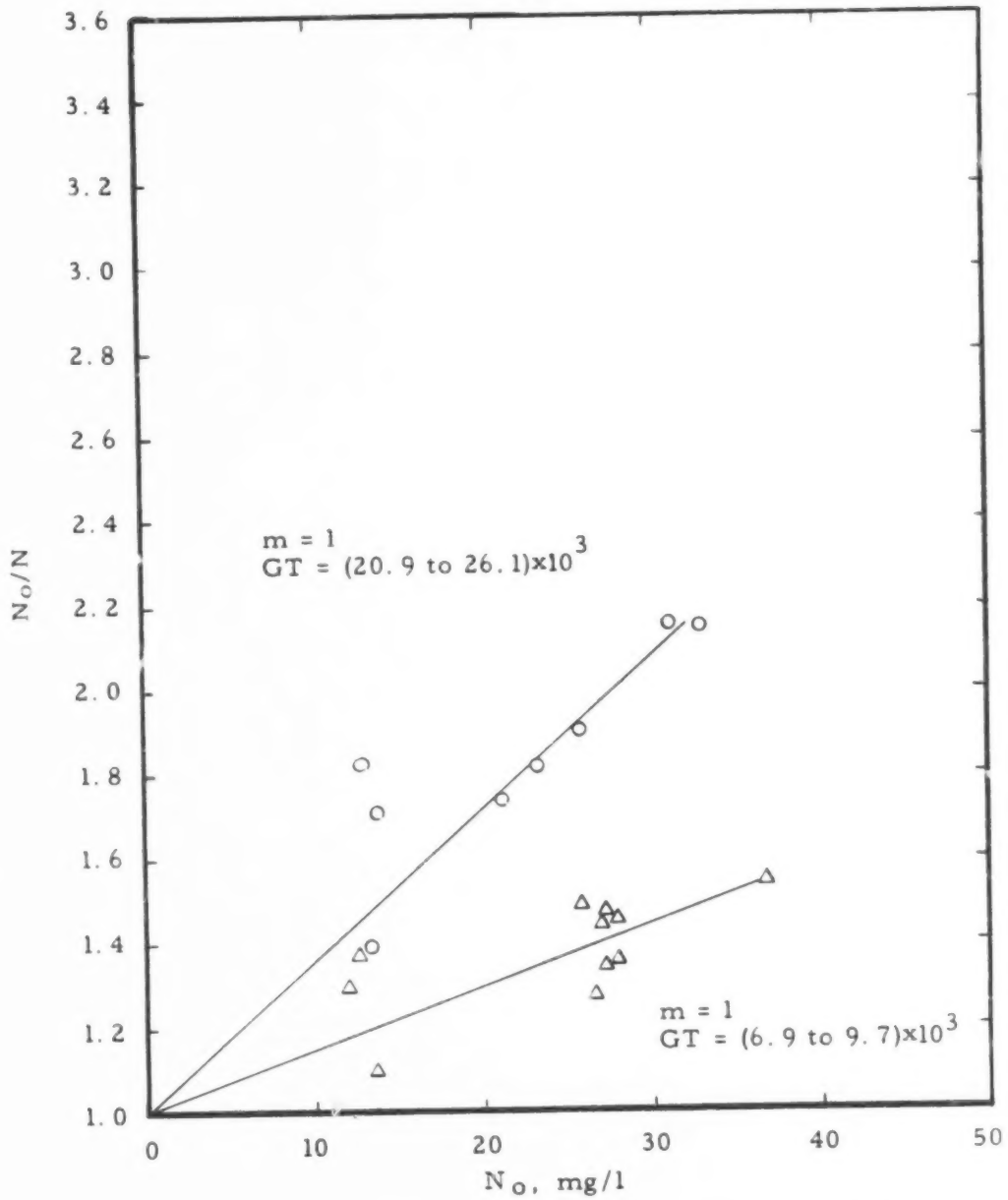

FIGURE 35 -- Effect of Floc Mass on Degree of Flocculation

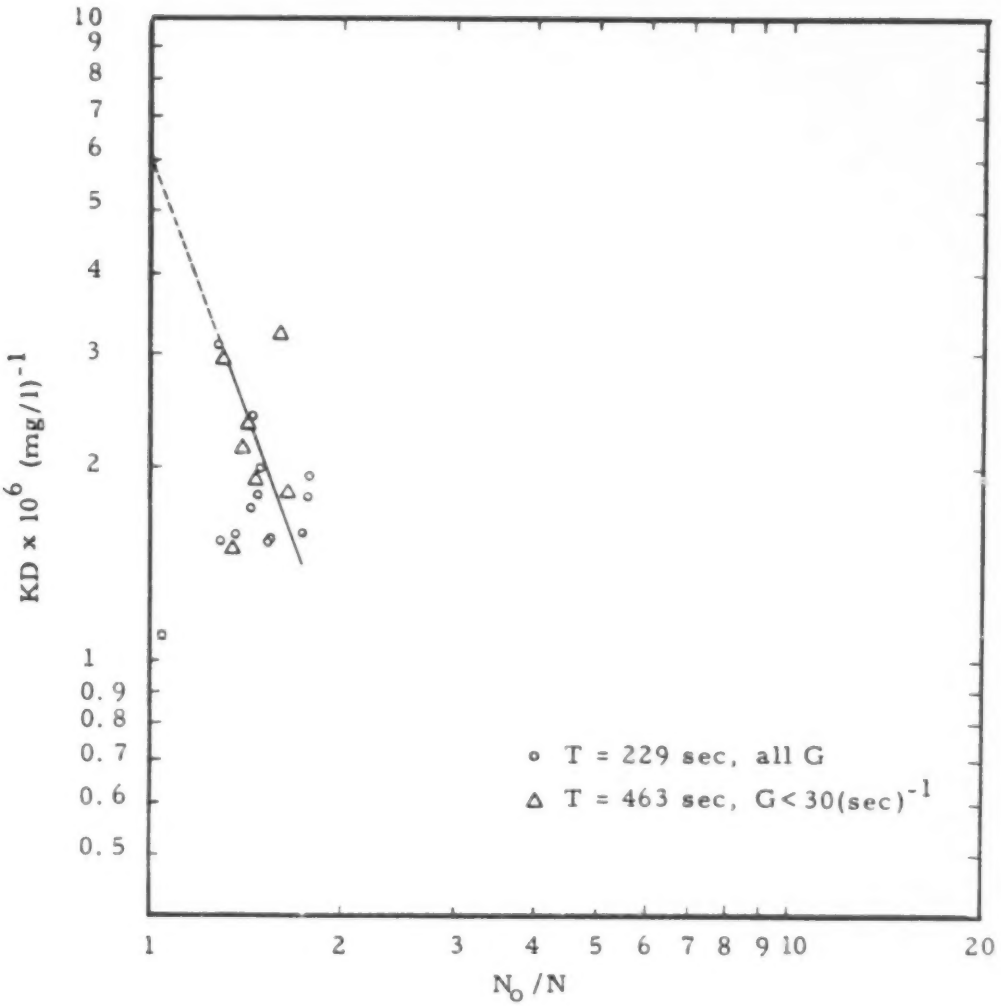

FIGURE 36 -- KD for Reactor 1

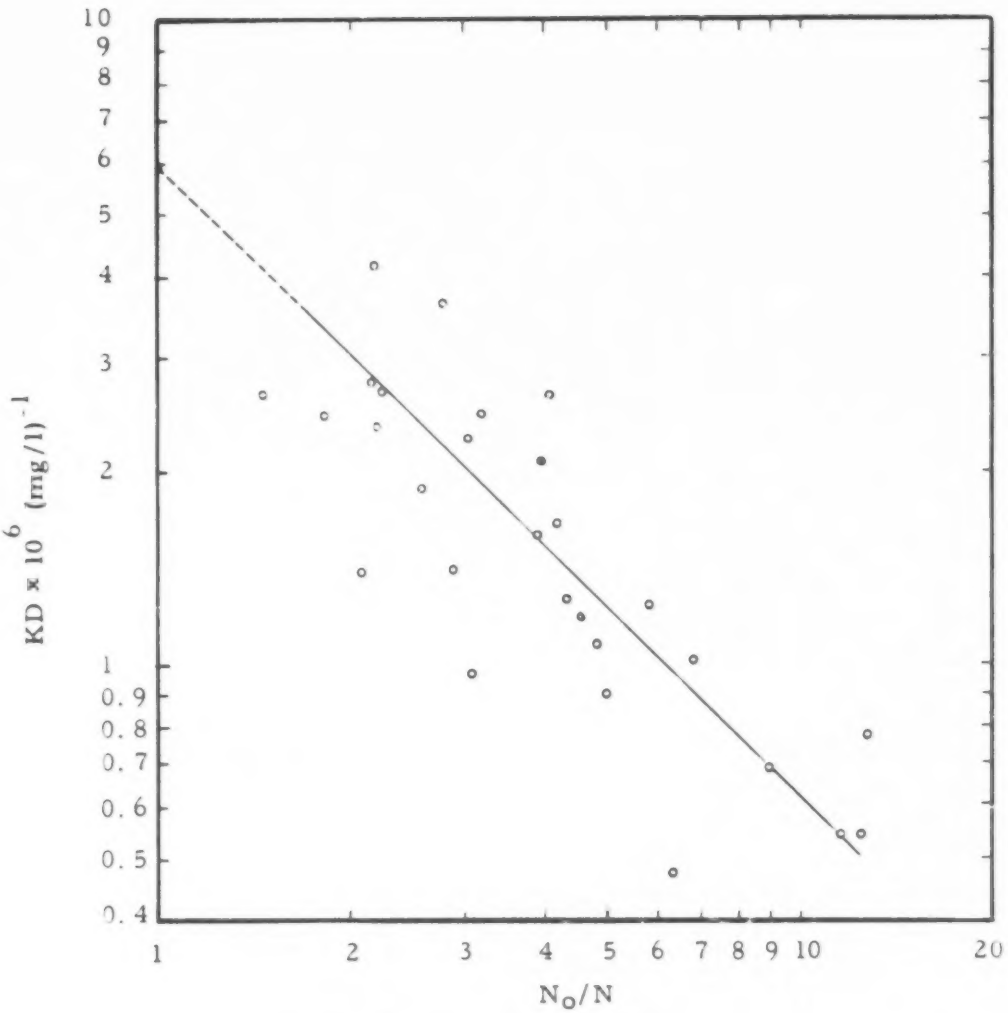

FIGURE 37 -- KD for Reactor 2

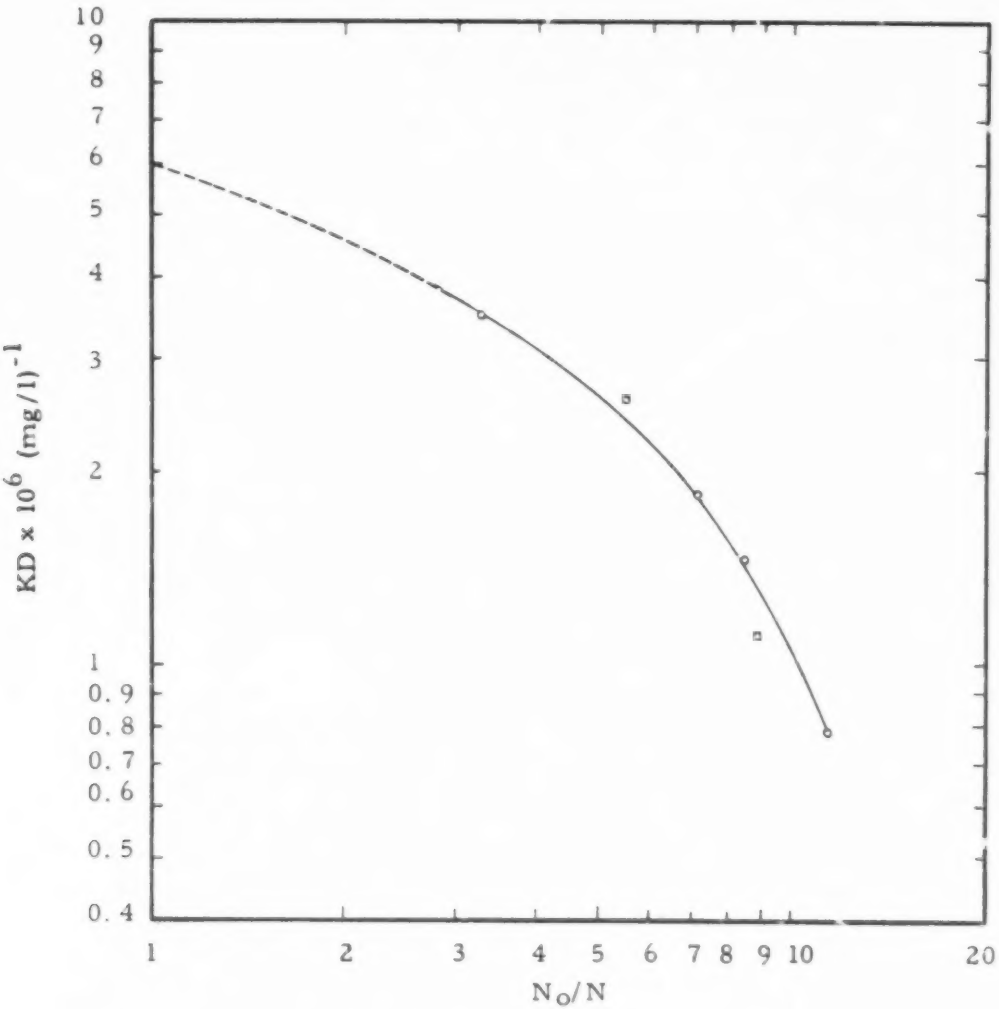

FIGURE 38 -- KD for Reactor 4

$$D = \frac{2 \times 10^{-6}}{0.75 \times 10^{-6}} = 2.67 \ .$$

It may be that K varied slightly under the experimental conditions, e.g., K and Φ may depend upon G. No such dependence could be demonstrated, however. Because of the extrapolation procedures used and the significant scatter of the data on Figures 36 to 38, there are considerable errors in the computed values of K and D.

Figure 39 presents the experimentally determined D functions from Figures 36 to 38 together with the computer-derived δ_m' functions from Figure 16. The experimentally determined functions are similar in some respects to the computer derived functions, but the latter are biased toward high values, for the reason cited earlier. It appears that D is similar or related to the mathematically defined size distribution function, but, the exact relationship could be determined only if the floc size distribution were known. The experimentally determined function can be utilized mathematically in the same manner as the computed functions.

The results of the flocculation-sedimentation experiments are shown in Figure 40. The lines indicated are

$$\frac{N_o}{N} = (1 + KDGN_oT)^m \qquad (31)$$

where $K = 0.75 \times 10^{-6}$ $(mg/l)^{-1}$ and the values of D are from Figure 39. Data for a mean velocity gradient of 70 to 100 sec^{-1} were analyzed separately because of the possibility of excessive floc breakup at high G, but this effect could not be demonstrated.

Rate Constant

The rate constant is nearly independent of all flocculation parameters and largely dependent on the circumstances of coagulation such as turbidity, coagulant dose, pH, etc. Since coagulation was controlled to yield maximum reduction in residual turbidity, it may be assumed that rapid flocculation was approached ($\alpha \cong 1$). For a system containing many relatively large flocs, the average collision radius can be assumed to be equal to the average physical radius ($a = 1$). Assuming a floc density of 1.02 and a density of 2.65 for the equivalent kaolin, $\Phi/N_o = 31.1 \times 10^{-6}$ $(mg/l)^{-1}$ (Equation 80). This indicates a value of $\Phi = 0.00078$ for 25 mg/l, a typical concentration in these studies. Then (cf. Equation 82)

$$K = \frac{31.1}{\pi} \times 10^{-6} = 9.9 \times 10^{-6} (mg/l)^{-1} \ .$$

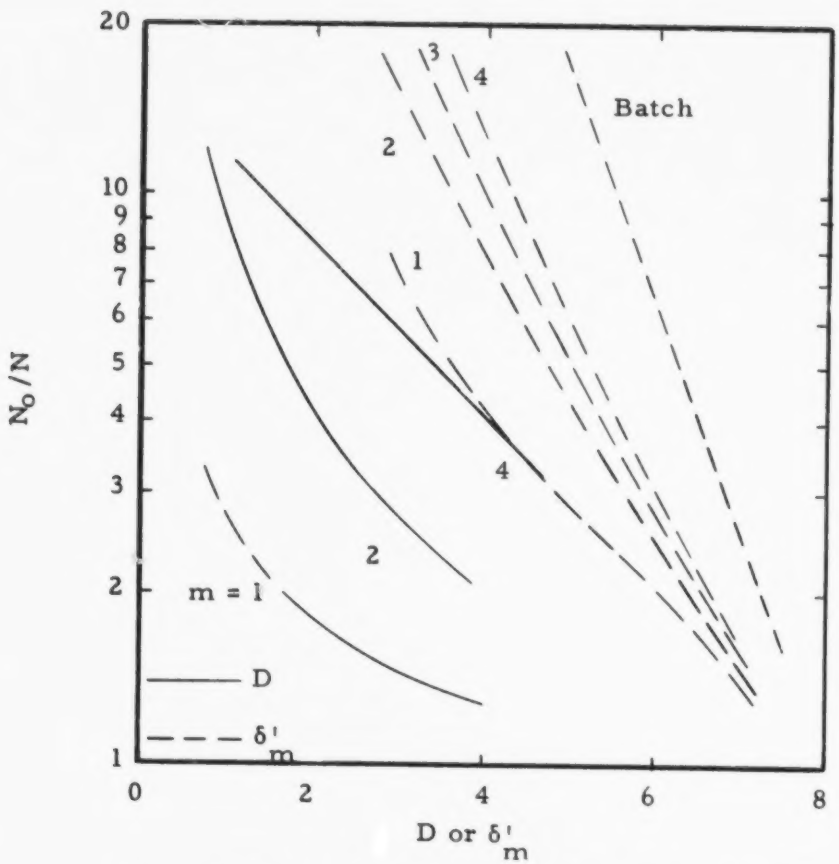

FIGURE 39 -- Experimentally Determined Values of D Function and δ'_m from Flocculation Simulation Studies

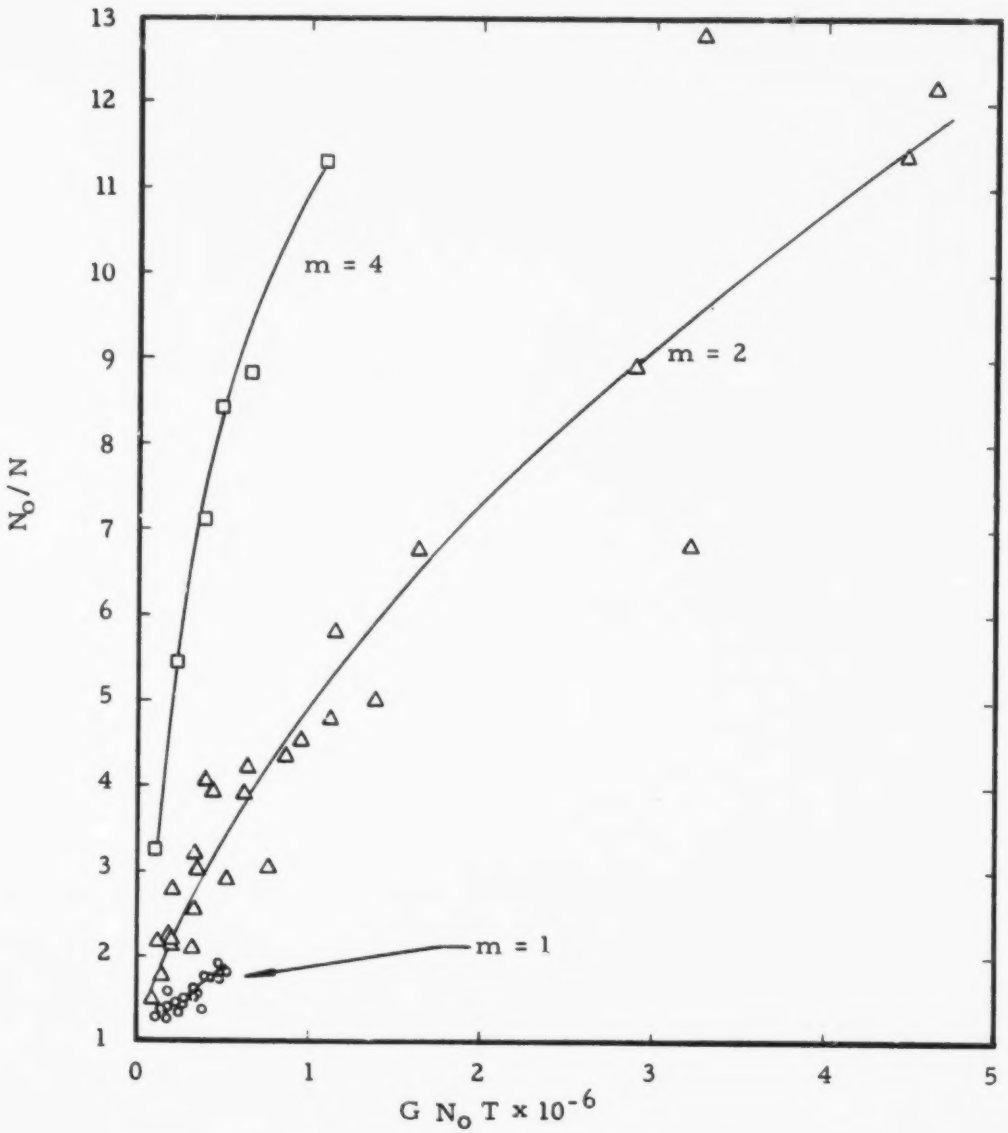

FIGURE 40 -- Degree of Flocculation in a Series of Continuous Stirred-Tank Reactors

The experimental value is

$$K = 0.75 \times 10^{-6}(mg/l)^{-1} .$$

The theoretical value of K is based upon the rate of decrease of primary particles. A floc composed of two primary particles is removed from consideration as an n_1 particle. On the other hand, a floc composed of two primary particles may have such a small settling velocity that it is measured as a portion of the residual floc mass N. Consequently, it would be indicated that no removal (aggregation) has occurred. A reaction constant K based upon the residual primary particles and small flocs will thus be smaller than one based upon primary particles only.

The assumption of constant floc density must be examined. The particle size distribution of the kaolin used for experimental purposes (Figure 25) was such that about half the weight was composed of particles of one-micron diameter or smaller. On the basis of numbers of particles, the vast majority were less than one micron. Initially the flocculation of these fine particles is primarily perikinetic. There is a tendency for the fines to become significant in orthokinetic flocculation as small flocs rather than as individuals. If it may be presumed that the density of these flocs approaches the density of the larger ones, then the assumption of constant density for all flocs in the system is valid. The aggregation of a primary particle (of any size) with a large floc results in only a slight change in overall density because the volume of a primary particle is small relative to the volume of the floc formed. The assumption of constant volume is invalid for the aggregation of primary particles. In summary, the validity of the assumption of a constant density equal to the density of the larger flocs cannot be demonstrated for all collision possibilities. It may well be true that the "effective density" is an average density determined by the probability of collision of various sizes of flocs. This effective density would be greater than the density of the large flocs but less than the density of the primary particles. An increase in density greatly reduces the estimated value of K. It is also likely that in real systems, having a spectrum of du/dz values, the breakup and reflocculation of weak flocs may function to increase floc density with time—assuming that the more dense flocs are of greater strength.

The assumption that $\alpha \rightarrow 1$ may be unduly optimistic. Although this value has been observed experimentally [5] at the beginning of perikinetic flocculation, it may be unrealistic for these experimental conditions and for water purification practice in general. If the other initial assumptions are valid, a value $\alpha = 0.076$ is indicated by the observed constant.

It is implied in the treatment of K as a constant that the density of the floc is a constant (Equation 80). Working with flocculating kaolin, Michaels and Bolger [26] observed little change

in floc size at velocity gradients between 21 and 42 per second. At less than 21 per second, the size increased significantly with decreasing gradient. Investigating the properties of estuarial sediments (at concentrations of 20 g/l and higher), Krone [27] determined the relationship between floc density and shear strength. Extrapolation of Krone's data indicates that a small change in density would be expected at the velocity gradients used in these experiments. It appears likely that there would be a variation in density with velocity gradient for the kaolin-alum system. The data presented herein are not sufficient to establish the extent of this change, however.

The considerations above are all related to the structure of the floc. Sufficient information is not presently available to resolve the many questions raised and additional research on the structure of floc is indicated.

Batch Reactor Analysis

Hudson [24] reported the results of jar with Detroit River water for various conditions of flocculation and at several alum concentrations. The tests were made with 1500-ml samples of 70°F and with and without a two-minute rapid mix followed by 10 to 30 minutes of flocculation at various values of G. After thirty minutes of settling, the turbidity of samples drawn from 5 inches below the surface was measured with a Baylis-type turbidimeter.

An analysis of Hudson's data can be made by first assuming N_o to be constant for all alum doses and equal to 20 ju. These assumptions are, of course, approximations, since N_o must depend to some extent on the alum dose. However, on this basis the correlation between N/N_o and GT conforms to Equation 83 and permits the calculation of KD for alum doses of 12, 15, 20, and 30 mg/l. By extrapolation to $N_o/N = 1$, where D = 8, corresponding values of K were calculated and are shown below.

Alum Dose, mg/l	KN_o	$K, (ju)^{-1}$
30	400×10^{-6}	20×10^{-6}
20	200×10^{-6}	10×10^{-6}
15	75×10^{-6}	3.8×10^{-6}
12	42×10^{-6}	2.1×10^{-6}

It is evident from the above data, and as was concluded by Hudson, that the rate constant depends on the alum dose. The question that remains unanswered is the extent that changing the alum dose influences the floc volume fraction (ϕ) and the aggregation-collision ratio (α). The relationship of D to N_o/N for Hudson's batch system indicated that a single size distribution function nearly characterized all alum doses (Figure 41). Moreover, recognizing that a batch system corresponds to a continuous one of $m = \infty$, Hudson's distribution function

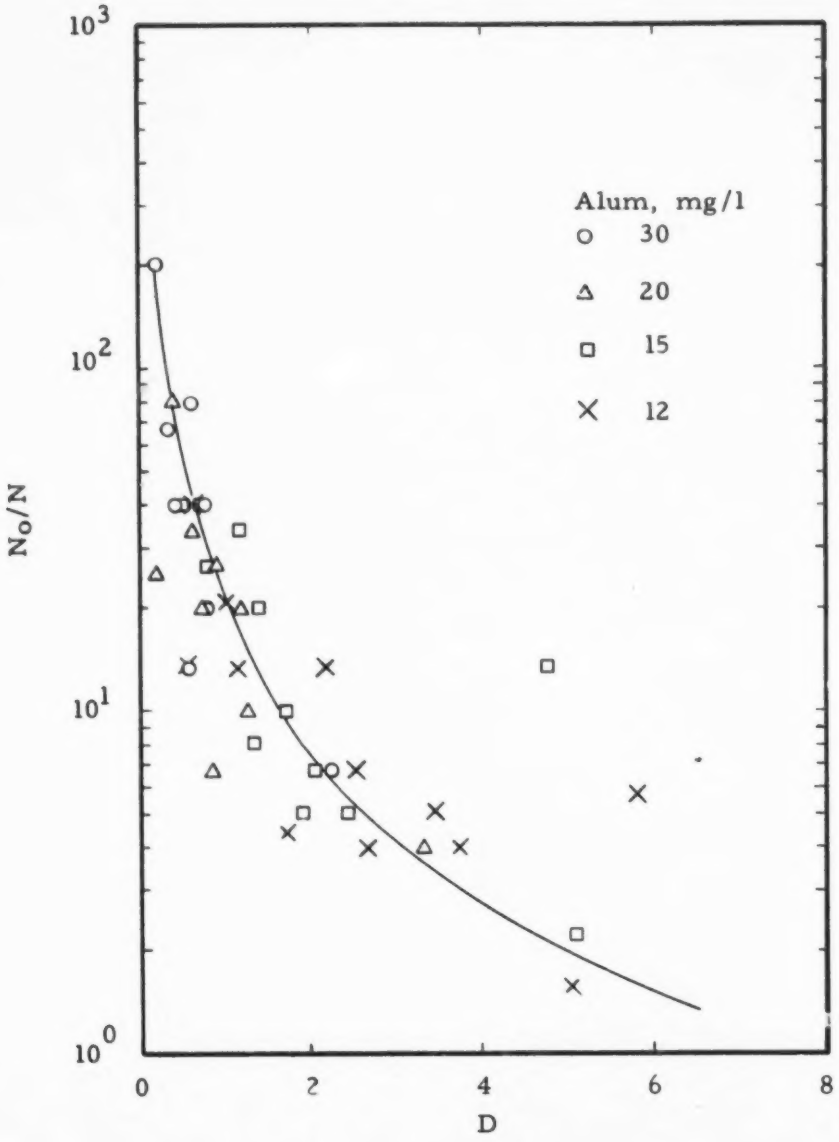

FIGURE 41 -- D Function as Derived from Hudson's Jar Test Data

conforms in a general way to those presented in Figure 39, but to m = 1 or 2, rather than m = ∞.

For each alum dose Hudson observed a critical value of G above which there was increasing turbidity with G. These values were 27 sec^{-1} for 30 and 20 mg/l, 59 sec^{-1} for 15 mg/l, and 78 sec^{-1} for 12 mg/l. This observation, together with the increase in K with alum dose noted earlier, suggests a progressive change in floc structure. It appears that as the alum dose increased, the floc volume fraction increased at a greater rate and the resulting less dense and relatively weak floc was eroded to produce significant numbers of primary particles and small flocs. The shear stress on the surface of the floc may be estimated by [21]

$$\tau = \frac{1}{8} \mu \frac{du}{dz} \qquad (84)$$

where τ is the shear stress. For a viscosity of one centipoise, and using G for du/dz

Alum, mg/l	Surface Shear Stress dynes/sq cm
30	0.034
20	0.034
15	0.074
12	0.098

It thus appears that floc strength limits the range of conditions over which the present kinetic equation applies (cf. Equation 60) and that the strength is a function of alum dose as well as many other coagulation parameters. By an appropriate selection of alum dose and coagulant aids, it is likely that both the reaction constant K and floc strength may be increased, thus permitting the use of larger shearing rates with perhaps improved flocculation economy.

SUMMARY

The progress of flocculation of a kaolin-water system was observed in a series of four continuous stirred-tank reactors. The degree of flocculation (N_o/N) was determined by the mass of floc in suspension both before and after sedimentation. A theoretical equation relating the degree of flocculation to various system parameters was developed.

The degree of flocculation is dependent upon the number of compartments into which the flocculator is divided (m), the product of mean velocity gradient G, floc concentration N_o, retention period T, and an additional term KD. It was shown that D is similar to the size distribution function δ_m as determined in the computer studies

and is considered to be the experimentally determined size distribution function. The observed value of K was compared with a predicted value and several reasons for discrepancy were considered.

VII. IMPLICATIONS OF RESULTS IN PROCESS DESIGN AND OPERATION

Some implications of the results of this study will be considered with respect to the design and operation of process units. The equations theoretically derived should apply generally to flocculating systems. However, this discussion will be limited to flocculation as utilized in water purification practice.

PREVIOUS DESIGN EQUATIONS

The summation of GT products for each of a series of reactors has been proposed and apparently widely used as a parameter of flocculator performance. The usefulness of this relationship can be examined in light of the results of the laboratory experiments. For a summation of $GN_oT = 0.5 \times 10^{-6}$, floc removals of 42, 59, and 71 per cent were observed for the systems composed of 1, 2, and 4 reactors. Thus the effectiveness of flocculation increases significantly with compartmentalization, for a constant sum of GT (or GN_oT). Thus the simple summation of GT is inadequate to correlate these results.

The primary deficiency of the GT parameter is the failure to consider compartmentalization. The results of experiments conducted on a batch basis may be correlated using GT. The results of other experiments conducted in a given number of continuous stirred-tank reactors also may be correlated by GT. However, the type of relationship between GT and performance is vastly different in these two instances; GT alone is insufficient to correlate results from one type of reactor with the other. A second deficiency in this parameter is that the dependent variable is not specified. Thus it is uncertain whether this parameter is proportional to the per cent removal, the absolute decrease in turbidity, etc. It is not surprising that the summation of GT, as calculated for representative water purification plants, ranges over better than an order of magnitude.

APPLICATION OF THE RATE EQUATION TO THE DESIGN OF A SERIES OF REACTORS

The design equation for a series of equal continuous stirred-tank reactors is

$$\left(\frac{N_o}{N}\right)_m = (1 + KDGN_oT/m)^m \qquad (81)$$

where N_o and N are the masses of floc before and after sedimentation in mg/l; m, the number of the reactor; K, the reaction constant; D, the floc size distribution function; G, the mean velocity gradient in sec^{-1}; and T, the retention period in seconds. The results of experiments with kaolin indicate a value of K of 0.75×10^{-6} $(mg/l)^{-1}$ and values of D as shown in Figure 39. The usefulness of Equation 81 in describing the results of flocculation-sedimentation experiments was demonstrated in Chapter VI.

The use of Equation 81 permits rational consideration of the number of reactors as a design variable. The number of reactors into which the total flocculator volume is divided appears as a significant parameter of performance. The importance of m approaches that of the other parameters (e.g., G).

In the usual design situation, N_o may be estimated for the raw water to be treated and N for the water to be applied to the filters. Using the ratio N_o/N, values of D can be determined and the product GT calculated for various values of m. If, however, values of G, N_o, and T are known, calculation of N is less direct since the proper value of D is dependent upon N. Graphical presentation of the design equation is especially helpful in this case. See Figure 42 presenting data from Figures 36 to 38.

The proper number of compartments to obtain a given removal is susceptible to evaluation on the basis of an economic comparison. The interrelationship of all parameters must be considered. For example, if 90 per cent removal is required, $GN_oT = 3 \times 10^6$ for four compartments in series and 7×10^6 for two compartments. Should the designer elect to maintain a constant value of G and reduce T by one half, the total volume required is reduced by one half. Also, the required energy imparted to the water by stirring is reduced by one half since G is a function of energy input per unit volume of suspension. If it were desired to maintain the same volume, the energy requirement is reduced to one-fourth. However, increased compartmentalization would tend to increase the cost of construction as the number of paddles and perhaps driving units would be increased. The total cost of the flocculator basins would increase because of the greater number of dividing walls and connecting channels (for the same total retention period). Even if the total size were decreased, the total cost might well increase because of the more complex construction. An increase in the number of paddles will increase the energy lost in bearing friction. This increase would tend to offset the decrease cited previously. Finally, consideration could be given to reducing the coagulant dosage and offsetting a lower reaction rate by increased G and T.

For a given GN_oT, the degree of flocculation or percentage removal of floc increases as the total is divided into an increasingly greater number (m) of smaller reactors. At the limiting condition of an infinite number of infinitely small reactors, the maximum removal is obtained as predicted by integration of the rate equation on a batch (plug flow) basis. Although a baffled channel flocculator might tend to approach plug flow conditions, this type of flocculator is little

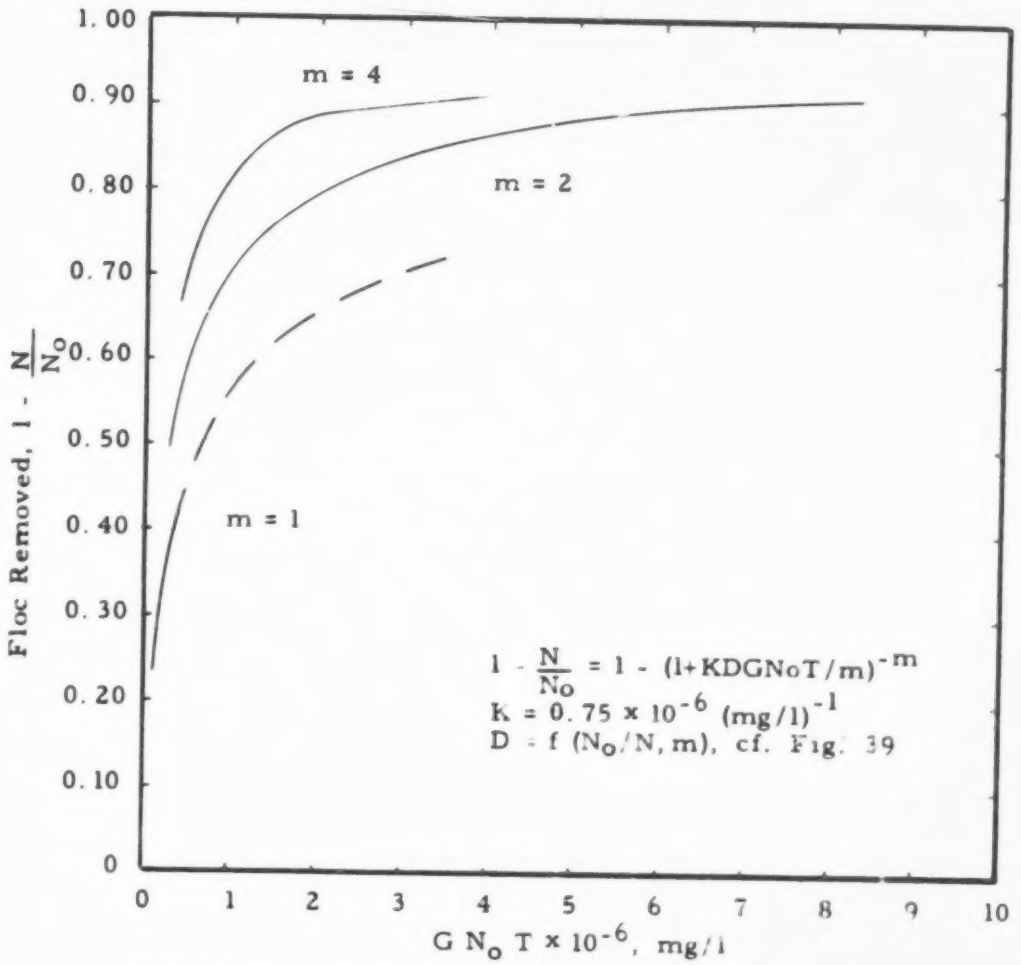

FIGURE 42 -- Role of Compartmentalization in Flocculator Performance

used in the U. S. because of its lack of flexibility. The degree of flocculation to be excepted in a batch or plug flow system is expressed by

$$\ln \frac{N_o}{N} = KDGN_oT \qquad (83)$$

$$\frac{N_o}{N} = e^{KDGN_oT}$$

where D is the distribution function for a batch reaction.

SOLIDS CONTACT UNITS

The rate of flocculation has been shown to have first order dependence on the floc volume fraction. Unusually high floc concentrations can be obtained either by recycling floc after gravity separation or by effecting separation within the unit. The high performance obtained from solids contact units is probably due in part to increased rate of flocculation caused by high floc concentration and by the large equivalent m in the sludge blankets of certain units.

VIII. SUMMARY AND CONCLUSIONS

The performance of a water treatment plant flocculator is largely determined by its effectiveness in promoting orthokinetic flocculation. Because the kinetics of flocculation have been imperfectly understood, the design and operation of process units has been based upon empirical and subjective criteria. To provide a rational basis for design, the major parameters determining flocculator performance have been identified and their interrelationship expressed in a rate equation. Integrated forms of the rate equation were shown to adequately describe the results of laboratory flocculation experiments and flocculation simulation studies.

Generalized equations expressing the rate of orthokinetic flocculation of a polydispersed system were derived from the Smoluchowski orthokinetic equation and further theoretical considerations. These equations describe the rate of change of concentration of the total number of flocs and of primary flocs only for conditions either of limited or of unlimited maximum floc size. The form of all of these equations is similar, differing only in the definition of the appropriate size distribution function.

The progress of flocculation was simulated by repeated application of the Smoluchowski equation using a digital computer. Several size distribution functions were determined for batch reactions and for reactions in a series of continuous reactors. The computer results supported the first order nature of the equations and the dependence upon size distribution.

The rate of flocculation of a kaolin-alum system was experimentally determined in a series of continuous stirred-tank reactors. The results indicated agreement with the integrated form of the rate equation after substitution of parameters susceptible to laboratory measurement. The experimentally determined size distribution function was similar to the functions determined in the computer simulation of flocculation. Analysis of batch flocculation data reported by Hudson [24] was shown to be consistent with the theoretical equation to a limit which appears to be dependent upon floc strength.

Within limits, an economic analysis can be used to determine the optimum relationship between the various rate-determining parameters for a desired degree of flocculation.

The following conclusions may be drawn from the theoretical analysis, the laboratory work, and the recent work of others:

1. The degree of completion of the flocculation reaction obtained in continuous flow or batch reactors is a

function of the product of a rate constant, the mean velocity gradient, the amount of floc in the system, the retention period, and a parameter characterizing the floc size distribution.

2. The compartmentalization of a continuous flow reactor exerts a considerable influence on the degree of flocculation obtained and on overall system economy. In terms of performance of a continuous flow system at constant overall residence time, a single, completely mixed reactor is the least satisfactory geometry, whereas an infinitely large number of infinitely small reactors in series is most efficient.

3. The increase in degree of flocculation with mean velocity gradient appears to reach a limit that depends upon floc strength and probably on the distribution of shearing rate in the reactor. The general rate equation cannot entirely accommodate nonuniform turbulence as it was derived for the average velocity gradient.

4. The flocculation rate constant is a function of the physical-chemical parameters generally associated with coagulation. In a sense, the rate constant is the link between flocculation and coagulation.

APPENDIXES

APPENDIX A

LIST OF SYMBOLS

SYMBOL	DEFINITION
A	Area; coagulant dose
a	Ratio of the collision radius of a floc to its physical radius
C	Residence time function
C_d	Drag coefficient
D	Diffusion coefficient; experimentally determined value of the size distribution function
du/dz	Velocity gradient
F	Residence time function
G	Mean velocity gradient
I	Number of collisions per unit time as a result of Brownian motion
i	Number of primary particles comprising an i-fold floc
J	Number of collisions per unit time as a result of velocity gradient
j	Number of primary p
K	Rate constant
k	Boltzmann constant; ratio of fluid velocity to paddle velocity

Pages 103 and 104 are blank.

APPENDIX A (continued)

m	Number of identical reactors in series
N	Mass of floc in suspension after flocculation and sedimentation
N_o	Total mass of floc
n	Number of particles or flocs per unit volume
n_1	Concentration of primary particles
n_i	Concentration of i-fold particles
n_j	Concentration of j-fold particles
n_k	Concentration of k-fold particles
n_o	Concentration of primary particles in reactor influent
n_t	Total number of particles per unit volume
p	Number of primary particles comprising the maximum size of floc
R	Collision radius; collision distance
r	Radius
r_1	Radius of a primary particle
S	Speed of a rotating shaft; concentration of coagulant in the floc
T	Absolute temperature; coagulation time; mean residence time in a reactor system
t	Time

APPENDIX A (continued)

V	Volume
w	Power dissipated per unit volume of fluid
α	Fraction of collisions which results in aggregation (aggregation - collision ratio)
β	Size distribution function
γ	Size distribution function
δ	Size distribution function; thickness of the Stern layer
δ'_m	Effective size distribution function
ϵ	Size distribution function; system phase shift in residence time distribution equation
η	Coefficient of exponent in residence time distribution equation
θ	Flocculation factor
μ_o	Viscosity of a fluid
μ_s	Viscosity of a suspension
ρ	Density
τ	Shear stress
ϕ	Floc volume fraction
ψ_o	Surface or total potential
ψ_δ	Potential over the diffuse double layer

APPENDIX B

COMPUTER PROGRAM

Preceding page blank

```
$JOB   2522    15,100,100            HOWARD S. HARRIS
$FMS
*      FORTRAN
*      DECKS
       SUBROUTINE RIN(PART,FINP,BETA,ALPHA,ITER)
       DIMENSION PART(2),FINP(1)
       READ 1,ALPHA,BETA,ITER
       READ 2,(PART(I),I=1,100)
       READ 2, (FINP(I),I=1,100)
     1 FORMAT(F12.11,F10.8,I5)
     2 FORMAT(5F14.4)
       BETA=1.0-BETA
       PRINT 1, ALPHA,BETA,ITER
       PRINT 2,(PART(I),I=1,100)
       PRINT 2,(FINP(I),I=1,100)
       RETURN
       END
*      FORTRAN
       FUNCTION CUBF(I,J)
       X=I
       Y=J
       CUBF=(X**.333+Y**.333)**3
       RETURN
       END
*      FORTRAN
*      DECKS
       SUBROUTINE PROUT(N,PART,ITER,ALPHA,BETA)
       DIMENSION PART(1),B(200),X(100),Y(100)
C
C      REACTOR DISTRIBUTION PRINTOUT
C
       IF(N-10) 1, 1, 7
     1 PRINT 2
     2 FORMAT(60H ************************************************
      1****,//)
       PRINT 3,N
     3 FORMAT(17H  ITERATION NO.  ,I4,//)
       PRINT 4,
     4 FORMAT(41H           REACTOR  PARTICLE  DISTRIBUTION,//)
       PRINT 5, (I,PART(I),I=1,100)
     5 FORMAT(4(I5,E15.8))
       TAU=1.0-BETA
       PRINT 6, ALPHA,TAU
     6 FORMAT(//,9H  ALPHA =,E15.8,12H      BETA  =,F10.8)
       RETURN
C
C      REPETITIVE PRINTOUT
C
     7 IF(N/10*10-N) 8,1,8
     8 IF(N-ITER+1) 9,10,9
     9 RETURN
```

```
C
C       FINAL PUNCHOUT AND SYSTEM PARAMETERS
C
   10 PUNCH 11, (PART(I), I=1,100)
   11 FORMAT(5F14.4)
C
C       INPUT TO REACTOR NUMBER TWO
C
      DO 12 I=1,100
           B(I)=PART(I)*TAU
   12 CONTINUE
C
C       PUNCH NEW INPUT ARRAY B(I) = I2(I)
C
      PUNCH 13, (B(I),I=1,100)
   13 FORMAT(5F14.4)
C
C       PRINT NEW INPUT ARRAY B(I)
C
      PRINT 2
      PRINT 15
   15 FORMAT(29H  REACTOR OUTPUT DISTRIBUTION,//)
      PRINT 16,(I,B(I),I=1,100)
   16 FORMAT(4(I5,E15.8))
      PRINT 14
   14 FORMAT(//,60H ************************************************
     1*******,//)
C
C       CALCULATE DELTA TIMES NUMB AND PRINT
C
      D=0.0
      SD=0.0
      DO 17 I=1,100
      X(I) =I
           D=PART(I)*((X(I)**0.3333+1.0)**3.0)
      SD=SD+D
   17 CONTINUE
      PRINT 6,ALPHA,TAU
      PRINT 18,SD
   18 FORMAT(14H  DELTA*NUMB =,E15.8,//)
C
C       CALCULATE THE GAMMA DENOMINATOR
C
      D=0.0
      SD=0.0
      DO 20 I=1,100
           DO 19 J=1,100
           X(I)=I
           Y(J)=J
           D  =PART(I)*PART(J)*(X(I)+Y(J))
      SD=SD+D
   19      CONTINUE
   20 CONTINUE
```

```
      PRINT 21,SD
   21 FORMAT(22H  GAMMA DENOMINATOR  =,E15.8,//)
C
C     CALCULATE THE GAMMA NUMERATOR
C
      D=0.0
      SD=0.0
      DO 23 J=1,100
      L=100-J
           DO 22 I=1,L
           X(I)=I
           Y(J)=J
           D=PART(I)*PART(J)*((X(I)**0.3333+Y(J)**0.3333)**3.0)
      SD=SD+D
   22      CONTINUE
   23 CONTINUE
      PRINT 24, SD
   24 FORMAT(20H  GAMMA NUMERATOR  =,E15.8,//)
C
C     CALCULATE BETA FUNCTION
C
      D=0.0
      SD=0.0
      DO 26 I=1,100
           DO 25 J=1,100
           X(I)=I
           Y(J)=J
           D=PART(I)*PART(J)*((X(I)**0.3333+Y(J)**0.3333)**3.0)
      SD=SD+D
   25      CONTINUE
   26 CONTINUE
      PRINT 27,SD
   27 FORMAT(17H  BETA FUNCTION =,E15.8,//)
C
C     CALCULATE TOTAL NUMBER OF PARTICLES
C
      T=0.0
      DO 28 I=1,100
           T=T+PART(I)
   28 CONTINUE
      PRINT 29,T
   29 FORMAT(29H  TOTAL NUMBER OF PARTICLES =,E15.8,//)
      PRINT 30
   30 FORMAT(12H  END OF RUN,//)
      PRINT 14
      RETURN
      END
```

```
*       FAP
          COUNT   200
          CLA     UNDER-1
          STO     8
          AXT     100,1
          PXA     ,1
          STO     NUMB,1
          STZ     DELT,1              ZERO ARRAY DELT SETUP ARRAY NUMB
          TIX     *-3,1,1
          AXT     100,1
BLAH1     AXT     100,2
BLAH2     PXA     ,1
          SXD     I,1
          SXD     J,2
          SUB     =1
          XCA
          MPY     =100
          XCA
          ADD     NUMB,2
          STO     TEMP
          CALL    $CUBE,I,J
          LXA     TEMP,4
          STO     CUBE,4
          TIX     BLAH2,2,1
          TIX     BLAH1,1,1
          CALL    $RIN,PPART,FINP,OMBET,ALPHA,ITER
          STZ     N           (NUMBER OF LOOPS)
          CLA     5
          STO     TIME
INCO      AXT     100,1
INC1      AXT     100,2
INC2      PXA     ,1
          SUB     =1
          XCA
          MPY     =100
          XCA
          ADD     NUMB,2
          PAX     ,4
          LDQ     CUBE,4
          FMP     PART,1
          XCA
          FMP     PART,2
          XCA
          FMP     ALPHA
          STO     DEL
          CLA     DELT,1
          FSB     DEL
          STO     DELT,1
          CLA     DELT,2
          FSB     DEL
          STO     DELT,2
          PXA     ,1
          ADD     NUMB,2
```

```
          PAX     ,4
          TXL     *+6,4,100
          ARS     1
          PAX     ,4
          LDQ     DEL
          FMP     =2.0
          STO     DEL
          CLA     DELT,4
          FAD     DEL
          STO     DELT,4
          TIX     INC2,2,1
          TIX     INC1,1,1
          AXT     100,1
          CLA     PART,1
          FAD     DELT,1
          XCA
          FMP     OMBET
          FAD     INPUT,1
          STO     PART,1
          STZ     DELT,1
          TIX     *-7,1,1
          CLA     N
          ADD     =010
          STO     N
          CALL    $PROUT,N,FPART,ITER,ALPHA,OMBET
          CLA     N
          CAS     ITER
          TRA     INCO
          TRA     *+2
          TRA     INCO
          CLA     5
          SUB     TIME
          STO     TIME
          TSX     $EXIT,4
          BSS     99
FPART     BSS     1
PART      BSS     99
FINP      BSS     1
INPUT     BSS     100
DELT      BSS     100
NUMB      BSS     1100
CUBE      BSS     0
ITER      PZE
N         PZE
TEMP      PZE
DEL       PZE
ALPHA     PZE
OMBET     PZE
I         PZE
J         PZE
TIME      PZE
```

```
UNCNT   PZE
        TRA     UNDER
UNDER   CLA     UNCNT
        ADD     =1
        STO     UNCNT
        ZAC
        LDQ     =0
        TRA*    0
        END
```

APPENDIX C

CHEMICAL ANALYSIS OF TAP WATER

Analysis of treated Mokelumne River water as reported by the East Bay Municipal Utility District.

Constituent or Property	Reported as	Concentration *	Date
Alkalinity	$CaCO_3$	21	10/64
Conductance	---	53	10/64
pH	---	9.5	10/64
Hardness	$CaCO_3$	22.8	10/64
Non-carbonate hardness	$CaCO_3$	3.8	10/64
Carbonate hardness	$CaCO_3$	19.0	10/64
Total Dissolved Solids	---	24	10/64
Aluminum	Al	0.02	10/64
Calcium	Ca	7.5	10/64
Iron	Fe	0.02	10/64
Magnesium	Mg	1.0	10/64
Manganese	Mn	0.00	6/64
Potassium	K	0.9	10/64
Sodium	Na	1.8	10/64
Bicarbonate	HCO_3	16.1	10/64
Boron	B	0.01	6/64
Carbonate	CO_3	3.5	10/64
Chloride	Cl	2	10/64
Fluoride	F	0.04	6/64
Phosphate	PO_4	0.015	6/64
Silica	SiO_2	9.6	10/64
Sulfate	SO_4	1.2	10/64

*Conductance in micromhos/cm. Other results, except for pH, are in mg/l.

Pages 117 and 118 are Blank.

APPENDIX D

RESULTS OF FLOCCULATION - SEDIMENTATION EXPERIMENTS

First Reactor in Series

Second Reactor in Series

Fourth Reactor in Series

Preceding page blank

APPENDIX D

RESULTS OF FLOCCULATION - SEDIMENTATION EXPERIMENTS

FIRST REACTOR IN SERIES

Run no.	Retention Period T (sec)	Mean vel. Gradient $G\ (sec)^{-1}$	Floc Mass N_o mg/l	N_o/N	$GN_oT\times10^{-6}$	$KD\times10^{6}$
20	463	34.7	11.2	1.80	.180	4.44
21	463	35.1	13.5	1.76	.219	3.47
23	463	35.1	13.8	1.72	.224	3.21
26	463	55.6	12.8	1.83	.330	2.52
27	463	55.6	13.2	1.39	.340	1.15
28	463	18.4	11.8	1.30	.101	2.97
29	463	25.8	15.0	1.42	.179	2.35
30	463	35.1	15.4	1.79	.250	3.16
31	463	26.1	15.0	1.39	.181	2.15
32	463	45.1	13.7	1.71	.286	2.48
33	463	26.1	15.1	1.59	.182	3.24
34	463	35.1	22.3	1.65	.362	1.80
35	463	35.1	21.9	1.65	.356	1.82
36	463	56.4	25.6	1.90	.668	1.35
37	463	56.4	31.0	2.16	.810	1.43
38	463	45.1	32.9	2.15	.687	1.67
39	463	18.6	27.0	1.35	.233	1.50
40	463	18.6	27.8	1.46	.239	1.92
41	463	26.1	29.2	1.64	.353	1.81

Preceding page blank

APPENDIX D (continued)

42	229	42.0	25.6	1.49	.246	1.99
42	229	24.0	26.8	1.45	.258	1.74
44	229	60.0	25.6	1.54	.352	1.53
45	229	30.3	26.3	1.28	.182	1.54
46	229	35.6	27.8	1.36	.227	1.58
47	901	33.7	22.5	2.16	.683	1.70
48	901	33.7	24.2	2.32	.735	1.80
49	901	55.1	24.2	2.92	1.201	1.60
50	901	16.4	21.5	1.64	.318	2.01
51	901	24.4	23.1	1.82	.508	1.61
52	901	78.9	24.5	2.82	1.742	1.04
53	901	67.2	24.5	3.50	1.483	1.68
54	463	67.9	23.6	2.41	.742	1.90
55	463	80.4	22.9	2.69	.852	1.98
56	463	93.4	21.3	2.48	.921	1.61
57	229	71.4	24.4	1.78	.399	1.95
58	229	83.0	227.	1.78	.431	1.81
59	229	96.4	21.1	1.74	.466	1.59
60	229	42.5	12.5	1.38	.122	3.11
61	901	33.7	12.5	1.39	.380	1.03
62	229	42.5	27.0	1.48	.253	1.82
63	463	34.7	24.0	1.66	.386	1.71
64	463	34.7	32.0	2.16	.514	2.26
65	463	34.7	29.5	1.93	.474	1.96
66	901	33.7	28.0	2.22	.850	1.44
67	229	42.5	36.5	1.55	.355	1.55
68	901	16.4	11.7	1.70	.173	4.05
69	901	55.1	12.0	2.50	.596	2.52
70	229	60.9	13.1	1.44	.183	2.40
71	229	30.7	13.5	1.10	.095	1.05

$$KD = \frac{(N_o/N) - 1}{GN_o T/m}$$

APPENDIX D

RESULTS OF FLOCCULATION - SEDIMENTATION EXPERIMENTS

SECOND REACTOR IN SERIES

Run no.	Retention Period T/m sec	Mean Vel. Gradient G			Floc Mass N_o mg/l	N_o/N	$(N_o/N)^{1/2}$	$GN_oT/m \times 10^{-6}$	$KD \times 10^6$
		First Chamber $(sec)^{-1}$	Second Chamber $(sec)^{-1}$	Mean G $(sec)^{-1}$					
72	463	18.6	16.2	17.4	14.1	2.17	1.47	.114	4.12
73	463	35.2	33.9	34.6	13.0	2.20	1.49	.208	2.36
74	463	56.4	55.6	56.0	12.3	2.56	1.60	.319	1.88
75	229	43.1	33.9	38.5	15.8	1.80	1.34	.139	2.45
76	901	34.1	33.9	34.0	12.6	4.07	2.02	.386	2.64
77	901	34.1	33.9	34.0	28.0	4.31	2.08	.858	1.26
78	901	34.1	33.9	34.0	20.5	4.19	2.04	.628	1.66
79	229	43.1	33.9	38.5	21.3	2.24	1.50	.188	2.66
80	463	35.2	33.9	34.6	20.9	3.03	1.74	.335	2.21
81	463	18.6	16.2	17.4	23.3	2.16	1.51	.188	2.71
82	463	56.4	55.6	56.0	23.8	3.90	1.98	.617	1.59
83	463	35.2	33.9	34.6	31.5	2.89	1.70	.505	1.39
84	463	18.6	16.2	17.4	40.4	3.20	1.79	.325	2.43
85	463	56.4	55.6	56.0	36.2	4.52	2.13	.939	1.20

APPENDIX D (continued)

86	229	43.1	33.9	38.5	36.5	2.10	1.45	.322	1.40
87	229	32.2	16.8	24.5	13.8	1.45	1.20	.077	2.60
88	229	87.3	82.8	85.0	39.1	3.03	1.74	.761	0.97
89	463	83.4	82.8	83.1	29.2	4.79	2.19	1.123	1.06
90	901	83.9	83.9	83.9	43.5	12.80	3.58	3.288	0.78
91	901	83.9	83.9	83.9	15.1	5.80	2.41	1.141	1.24
92	901	17.4	17.0	17.2	12.3	2.80	1.69	.191	3.61
93	901	17.4	17.0	17.2	27.5	3.93	1.89	.426	2.09
94	901	84.9	84.9	84.9	58	11.39	3.38	4.437	0.54
95	901	59.3	59.1	59.2	60	6.32	2.51	3.200	0.47
96	901	100	100	100	32.0	8.90	2.98	2.883	0.69
97	463	59.9	59.1	59.5	49.7	4.97	2.23	1.369	0.90
98	1667	35.7	35.6	35.6	27.1	6.78	2.60	1.608	1.00
99	1667	83.9	83.9	83.9	33.0	12.21	3.50	54.615	0.54

$$KD = \frac{(N_o/N)^{1/2} - 1}{GN_o T/m}$$

APPENDIX D

RESULTS OF FLOCCULATION - SEDIMENTATION EXPERIMENTS

FOURTH REACTOR IN SERIES

Run no.	Retention Period T/m sec	Mean Velocity Gradient G				Mean G sec^{-1}	N mg/l	N_o/N	$(N_o/N)^{\frac{1}{4}}$	$GN_oT/m \times 10^{-6}$	$KD \times 10^6$
		First Chamber sec^{-1}	Second Chamber sec^{-1}	Third Chamber sec^{-1}	Fourth Chamber sec^{-1}						
100	229	45.2	35.6	36.8	35.6	38.4	42.0	8.07	1.68	.369	1.84
101	229	31.4	16.4	18.7	16.4	20.5	43.5	5.44	1.53	.204	2.60
102	229	62.4	56.3	57.0	56.3	58.0	36.2	8.44	1.70	.481	1.46
103	229	85.2	80.7	81.2	80.7	82.0	34.5	8.85	1.73	.648	1.13
104	229	31.4	16.4	18.7	16.4	20.5	20.5	3.26	1.34	.096	3.54
105	463	81.4	80.7	80.7	80.7	81.0	28.5	11.30	1.84	1.069	0.79

$$KD = \frac{(N_o/N)^{\frac{1}{4}} - 1}{GN_oT/m}$$

REFERENCES

1. Guoy, G. "Sur La Constitution De La Charge Electrique A La Surface D'un Electrolyte." J. Phys. 9: 457, 1910.

2. Chapman, D. L. "A Contribution to the Theory of Electrocapillarity." Phil. Mag., 25: 475, 1913.

3. Stern, O. "Zur Theorie Der Elektrolytischen Doppelschicht." Z. Electrochem., 30: 508, 1924.

4. Grahame, D. C. "The Electrical Double Layer and the Theory of Electrocapillarity." Chem. Revs., 41: 441, 1947.

5. Kruyt, H. R., (Editor), Colloid Science I, Elsevier Publishing Co., New York; 1952.

6. Von Smoluchowski, M., "Drei Vorträge über Diffusion, Brownsche Molekularbewegung und Koagulation von Kolloidterlchen." Physik. Z., 17: 557, 1916.

7. Von Smoluchowski, M., "Drei Vorträge über Diffusion, Brownsche Molekularbewegung und Koagulation von Kolloidterlchen." Physik. Z., 17: 585, 1916.

8. Von Smoluchowski, M. "Versuch einer Mathematischen Theorie der Koagulationskinetik kolloide Lösungun." Z. Physik. Chem., 92: 155, 1918.

9. Muller, H. "Die Theorie der Koagulation Polydisperser Systeme." Kolloid Z., 38: 1, 1926.

10. Muller, H. "Zur Theorie der Electrischen Landung und der Koagulation der Kolloide." Kolloidchem. Beihefte, 26: 257, 1928.

11. Fuchs, N. "Über die Stabilität und Aufladung der Aerosole." Z. Physik., 89: 736, 1934.

12. Von Smoluchowski, M. "Versuch uner mathematischen Theorie der Koagulationskinetik kolloider Lösungen." Z. Physik. Chem., 92: 129, 1917.

Preceding page blank

REFERENCES (continued)

13. Muller, H. "Zur allgemeinen Theorie der raschen Koagulation." Kolloidchem. Beihefte, 27:223, 1928.

14. Tuorila, P. "Über orthokinetische und perikinetische Koagulation." Kolloidchem. Beihefte, 24:1, 1927.

15. Levich, V. G. Physiocochemical Hydrodynamics, 2nd ed. Englewood Cliffs, New Jersey: Prentice-Hall, Inc., 1962.

16. Manley, R. St. J. and S. G. Mason. "Particle Motions in Sheared Suspensions: II Collisions of Uniform Spheres." J. Colloid Sci., 7:354, 1952.

17. Swift, D. L. and S. K. Friedlander. The Coagulation of Hydrosols by Brownian Motion and Laminar Shear Flow. Baltimore: Department of Chemical Engineering, The Johns Hopkins University, October, 1963.

18. Langelier, W. F. "Coagulation of Water with Alum by Prolonged Agitation." Eng. News Rec., 86:924, 1921.

19. Camp, T. R., D. A. Root and B. V. Bhoota. "Effects of Temperature on Rate of Floc Formation." JAWWA, 32:1913, 1940.

20. Camp, T. R. and P. C. Stein. "Velocity Gradients and Internal Work in Fluid Motion." J. Boston Soc. Civil Eng., 30:219, 1943.

21. Camp, T. R. "Flocculation and Flocculation Basins." Trans, ASCE, 120:1, 1955.

22. Fair, G. M. and R. S. Gemmell. Some Aspects of Orthokinetic Flocculation. Cambridge: Div. of Engineering and Applied Physics, Harvard University, 1963.

23. Tambo, N. A Fundamental Investigation of Coagulation and Flocculation. Sapporo, Japan: Dept. of Sanitary Engineering, Hokkaido Univ., 1964.

24. Hudson, H. E. "Physical Aspects of Flocculation." J. AWWA, 57:893, 1965.

REFERENCES (continued)

25. Michaels, A. S. and J. C. Bolger. "Settling Rates and Sediment Volumes of Flocculated Kaolin Suspensions." I & EC Fundamentals, 1:24, 1962.

26. Michaels, A. S. and J. C. Bolger. "The Plastic Flow Behavior of Flocculated Kaolin Suspensions." I & EC Fundamentals, 1:153, 1962.

27. Krone, R. B. A Study of the Rheologic Properties of Estuarial Sediments. Berkeley: Hydraulic Engineering Lab. and Sanitary Engineering Research Lab., University of California, Sept., 1963.

28. Danckwerts, P. V. "Continuous Flow Systems, Distribution of Residence Times." Chemical Engineering Science, 2:1, 1953.

29. Levenspiel, O. Chemical Reaction Engineering. New York: John Wiley and Sons, Inc., 1962.

30. Wolf, D. and W. Resnick. "Residence Time Distribution in Real Systems." I & EC Fundamentals, 2:287, 1963.

31. Feuerstein, D. L. and R. E. Selleck. "Fluorescent Tracers for Dispersion Measurements." Journal of the Sanitary Engineering Division, ASCE, 89:1, 1963.

32. Vennard, J. K. Elementary Fluid Mechanics, 3rd edition, New York: John Wiley and Sons, Inc., 1954.

33. Handbook of Chemistry and Physics, 44th ed., Cleveland: Chemical Rubber Publishing Co., 1962.